

AD-A040 137

AMMANN AND WHITNEY NEW YORK
BLAST CAPACITY EVALUATION OF BELOWGROUND STRUCTURES. (U)

MAY 77 R ARYA, A AMMAR, S WEISSMAN, N DOBBS DAAA21-76-C-0125

UNCLASSIFIED

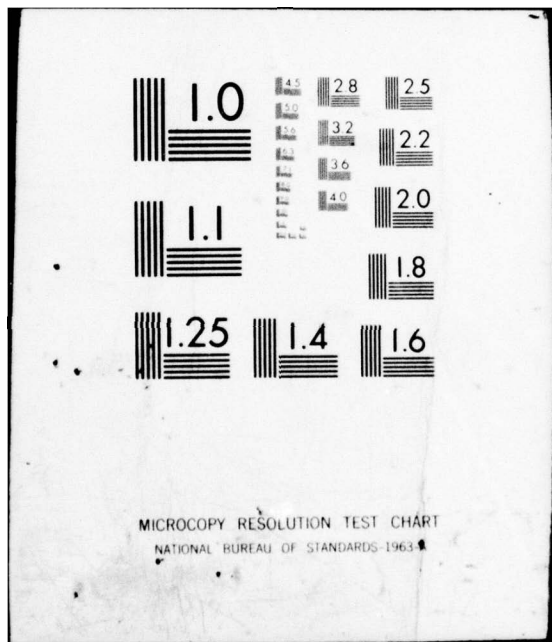
ARLCD-CR-77006

F/G 19/4

NL

1 OF 2
AD
A040137





MICROCOPY RESOLUTION TEST CHART
NATIONAL BUREAU OF STANDARDS-1963

ADA 040137

12
NW

AD

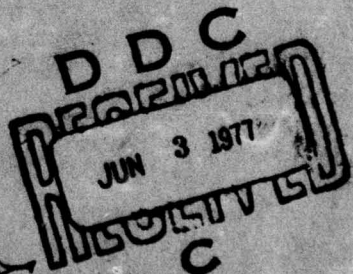
COPY NO. 35

CONTRACTOR REPORT ARLCD-CR-77006

BLAST CAPACITY EVALUATION OF
BELOWGROUND STRUCTURES

RAM ARYA ALBERT AMMAR
NORVAL DOBBS SAMUEL WEISSMAN
AMMANN & WHITNEY
PAUL PRICE
ARRADCOM COORDINATOR

MAY 1977



US ARMY ARMAMENT RESEARCH AND DEVELOPMENT COMMAND
LARGE CALIBER
WEAPON SYSTEMS LABORATORY
DOVER, NEW JERSEY

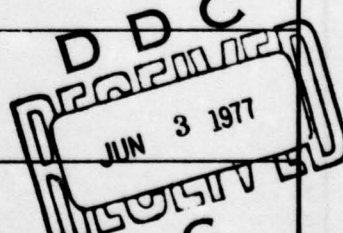
APPROVED FOR PUBLIC RELEASE: DISTRIBUTION UNLIMITED.

12
NW
DDC FILE COPY

Unclassified

SECURITY CLASSIFICATION OF THIS PAGE (When Data Entered)

(9) Contractor ref't.)

REPORT DOCUMENTATION PAGE		READ INSTRUCTIONS BEFORE COMPLETING FORM
1. REPORT NUMBER Contractor Report ARLCD	2. GOVT ACCESSION NO. CR-770064	3. RECIPIENT'S CATALOG NUMBER
4. TITLE (If different from item 1) Blast Capacity Evaluation of Belowground Structures		5. TYPE OF REPORT & PERIOD COVERED
6. AUTHORITY Ram Arya, Albert Ammar, Samuel Weissman, Norval Dobbs, (Ammann & Whitney), Paul Price, ARRADCOM Coordinator		7. PERFORMING ORG. REPORT NUMBER
8. CONTRACT OR GRANT NUMBER(s)		9. PROGRAM ELEMENT, PROJECT, TASK AREA & WORK UNIT NUMBERS DAAA-21-76-C-0125
10. CONTROLLING ORGANIZATION NAME AND ADDRESS ARRADCOM, LCWSL Manufacturing Technology Division (DRDAR-LCM) Dover, New Jersey 07801		11. REPORT DATE May 1977
12. MONITORING AGENCY NAME & ADDRESS (if different from Controlling Office)		13. APPROVALS 127 PA
14. DISTRIBUTION STATEMENT (of this Report)		15. SECURITY CLASS. (of this report) Unclassified
16. DISTRIBUTION STATEMENT (of the abstract entered in Block 20, if different from Report)		15a. DECLASSIFICATION/DOWNGRADING SCHEDULE
17. SUPPLEMENTARY NOTES  18. KEY WORDS (Continue on reverse side if necessary and identify by block number) Underground structures Reinforced concrete walls Blast resistant capacity Earth mounded structures Single revetted barricades High explosive effects		
19. ABSTRACT (Continue on reverse side if necessary and identify by block number) A series of ten explosion tests was performed to evaluate the capacity of belowground reinforced concrete structures (with open roofs) to resist the effects of internal explosions. Test results indicated that a full-scale belowground structure having the shape and three times the dimensions of the cells tested will have a capacity to resist a maximum of 2,700 to 3,600 kg (6,000 to 8,000 lbs) of H.E. Further testing is needed to establish quantitative means for determining the capacities of these structures. Also, additional structural configurations should be developed for use with large quantities of explosives.		

ACKNOWLEDGMENTS

The authors wish to express their sincere appreciation to the following persons for their assistance and guidance during the test program and/or report preparation: Messrs. Irving Forsten, Jack Canavan and Joseph Caltagirone of Picatinny Arsenal, Dover, New Jersey; Messrs. Phillip Miller and Charles Warnecke of U.S. Army Dugway Proving Ground, Utah; and Drs. John Healey and Kirti Gandhi, Messrs. Michael Dede, Aniello Maggio, Frank Wendling and Vambola Kald of Ammann & Whitney, Consulting Engineers, New York, New York.

ACCESSIONED BY	
RTTB	White Section
BIG	Buff Section
UNARMED	
JUSTIFICATION	
BY.....	
DISTRIBUTION/AVAILABILITY CODES	
DIAL.	AVAIL. 200/OF SPECIAL
A	

TABLE OF CONTENTS

	Page
SUMMARY	1
INTRODUCTION	3
Background	3
Purpose and Objective	3
Format and Scope of Report	3
TEST DESCRIPTION	5
General	5
Test Structures	5
Test Sequence	6
Explosive Charges	7
Instrumentation and Measurements	7
Deflection Gages	7
Hand Measurements	8
Damage Survey	8
Measurement of Backfill Movement	8
Photographic Documentation	9
TEST RESULTS	10
General	10
Structural Damage	10
Test Numbers 1 through 3	10
Test Number 4	11
Test Number 5	11
Test Number 6	12
Test Number 7	13
Test Number 8	14
Test Number 9	15
Test Number 10	16
Deflection Measurements	16
Hand Measurements	16
Deflection Gage Measurements	18
Evaluation of Test Results	19

TABLE OF CONTENTS
(Continued)

	Page
Comparison of Test Results with Existing Facilities	21
Radford AAP TNT Line Accident	21
Lone Star AAP 105mm Projectile Melt/Pour Facility	22
Single Revetted Barricades Tests	23
 CONCLUSIONS AND RECOMMENDATIONS	25
 REFERENCES	26
 TABLES	
Table 1 Charge properties and instrumentation	27
Table 2 Summary of permanent deflections (hand measurement)	28
Table 3 Summary of maximum and permanent deflections	29
 FIGURES	
Fig 1 White Sage Flat Test Site	31
Fig 2 Test structures layout	32
Fig 3 Structural details of test structures	33
Fig 4 Top view of concrete apron	35
Fig 5 Construction phase of test structures	36
Fig 6 Typical setup for Composition C-4 charges	37
Fig 7 Attachment location of deflection gages	38
Fig 8 Instrumentation details	39
Fig 9 Hand measurement and damage survey grid	41
Fig 10 Post-test view of Cell No. 1 west wall (Test No. 2)	42
Fig 11 Post-test view of Cell No. 1 west wall (Test No. 3)	43
Fig 12 Typical post-test apron and soil crack pattern (Test No. 4)	44
Fig 13 Post-test damage to Cell No. 1 east wall (Test No. 4)	45
Fig 14 Shear plane in soil	46
Fig 15 Post-test damage to Cell No. 1 east wall (Test No. 5)	47
Fig 16 Pre-test view of secondary debris source, Cell No. 1 (Test No. 5)	48

TABLE OF CONTENTS
(Continued)

	Page
Fig 17 Post-test damage to Cell No. 1 apron (Test No. 5)	49
Fig 18 Post-test damage to Cell No. 1 north wall (Test No. 6)	50
Fig 19 Post-test damage to Cell No. 1 apron (Test No. 6)	51
Fig 20 Post-test soil crack pattern (Test No. 6)	52
Fig 21 Post-test exterior view of Cell No. 1 (Test No. 7)	53
Fig 22 Post-test damage to Cell No. 1 (Test No. 7)	55
Fig 23 Post-test damage to Cell No. 1 north wall (Test No. 7)	57
Fig 24 Break-up of Cell No. 1 concrete apron (Test No. 7)	58
Fig 25 Post-test damage to Cell No. 2 (Test No. 8)	59
Fig 26 Post-test damage to Cell No. 2 east wall (Test No. 8)	61
Fig 27 Post-test damage to Cell No. 2 floor slab (Test No. 8)	62
Fig 28 Location of charges and damage to Cell No. 2 (Test No. 8)	63
Fig 29 Post-test damage to Cell No. 2 concrete apron (Test No. 8)	64
Fig 30 Cell No. 1 after removal of apron	65
Fig 31 Post-test damage to Cell No. 1 north wall (Test No. 9)	66
Fig 32 Post-test damage to Cell No. 2 (Test No. 10)	67
Fig 33 Permanent deflection contours, Cell No. 1 (Test No. 4)	69
Fig 34 Permanent deflection contours, Cell No. 1 (Test No. 5)	70
Fig 35 Permanent deflection contours, Cell No. 1 (Test No. 6)	71
Fig 36 Permanent deflection contours, Cell No. 1 (Test No. 7)	72
Fig 37 Permanent deflection contours, Cell No. 2 (Test No. 8)	73
Fig 38 Deflection-time measurements, Gage No. 2 (Test No. 4)	75
Fig 39 Deflection-time measurements, Gage No. 5 (Test No. 4)	76

TABLE OF CONTENTS
(Continued)

	Page
Fig 40 Deflection-time measurements, Gage No. 6 (Test No. 4)	77
Fig 41 Deflection-time measurements, Gage No. 2 (Test No. 5)	79
Fig 42 Deflection-time measurements, Gage No. 3 (Test No. 5)	80
Fig 43 Deflection-time measurements, Gage No. 5 (Test No. 5)	81
Fig 44 Deflection-time measurements, Gage No. 6 (Test No. 5)	82
Fig 45 Deflection-time measurements, Gage No. 7 (Test No. 5)	83
Fig 46 Deflection-time measurements, Gage No. 5 (Test No. 6)	84
Fig 47 Deflection-time measurements, Gage No. 7 (Test No. 6)	85
Fig 48 Deflection-time measurements, Gage Nos. 1 & 2 (Test No. 7)	87
Fig 49 Deflection-time measurements, Gage Nos. 3 & 4 (Test No. 7)	88
Fig 50 Deflection-time measurements, Gage No. 6 (Test No. 7)	89
Fig 51 Deflection-time measurements, Gage No. 7 (Test No. 7)	91
Fig 52 Deflection-time measurements, Gage No. 1 (Test No. 8)	92
Fig 53 Deflection-time measurements, Gage No. 2 (Test No. 8)	93
Fig 54 Deflection-time measurements, Gage No. 3 (Test No. 8)	94
Fig 55 Deflection-time measurements, Gage No. 4 (Test No. 8)	95
Fig 56 Deflection-time measurements, Gage No. 5 (Test No. 8)	96
Fig 57 Deflection-time measurements, Gage No. 6 (Test No. 8)	97
Fig 58 Floor plan - Building 9502, RAAP	98
Fig 59 Section - Building 9502, RAAP	99
Fig 60 Post-explosion view of Building 9502, RAAP	100
Fig 61 Floor plan - Automatic Inspection Building, LSAAP	101

TABLE OF CONTENTS
(Continued)

	Page
Fig 62 Section - Automatic Inspection Building, LSAAP	102
Fig 63 Section - Single Revetted Barricades Test Structure	103
Fig 64 Post-explosion view of Wall No. 1 - Barricade Tests	104
Fig 65 Post-explosion view of Wall No. 2 - Barricade Tests	105
APPENDIX - INTERNATIONAL SYSTEM OF UNITS	107
General	109
SI Units and Prefixes	109
Base Units	109
Supplementary Units	109
Derived Units	110
Prefixes	111
Mass, Force and Weight	112
Conversion and Rounding Rules	112
Selected Conversion Factors	113
DISTRIBUTION LIST	115

SUMMARY

Modern-day explosive manufacturing and loading facilities require increased protection to achieve a safe operating system. However, this increased protection is expensive and in many cases difficult to obtain. Where relatively large quantities of explosives are involved, economy of construction can be realized with the use of belowground reinforced concrete structures. Since they are located below the ground surface, these structures can utilize barricaded intraline separation distances for their siting and thereby realize cost saving for utilities and other facilities connecting various buildings.

At the present time, the design of belowground structures is based upon requirements for conventional loads, i.e., the walls are designed as retaining walls without considering the effects produced by an internal explosion. In order to provide insight into the blast-resistant capacities of belowground structures a series of tests was performed at Dugway Proving Ground under the direction of Picatinny Arsenal. This series consisted of ten tests on two one-third scale models of a typical belowground operating building. Each structure was a 2.44 m (8 ft) cube consisting of four concrete walls and a floor slab and an open roof. The top of the structure was at the ground level. Concrete aprons were used to provide lateral support at the top of the walls. The apron was removed prior to performing the last test on each structure. Eight tests were performed on one of the models, whereas the second structure was subjected to the effects of only two explosions. The quantities of explosives used in the first three tests (Cell No. 1) were small, 2.7 kg (6 lbs) and less. Tests 4, 5, 6, 7 and 9 of Cell No. 1 used explosive quantities of 11.2, 19.5, 28.8, 36.9 and 68.0 kg (25, 43, 63, 81 and 150 lbs), respectively. Tests 8 and 10 were performed on Cell No. 2 and utilized explosive quantities of 86.7 and 113.4 kg (191 and 250 lbs), respectively. The center of gravity of all explosive charges (Composition B or C-4) was located at the geometric center of the structures. Electronic instrumentation, as well as hand measurements, were used to determine the wall deflections. Also, both still and motion picture camera coverage was provided for documentation purposes.

The cell used in the first seven tests and Test 9 survived the combined effects of the eight explosions; on the other hand the second cell failed during the second test performed on it. Based upon these results, it is estimated that the maximum blast-resistant capacity of the full-scale structures of the

configuration tested is in the order of 2,700 to 3,600 kg (6,000 to 8,000 lbs) of H.E.

It is proposed that additional tests be performed to provide quantitative means for determining the blast-resistant capacity of belowground reinforced concrete structures and to develop various configurations of these structures for large explosive quantities.

INTRODUCTION

Background

To provide economy of construction and still achieve safety needs, new explosive manufacturing and loading plants are utilizing more and more belowground construction. However, presently there is relatively little quantitative data available whereby the explosive capacity of a belowground structure can be determined; particularly when the potential explosion is within the building itself (donor structure).

In order to obtain necessary data relating to the performance (capacity and damage which may be sustained by below-ground structures) a series of tests was performed under the direction of the Manufacturing Technology Directorate of Picatinny Arsenal as part of its overall Safety Engineering Support Program for the U.S. Army Armament Command. This report, which was prepared with the assistance of Ammann & Whitney, Consulting Engineers, summarizes the results of these tests and provides conclusions and recommendations for further evaluation of belowground structures.

Purpose and Objectives

The main purpose of the test series was to evaluate the blast-resistant capacities of fully vented (open roof) below-ground structures when subjected to the blast output of internal explosions.

The objectives of the tests are summarized as follows:

1. To evaluate the strength afforded by the reinforced concrete and the surrounding soil, as a composite unit, to resist the blast output of an explosion.
2. To determine the modes of failure of the structure when overloaded by blast.
3. To determine quantitatively the upper explosive limit of belowground reinforced concrete protective structures.

Format and Scope of Report

This report is organized into three basic areas. The second section of the body of the report considers the test setups including description of the test structures and the instrumentation. Damage sustained by the structures is

described in the third section; while the conclusions based upon the test results, as well as recommendations for further testing, are presented in the fourth section.

Since future standards of measurements in the United States will be based upon the SI Units (International System of Units) rather than the United States System of Units now in use, all measurements presented in this report will conform to that of the SI units. However, for those persons not fully familiar with the SI Units, United States equivalent units of particular test data are presented in parenthesis adjacent to the SI units. Also, a list of units, symbols, and United States conversion factors for SI units is presented in the Appendix.

TEST DESCRIPTION

General

Ten tests were performed at the White Sage Flat Test Facility range of Dugway Proving Ground (DPG) at Dugway, Utah. Eight tests were conducted during June 1975 while the remaining two tests were completed in September 1975. Figure 1 illustrates the site layout of this test series.

Two structures were tested; both of which were identical in terms of general dimensions, foundation type and surrounding soil conditions. In order to determine the structural response of each test structure, both electronic and hand measurements of the structural deflections produced by the blast were recorded. Photographic coverage of both pre- and post-test conditions of each structure was made in order to define the damage incurred due to the blast.

Test Structures

Each structure was constructed of reinforced concrete and was positioned belowground. The top of the structure was level with the ground surface. As will be shown, the size of the test structure was representative of a one-third scale model of a typical belowground operating building.

Figure 2 illustrates the layout of the test structure while Figure 3 shows the structural details.

Each structure was rectangular in shape and consisted of four walls and a foundation slab. The overall interior dimensions of each structure was 2.44 m (8 ft) cube while the concrete thickness of each wall and the slab was 0.2 m (8 in.) and 0.25 m (10 in.), respectively. The amount of reinforcement in the individual members was determined by considering the structures' capacity to sustain the exterior soil pressures and complied with the minimum flexural reinforcement as specified in the TM 5-1300 (Ref 1). Laced reinforcement was not used in these walls.

Positioned at the top of each test structure was a reinforced concrete apron having a width and thickness of 0.91 m (3 ft) and 0.2 m (8 in.), respectively. The apron was continuous around the structure and was cast monolithically to the exterior of the walls (Fig 4). As will be shown later, this apron provided a significant increase in strength to the walls and, thererby, increased the explosive capacity of the structure.

Initially it was planned to construct each test structure totally below ground. However, in order to avoid an elaborate and complicated installation of instrumentation for measuring wall deflections, it was decided to position the structure partly below the natural terrain for a depth of 0.86 m (2 ft-10 in.) and backfill around that portion of the structure extending above ground. In order to simulate the infinite soil conditions which would be associated with the structure positioned completely below ground, the backfill above the natural grade was extended horizontally in all directions away from the structure for a distance of 7.6 m (25 ft) and at that point allowed the fill to slope at the rate of 2 on 1 to the elevation of the natural terrain.

Prior to construction, the entire site allocated for the construction of each structure (structure and backfill) was stripped of loose surface material and existing vegetation, by scraping. The fill used for backfilling both the belowground and upper portion of the structure consisted of well-graded sand-gravel material which was placed in 0.2 m (8 in.) thick layers which, in turn, were compacted to 92 percent of the maximum dry density as required by Reference 2.

Figure 5 illustrates the construction phase of the project. Additional construction photographs are presented in Reference 3.

Test Sequence

Of the ten tests performed, the first eight tests can be considered as response tests to determine the maximum capacity of the belowground structure as originally designed. The seven initial tests were performed on one of the test structures (hereafter referred to as Cell No. 1), while the eighth test was performed on the second structure or Cell No. 2. Testing of Cell No. 1 was performed in stages with progressively larger charges being used in each successive test (Table 1). The results of these tests were used to establish what was thought to be the upper limit of the explosive capacity of the structure. This so-called upper limit was then used as the explosive quantity of the test of Cell No. 2 in Test No. 8.

Although both cells were severely damaged after the completion of the first eight tests, the structures had not failed and, therefore, additional tests were scheduled to try to establish an insight as to the magnitude of the structure's capacity in the event that the previously mentioned concrete aprons were eliminated. For this purpose, Cell No. 1 was tested in Test No. 9, while Test No. 10 utilized Cell No. 2.

Modification of the structures was accomplished by removing the aprons with the use of a concrete saw.

Explosive Charges

The explosive used in Tests 1 through 8 was Composition B. Each charge had a cylindrical shape with an aspect ratio (length to diameter ratio) of one. The explosives used in Tests 9 and 10 were formed from Composition C-4 blocks. The blocks, which weighed 0.57 kg (1-1/4 lbs) each, were arranged to form a cubicle shape (Fig 6). All charges were initiated electrically from the control house.

The weights of the individual charges used in the various tests are given in Table 1.

Individual charges weighing 6.8 kg (15 lbs) or more were supported on wooden benches, while smaller charges were hung from cross-wires attached to the top of the cell walls. All charges were located at the geometric center of the cell.

As previously mentioned, the size of the test structure was selected such that it would represent a one-third scale version of a full scale operating building. Therefore, the full scale charge weights which would be associated with the representative full scale structure would be equal to 27 times the weight of the individual charges used in the tests. These full scale equivalent charge weights are also presented in Table 1.

Instrumentation and Measurements

Deflection Gages

Only one of the four walls of each cell was instrumented with electronic displacement gages. Displacement-time history measurements were recorded at nine locations of the wall (Fig 7). All gages were linear displacement transducers which operate on the principle of change in inductance in the coils of a linear differential transformer with change in position of the core. These gages had a 0.15 m (6 in.) stroke which, as will be discussed later, was exceeded in several of the tests.

Each gage was mounted at the mound side of the structure on steel support frames. The deflection rods (cores) were connected to steel rods (Fig 8) which passed through pipe sleeves. The steel rods were embedded in the concrete wall of the structure. Movement of the wall moved the deflection rods within the gage. The sleeves minimized any binding of the steel rods by the compacted earth.

Hand Measurements

Pre- and post-shot measurements of the curvature of three walls of each cell were made at the intersection of horizontal and vertical grid lines marked on the inner faces of the cell (Fig 9). These measurements were made to a fixed frame of reference consisting of a steel beam supported on two concrete blocks which were positioned adjacent to the cell. Each block, which was 0.36 m long by 0.31 m wide by 0.38 m deep (14 in. by 12 in. by 15 in.), was positioned to a pair of fixed bench marks located outside the blast affected area. The positions of the blocks both before and after each test was checked to determine whether movement of the blocks occurred during a test. Each end of the steel beam, which was portable, was located at the center of each block. The bottom flange of the beam was fitted with a "Unistrut" type channel which served as the rail for a trolley-type assembly which, in turn, supported a plumb line. The plumb line could be moved along the length of the beam to points opposite the grid lines on the walls. Measurements between the plumb line and the intersections of the grid lines were made with the use of a steel ruler. The measurements were made before and after each test and, thereby recorded the movement of the wall during the test. The beam with the trolley and plumb line was removed during each test.

Details of the hand measurement equipment are illustrated in Figure 8.

Damage Survey

The entire inner surface (four walls and floor) of the cell, as well as the upper surface of the apron was painted white and marked with a grid of 13 mm (1/2 in.) wide black lines. The white-lined surface facilitated detection of cracks and location of areas of spalled concrete and reinforcement damage. The intersection of the black lines also served as the points used for performing the previously mentioned hand measurements.

Measurement of Backfill Movement

No special electronic instrumentation was used to measure soil movement around the structures during the tests. However, poles which were placed in the backfill adjacent to the south and west sides of each structure were used to yield qualitative information about the nature of the gross movement of the soil relative to that of the structure. A total of nineteen poles were used at each of the above two sides of each cell and were arranged in a pattern illustrated in Figure 8. Each pipe was

38 mm (1-1/2 in.) in diameter with its exposed end painted orange for better visibility.

Photographic Documentation

For documentary purposes motion picture camera coverage of the tests was used to observe the cells during each detonation. Still photographs were taken to record the pre-shot setup in terms of site location, general arrangement, construction details and instrumentation; and to record post-shot test results.

Three movie cameras were utilized in the individual tests. One camera, with a speed of 500 frames per second, was used to record an overall view of the test; whereas the other two cameras, each having a speed of 3,000 frames per second, were used to photograph the cell and backfill movements. The positions of the cameras are shown in Figure 8. A hand motion picture camera was also used to make documentary films of the test series; recording the various phases of the construction, pre-test setup and post-test damage.

TEST RESULTS

General

Results of the tests are presented in terms of pictorial photos, crack patterns and displacement measurements. The photos and crack patterns illustrate the damage sustained by the various wall elements, whereas the displacement measurements indicate the motions to which the walls were subjected. Both permanent and time dependent displacements are presented. Because of the severe damage sustained by Cell No. 1 in Test No. 9, and Cell No. 2 in Test No. 10, the results of these tests are presented only in pictorial form.

Structural Damage

Test Numbers 1 to 3 - Cell No. 1 (0.9, 2.7 and 2.7 kg)

The damage sustained by the structure in Test Nos. 1 to 3 was relatively minor. There was no damage in Test No. 1 except very minor pitting of the concrete walls. After Test No. 2, some hairline cracks appeared in the vertical corners of the cell as shown in Figure 10. No sign of movement of the soil was visible in either Test No. 1 or Test No. 2.

In Test No. 3, the cracks sustained in Test No. 2 were increased and the spalling of concrete to a depth of 3 mm (1/8 in.) along the vertical cracks was observed (Fig 11). Formation of these cracks (in Test Nos. 2 and 3) indicated that yielding of the interior corner reinforcement was produced. Also, as will be shown later, these corner bars tended to pull out of their supports and thereby increased the size of the cracks.

Damage to the floor, if any, could not be observed because of water on the floor due to rain prior to testing. No spalling or cracking of the concrete was observed at any other place on the interior surface of the walls. Although the earth-fill behind the walls was not removed and, therefore, the exterior surfaces of the walls could not be observed, it was felt that vertical tensile cracks at the center of each wall were formed in these tests.

Diagonal hairline cracks were formed in Test No. 3 at the four corners of the cell apron. Each crack extended approximately 0.46 m (1 ft-6 in.) away from the corner (Fig 12). A separation of approximately 3 mm (1/8 in.) was formed between the concrete and the soil around the periphery of the apron. This separation was an indication of the occurrence of horizontal movement (vibration) of the cell.

Test Number 4 - Cell No. 1 (11.2 kg)

Spalling of concrete in corners of the cell observed in Test No. 3 was appreciably increased and extended over the lower three-fourths of the cell height. Depth of spall was as large as 19 mm (3/4 in.) with some reinforcing bars in the corners visible. Cracks appeared along the intersection of floor slab and all four walls. Approximately 0.3 m (1 ft) below the top of the walls, horizontal hairline cracks were formed. These cracks were formed by the yielding of vertical reinforcement at the interface of the walls which, in turn, was produced by the blast loads acting on the top of the aprons. Hairline cracks were formed in the floor slab which radiated from its center. All this damage is illustrated in Figure 13.

The above described damage indicated that walls were being pushed into the soil by the blast loads and were acting as plates supported on four sides; the top support being furnished by the apron acting as a series of interconnected deep beams. The apron crack pattern, as shown in Figure 12, illustrates the above-mentioned beam action of the apron. It may also be noted from Figure 12 that cracks were formed in the soil at the location of the poles indicating the soil movement has occurred. These cracks were situated at the poles because of the soil weakness produced at these locations by insertion of the poles. The significance of the cracks is the extent away from the structure to which the soil is effective in resisting the movement of the structure, i.e., the angle of friction (θ) between the structure and the supporting soil is equal to or greater than 65 degrees (Fig 14). This relatively large friction angle is in part attributed to the vertical compression forces produced by the downward motion of the concrete apron and to a lesser extent by the blast loads acting on the surface of the backfill surrounding the structure.

Test Number 5 - Cell No. 1 (19.5 kg)

Concrete spalling in the corners extended the full height of the cell. Vertical and horizontal reinforcement bars in the corners were visible. The vertical bars were pushed out by horizontal bars which tried to pull out of their supports. Similarly, vertical bars at the junction of floor slab and walls were visible. Horizontal cracks were formed at the junction of apron and walls (Fig 15). Total deflection near the center of walls was as large as 100 mm (4 in.). Except for some concrete scabbing of the walls, the debris placed adjacent to the charge in this test (Fig 16) did not cause any structural damage. However, some pieces of debris were thrown as far away as 38.0 m (125 ft).

The general crack pattern of the apron in this test remained the same as that of Test No. 4. However, the cracks did widen a bit and a few new cracks around the outside corners of the apron were formed (Fig 17).

Like the concrete damage to the apron, the crack pattern formed in the soil in Test No. 4 did not change in Test No. 5 except that the cracks were widened. Soil was loose around the poles in the first three rows nearest the walls while, at the fourth row, the soil remained intact. Concrete pads located in the soil at opposite sides of the cell were moved towards one another a total of 13 mm (1/2 in.). This inward movement of the blocks was attributed to the upheaval of the backfill which, in turn, was caused by the outward deflection of the walls and/or the movement of the overall structure. Like the cracks, the upheaval of the soil was evidence that soil was compressed by the structure and thereby assisted the structure in resisting the blast output. In addition, the upheaval of the soil was an indication that the movement along the soil shear plane had occurred.

Test Number 6 - Cell No. 1 (28.8 kg)

Concrete was broken loose to full thickness of wall in the corners of the cell. Soil in the back of walls was visible at the corners. Vertical reinforcement near the corners was pulled towards the interior of the cell by the straightening action of horizontal bent bars in the corners. Some of these horizontal bent bars were broken. Spalling of concrete at the junction of apron and wall was complete at two walls and all the vertical reinforcement was exposed. All bars at the base of these walls (at the junction with the floor) were visible; some up to a height of 0.46 m (1 ft-6 in.). Several of these bars were broken. Vertical cracks were located at center of each wall. These cracks were attributed to tension force produced in a given wall by the blast loads acting on the two adjoining walls.

Damage to the cell after Test No. 6 is illustrated in Figure 18.

Cracks which had previously opened in the apron opened even further with the widest crack being as large as 8 mm (5/16 in.). This crack was located at center of outside of the apron (Fig 19). Concrete was crushed along cracks in the outside corners of the apron. Several pieces of concrete were detached from the inside corners of the apron (Fig 19).

Soil was displaced from near the edge of the apron and deposited near the first row of poles (Fig 19). Movement of the

soil immediately adjacent to the first row of poles was approximately 6 mm (1/4 in.). This movement was evident from the air space which was located at the rear of the poles after the test. Again, the concrete pads moved towards the cell. The total movement caused was approximately 32 mm (1-1/4 in.), which is indicative of the increase of the soil compression force from one test to the other.

The soil crack pattern is shown in Figure 20. These cracks were almost circular out to the edge of the earth-mound and as before, were formed at the locations of the various groups of poles. The large radius of the outer crack is an indication that the angle of friction (ϕ) was even larger than previously mentioned.

Test Number 7 - Cell No. 1 (36.9 kg)

Figure 21 illustrates the overall view of the damage to the cell including debris from the breakup of the wall and apron after Test No. 7. Damage to the walls and apron is illustrated in Figure 22. Most of the debris was formed from the breakup of the wall corners. All reinforcing bars at the corners were exposed for a wall length of 0.2 m (8 in.). Some of the earth-fill fell into the cell from behind the corners (Fig 23). Permanent deflections of walls into the soil were as large as 0.2 m (8 in.) and with uniform curvatures of the walls clearly visible. This uniform curvature is attributed to the support provided by the soil over the full length and height of the walls and again is evidence of the increased resistance of the walls provided by the earth-fill.

Concrete sections weighing 1 kg (2.2 lbs) or more were thrown out from the structure for a distance of 4.57 m (15 ft). Smaller sections were thrown even farther. The apron was badly damaged in the corners and concrete sections were dispersed as debris (Fig 24).

The cratering of the soil at the rear of the apron was extensive in this test. No visible tilting of poles took place. A considerable amount of soil was removed around the base of each pole. The crack pattern for soil was similar to the one shown for Test No. 6 (Fig 20), except that cracks as wide as 10 mm (3/8 in.) were formed. Concrete pads moved a total distance of 60 mm (2-3/8 in.) from their original position and were tilted towards the cell as before. A crater was formed in the floor slab about 0.46 mm (1 ft-6 in.) in diameter and about 51 mm (2 in.) deep. Radial cracks 0.61 m to 0.91 m (2 ft to 3 ft) long were formed.

Test Number 8 - Cell No. 2 (86.7 kg)

Two charges were used in this test, as previously mentioned, one weighing 43.4 kg (97.8 lbs), and the other weighting slightly less at 43.3 kg (97.5 lbs). These charges were placed side by side on a wooden bench and were detonated simultaneously. This was the first of two tests performed in Cell No. 2.

Extensive spalling of concrete and separation of concrete from the reinforcement of each wall took place (Fig 25). Pieces of concrete weighing upward to 4 kg (8.8 lbs) were thrown as far away as 10 m (30 ft). Most of the horizontal bent reinforcing bars at the corners on the inside face of the cell were broken. Also, many of the bars on the inside face at the junction of walls and floor were ruptured. All the vertical bars of east wall and most of the vertical bars of west wall on inside face were broken at the junction of apron; corresponding reinforcement of the other walls remained intact. The concrete was displaced from the four corners. Also, cavities behind each corner was formed by displacement of the backfill by the blast pressures. Figure 26 illustrates typical damage to each of the four walls.

Directly below the charge, the floor slab was crushed over a 1 m (3 ft-4 in.) diameter area; with the concrete in this area pushed into the soil. Outside of the depression, circular and radial cracks extended out to the walls (Fig 27).

Aprons had diagonal cracks as large as 13 mm (1/2 in.) in width. All four walls along with the apron were pushed into the soil. East and west sides of the apron were pushed upward in a convex form, whereas north and south sides of the apron were pushed down in a concave form. This variation of the apron deflections was attributed to the variation in the tension forces in walls due to the charge orientation; i.e. for cylindrical charges having an aspect ratio of one, the walls positioned parallel to the center-line of the double charge (Fig 28) are subjected to a greater portion of blast output than are walls which are oriented perpendicular to the charge center-line. Here, the larger loads acting on the east and west walls produced larger tension forces in the north and south walls and thereby caused the downward curvature of the aprons of these latter walls. As will be shown later, this variation in blast loads also affected the magnitudes of the wall displacements.

In addition to extensive diagonal cracking in apron corners, the concrete was disengaged at the outside corners (Fig 29). This was a result of the compression forces produced in the aprons due to their deep beam action. Compression failure also

occurred at the center of the east and west side of the apron. At these sections, the compression forces, in addition to those produced by the deep beam action, were produced by the convex deformation of the apron discussed earlier. The apron also had cracks in the center portions running from the outside face to the junction of walls and apron and are typical of tension cracks formed in beams.

Soil was displaced from the edges of the apron exposing the apron to a depth of up to 0.15 m (6 in.). Soil was loosened up to a distance of 3.66 m (12 ft) away from the edges of the apron and, therefore, no crack pattern for soil was visible. No visible tilting or movement of poles took place. The concrete pads were pushed out and were tilted away from the cell. This was probably caused by the loosening of the soil.

Although the total weight of charge used in this test was less than the combined weight of the charges of the first seven tests, the damage sustained by Cell No. 2 was at least equal to and in some respects greater than the combined damage to Cell No. 1. In the case of Cell No. 1, a total of seven separate charges were detonated independently and produced a larger elastic recovery of the plastic displacements than that which was produced by the double charge simultaneously initiated in Cell No. 2.

Test Number 9 - Cell No. 1 (68 kg)

For this test, the apron was sawed off along the outside face of walls (Fig 30) and 68 kg (150 lbs) of Composition C-4 charge was detonated at the center of the cell.

The added damage to the structure consisted of an increase in the removal of the concrete located at the four corners of the walls and near the intersection of the walls and floor slab, increase in the displacement of each wall panel into the earth-fill, additional cracking of the walls and the disengagement of the top of the wall which originally was part of the apron which was not removed prior to the test (Fig 31).

In general, it may be said that complete failure did not occur and that the structure functioned as an effective barricade, although some fragments were produced.

Regarding the effectiveness of the apron, the displacements at the top of the walls after this test were considerably larger than after the previous tests and, therefore, it may be concluded that the apron was effective in limiting wall displacements and

probably provided increased strength to the structure as a whole. However, its effectiveness in terms of quantitative measures has not been established and will need further study.

Test Number 10 - Cell No. 2 (113 kg)

Like the cell of Test No. 9, the structure of this test had its apron removed prior to testing.

Structural damage sustained in this test was considerably more than that of Test No. 9. Two of the walls completely collapsed while the remaining walls were on the verge of failure (Fig 32). A considerable amount of the wall debris was dispersed distances greater than barricaded intraline distances, with smaller fragments being projected beyond unbarricaded distances. The secondary missiles formed from the structure breakup would definitely be a source of danger to other structures separated from the test structure at the above mentioned safety distances.

The degree of damage to this structure can be associated with damage which is beyond incipient failure. Therefore, qualitatively it can be said that the charge capacity of this type of structure will be less than the combined weights of explosives of Test No. 8 and 10 or 200 kg (440 lbs).

Deflection Measurements

Hand Measurements

Post-test permanent deflection patterns of all walls except the east wall were obtained by hand measurements. These measurements were taken at the grid points as shown in Figure 9. Since there were no apparent permanent deflections, measurements were not taken for Tests 1 through 3. Also, because of the extensive damage which occurred in Test Nos. 9 and 10, deflection measurements for these tests were unobtainable.

Results of those hand measurements are summarized in Table 2; whereas Figures 33 to 37 illustrate the wall deflection contours. Except for Test Nos. 4 and 8, the deflections given in both the table and the contours are relative values, e.g. the values given in Figure 35 are the differences in measurements recorded after the sixth test and the fifth test. In case of Test Nos. 4 and 8, the values listed can be considered as absolute deflections; since, for the first three tests there were no apparent permanent deflections and the Test No. 8 was the first test performed on Cell No. 2.

The deflection patterns produced in Test Nos. 4 through 7 were similar for the three walls investigated in any one test. However, the patterns did vary from test to test both in magnitude and in shape.

In the initial test, for which measurements were recorded (Test No. 4), the maximum deflection was located near the center of each wall (Figure 33) adjacent to the charge. The magnitude of the wall displacement decreased with the increase in distance away from the center of the wall. The deflections along the intersection of each wall with the floor was equal to approximately one-half the maximum value while at the adjoining wall intersections the deflections varied from the previous mentioned value at the floor to about one-tenth to one-fifteenth of the maximum displacement at the top of the walls. It is theorized that the larger deflections at the wall and floor intersections were produced by the amplification of the blast loads by the multiple reflections of the blast wave in the corners of the structures.

Except for the south wall, the deflection along the top of each wall was constant, and about 1/10 to 1/15 of the maximum deflection of that wall. In case of the south wall, the deflection at the center of the top of the wall was one-fifth of that of the maximum value. This was attributed to the fact that the charge was positioned slightly off center and closer to the south wall. As was evident from the larger perpendicular cracks formed at the center of the south wall apron, the beam reinforcement yielded in this apron and increased the wall deflections. As will be shown, this increase in deflection at the top of the south wall was also observed in subsequent tests.

As may be seen from Figure 34, the wall deflection patterns after the fifth test differed substantially from those of Test No. 4. Here, the points of maximum deflection were located closer to the floor slab than were those of the previous test. Also the size of the crater (point of maximum deflection) increased in width which caused the deflections of the wall intersections to increase in the lower half of the walls. The deflections at the intersection of the walls and slab were only slightly smaller in magnitude than that of the maximum deflection.

After the sixth test, the zone of the maximum displacement had spread to encompass almost the entire lower half of each wall. As in the previous tests, the deflections at the top of the walls were small in comparison to those in the lower half of the cell. Here again, these reduced displacements were attributed to the support afforded by the apron. The deflection contours

for the walls of Test No. 6 are illustrated in Figure 35.

The spreading out of the zone of the maximum deflection to encompass larger areas of the walls was further continued in Test No. 7. At this point, the support furnished by one wall or the floor slab to another wall was negligible due to severe cracking of the concrete at their intersections. In essence, the main support for the lower portions of the walls was provided by the soil (backfill).

It may be noted that the relative wall displacements which occurred in Test No. 7 were smaller than those produced in Test No. 6. This can be attributed to the nonlinear compaction characteristics of the soil backfill, i.e. the change in soil resistance will increase with increasing soil compaction. It is surmised that the compaction of the soil in the previous tests was such as to produce a high soil resistance and thereby limited the soil displacements which, in turn, limited the wall deflections of Test No. 7.

Test No. 8 was the first test performed on Cell No. 2 and utilized a total explosive quantity equal to slightly less than the combined weights of the explosives used in Test Nos. 1 through 7.

The magnitude of the deflections (Figure 37) sustained by the north and south walls in Test No. 8 was equal to or slightly larger than the combined deflections (at a given point) produced in Test Nos. 4 through 7. On the other hand, the west wall and presumably the east wall deflections were approximately 60 percent larger than the combined deflections of the previous tests. These larger deflections were produced by the increase in the blast output due to the orientation of the two charges with their common axis parallel to the east and west walls (Figure 28). Like the previous tests, the deflections were fairly uniform in magnitude across the lower half of the walls, with considerably smaller displacements occurring near the top of the cell. It may be noted that the deflections at the top of the north wall of Cell No. 2 were larger than those combined in all seven tests of Cell No. 1. This was probably caused by the yielding of the reinforcement in the north wall section of the apron.

Deflection Gage Measurements

A summary of the maximum and permanent relative deflections recorded by each gage in each test from Test Nos. 4 through 8 is listed in Table 3, whereas the time histories of the deflections are illustrated in Figures 38 through 57. Figures 41 through 47

and Figures 50 and 51 are prepared from computer data output furnished by the DPG personnel. The remainder of the deflection gage measurements have been obtained from Reference 3. Since the gages did not trigger, deflection gage measurements from Tests No. 1 through 3 are not available. All deflections recorded have been presented both in the SI and U.S. units.

For comparison purposes, permanent deflections obtained from deflection gages and hand measurements are also listed in Table 3. It may be noted from Table 3 that, in most cases, the permanent deflections obtained from gage measurements of Test Nos. 4 and 5 compare very favorably with those of the hand measurements. For Test No. 6, the push rods of the gages struck the angles and were bent and therefore, the gage deflection measurements cannot be relied upon. In Test No. 7, gages 1 through 4 had a very short time base of 40 ms with the records ending near the maximum deflection and therefore, permanent deflections records could not be obtained. Also, the permanent deflection records of gages 6 and 7 were lost due to a broken electrical connection after the maximum deflections had been reached. However, all the maximum deflections obtained from gages in Test No. 7, in combination with the permanent deflections obtained from hand measurements, define fairly well the motions of the structure.

In Test No. 8, all the permanent deflections obtained from the hand measurements were 25 to 50 percent larger than those obtained from the gage measurements. Also the maximum deflections and permanent deflections obtained from the gages are of the same order of magnitude.

This can be explained by the fact that the damage to the structure was so severe that little or no elastic rebound of the walls themselves or the soil backfill occurred. However, the support furnished by the soil to the wall was evident from the near uniformity of the wall deflections.

Evaluation of Test Results

The single charge capacity (total explosive quantity detonated at one time) of the belowground cell configuration tested is difficult to estimate because of the structural modification which included the removal of the concrete aprons prior to the performance of Test Nos. 9 and 10. However, a guesstimate of this capacity can be made based upon the results of the tests of Cell No. 2.

The single charge capacity of the test cell was definitely more than the 87 kg (194 lbs) of explosives used in Test No. 8 but was probably less than the combined weights of the explosives of Test Nos. 8 and 10, or 200 kg (440 lbs). The strength afforded by the backfill was significant in so far as the overall charge capacity of the structure was concerned. This was demonstrated in the later tests of Cell No. 1 and the initial test of Cell No. 2 (Test No. 8). In both cases, the concrete at the intersections of the walls and floor was completely destroyed. However, the central sections of the walls remained intact with the reinforcement extending between adjoining members (wall panels and floor slab) also remaining intact. This type of structural failure was not considered to be a structural collapse. If the soil were not present, each wall panel would have failed initially at the center and then the failure spreading towards the corners. This type of wall collapse would have occurred at much smaller charge capacities than stated above.

In addition to the soil, strength was also afforded to each test structure by the concrete aprons located at the top of the cells. Here, the deflections at the top of the wall were minimized by the "ring action" of the apron which in turn reduced the maximum deflections at the center of the walls. By shifting the curve of maximum deflections to the lower portions of the structure, increase in the soil resistance was obtained due to the additional overburden. Also, the compressive forces in the soil, produced by the downward motion of concrete apron which in turn was caused by the downward motion of the structure as a whole, increased the angle of friction in the soil and, thereby, increased the soil capacity to resist the outward motion of the walls.

Based upon the above, it can be concluded that a full-scale belowground structure having dimensions equal to three times those of the test structure would have an upper explosive limit somewhere in the order of 2,700 to 3,600 kg (6,000 to 8,000 lbs) of HE when the charge is located at the geometric center of the cell and the upper portions of the walls are supported with system similar to the concrete aprons used in the tests. For cells with roof panels, where significant blast reflections occur from the roof panels the explosive limit stated above would be reduced as discussed later. The limiting explosive capacity is reached at full or near full containment of the output of an explosion. If the explosive charge in a given cell is distributed into two or more smaller charges, rather than being concentrated as in the majority of these tests, then individual wall capacities will differ depending upon the quantity and location of the individual charges. This was demonstrated in Test No. 8 where two cylindrical

charges were placed side by side in the middle of the cell such that the line connecting the centers of the charges was parallel to the east and west walls. In this case the deflections attained by those two walls were 60 percent higher than the deflections of the north and south walls. It is possible that in some extreme cases, the two parallel walls would fail whereas the other two walls would sustain very little damage. This would be classified as a structural failure and could occur at explosive weights less than the charge capacities of the test cells. The other factor involving the capacity of a belowground structure is the use of concrete aprons. The above mentioned capacities assume that the aprons are furnished. Without the aprons the capacity will be reduced.

Comparison of Test Results with Existing Facilities

Several existing and newly designed facilities have utilized belowground construction for the potential donor structures. However, the design of these structures only considered the requirements for conventional loadings (soil pressures) without giving consideration to blast effects associated with an explosion. The following examples illustrate the need for design criteria whereby the explosive limits of belowground structures can be determined.

Radford AAP TNT Line Accident

An accidental detonation took place in the Nitration and Purification Building (Building 9502) in Line A of the TNT Manufacturing Facility at Radford AAP. At the time of the incident, the quantity of explosive contained in the building was estimated to be equivalent to 3,600 kg to 5,500 kg (8,000 to 12,000 lbs) of TNT.

Building 9502 was a partially belowground structure; the aboveground portion was barricaded on all four sides by an earth-mounded barricade (Fig 58). The earth mound and the earth around the belowground portion of the structure (Fig 59) were supported by reinforced concrete walls. The intersecting walls formed the rectangular shaped structure having plan dimensions of 19.51 m (64 ft) by 17.37 m (57 ft). The overall height of the building was 9.14 m (30 ft). The aboveground barricade portion was 3.96 m (13 ft) high with the belowground portion being recessed in two levels. The floor of the basement level was located 2.59 m (8 ft - 6 in.) below the grade and the floor of the pit was located 3.05 m (10 ft) below that of the basement. The wall thickness varied from 0.31 m (1 ft) at the top of the barricade to 0.58 m (1 ft 10-3/4 in.) at the basement floor level. The pit

walls had a constant thickness of 0.31 m which was same as the top of the barricade retaining wall.

As described in Reference 4, the total building was destroyed (Fig 60) with only a crater remaining after the explosion. Equipment and the concrete retaining wall fragments, some of which as large as 23 kg (50 lbs), were found as far away as 915 m (3,000 ft).

The damage produced by this accident was larger than the damage sustained by Cell No. 2 after the performance of Test No. 10. The total quantity of explosive used in the two tests (Nos. 8 and 10) was approximately equal to a full-scale equivalent of 5,500 kg (12,000 lbs). This quantity was in the order of magnitude of the upper limit of the quantity of explosive estimated to be in Building 9502. However, it should be noted that Building 9502 did not have an apron at the top of the walls similar to the test cell used in Test No. 8, also, Building 9502 had a wooden roof which supported air handling equipment and the thickness of its walls in the upper half of the structure was equal to approximately one-third the thickness of full-scale version of the test structure. Therefore, the relative explosive capacity of the operating building was probably less than that of the test structure. Based on this reduced capacity and the comparative damage to the test and operating structures, it is estimated that the explosive capacity of Building 9502 was less than the estimated lower limit of the explosive quantity contained within the building, and was probably in the order of 2,700 kg (6,000 lbs). It may be further noted that the explosive within Building 9502 was distributed throughout the building rather than being concentrated as in the test. Distribution of the explosives usually has a tendency to reduce the TNT equivalency of the explosion resistant capacity of the structure; which was probably the case in the Radford incident.

Lone Star AAP 105 mm Projectile Melt/Pour Facility

The 105 mm Projectile Melt/Pour Facility at the Lone Star AAP is presently being modernized to reduce production costs and achieve increased safety of operation. This facility utilizes an automatic explosive flake inspection system; which was developed at the Iowa AAP as a part of Picatinny Arsenal's munitions production base modernization and expansion program for DRSAR and DRCPM. The two inspection systems needed to achieve the required production rate are housed in a two-story building (Building No. E-125). The lower portion of the structure is constructed below the ground; whereas the building content on the upper level is protected from explosions in the adjoining buildings by a laced

reinforced concrete wall at one side of the building and by interconnected blast resistant structural steel beams, columns and corrugated roof panels and metal siding on the other sides. An interior laced reinforced concrete wall was used to separate the two systems, and thereby prevent propagation of explosion from one system to the other.

Figures 61 and 62 illustrate the plan layout and the vertical section, respectively.

The blast wall separating the two systems was designed to withstand the blast output of 1,360 kg (3,000 lbs) of TNT with the major portion of the explosive in each cell being located below the ground. Although the explosive within the belowground portion of the building was distributed and thereby resulted in a TNT equivalency somewhat higher than that produced by the charge arrangement used in the tests, the total quantity of explosive contained within the building is much less than that used in the full scale version of the cell of Test Nos. 8 and 10 (Cell No. 2). Therefore, in the event of an explosion within the Building E-125, it may be expected that the belowground portion of the building in addition to the laced concrete walls will survive the effects of the blast output without failure.

Single Revetted Barricades Tests

In conjunction with this series of tests, a second series of explosion tests (Ref 5) was performed to evaluate the blast capacities of single revetted earth mounded barricades. The results of this series seem to verify the previously stated result of this study that earth-fill behind the concrete retaining wall provides a significant increase in the capacity of unlaced reinforced concrete walls to resist the blast overpressures from an explosion. To illustrate this feature, consider the setup and results of the earth-mounded barricade test series as described below.

Each of the two walls of the revetted barricade tests was a reinforced concrete cantilever wall which was 2.44 m (8 ft) high, 4.88 m (16 ft) long and 0.25 m (10 in.) thick. Support for each wall was provided by a 1.78 m (5 ft - 10 in.) wide reinforced concrete slab which was cast monolithically with the wall. The concrete slab, which extended the full length of the wall, had a thickness of 0.31 m (1 ft). Located to the rear of each wall was an earth-mound; the shape of which conformed to the requirements of Reference 6, i.e., the mound height was equal to that of the wall, the section of the mound adjacent to the wall was flat for a distance of 0.91 m (3 ft) and, beyond

the flat section the mound tapered to the ground on a 2 to 1 slope (Fig 63).

The first wall was tested three times using explosive weights of 23 kg (50 lbs), 68 kg (150 lbs) and 113 kg (250 lbs). All charges in these tests were positioned 1.22 m (4 ft) from the wall. A fourth test was performed on the second wall using an explosive weight of 227 kg (500 lbs) positioned 0.91 m (3 ft) from the wall.

Figures 64 and 65 illustrate the damage to the two walls at the completion of the test series. Wall No. 1 sustained severe damage but still remained intact while Wall No. 2 was considered to have failed. In case of the first wall, the rebound afforded by the soil during each test was significant and thereby limited the magnitude of the permanent deflections of the wall after each test. That is to say, the sum of the permanent displacements obtained from the individual tests was less than that would have been produced by the combined weight of explosive of 204 kg. In the case of Wall No. 2, however, the initial velocity of the wall produced by the explosive output was of sufficient magnitude to overpower the resisting capacity of the system (concrete and soil), and thereby produced soil displacements large enough to make the wall fail.

The severe damage to Wall No. 1 and the failure of the second wall occurred at the top of each wall immediately adjacent to the explosion. If a concrete support at the top of the wall had been used similar to the concrete aprons of the belowground test structures, then it may be expected that the blast capacities of both walls would have been increased. With the use of the top supports, the effects of the blast loads acting on the part of each wall immediately in front of the explosion would have been transferred to other portions of the walls where the blast loads were less intense. This redistribution of stresses would have reduced deflections of the center of the walls, and thereby, reduce the amount of damage to the overall structures.

A comparison of the results of the barricade and belowground structure tests indicated that although Wall No. 2 of the former test series was considered to have failed, the damage it sustained was considerably less than that of Cell No. 2 of the latter tests. This greater damage occurred even though the charge weight was larger and the separation distance was smaller in the barricade than in the cell test. These results are indicative of the comparative explosive capacities of 2,700 to 3,600 kg for the below-ground structure and 3,600 to 4,500 kg (8,000 to 10,000 lbs) as reported in Reference 5 for the earth bermed walls.

CONCLUSIONS AND RECOMMENDATIONS

Conclusions

The results of these tests indicate that when subjected to the effects of an internal explosion, belowground structures with no roof will have an upper explosive limit beyond which the structure will fail and thereby become a source of secondary fragments. This capacity is less than that which was considered in most past facility designs. Also, belowground structures which are provided with a support system for the top of the walls similar to the concrete aprons used in these tests will demonstrate an increase in blast resistant capacity above those belowground structures where the top support is not furnished. This increase in capacity will be a significant factor to be considered in a belowground structure's design.

For a belowground structure which has overall dimensions equal to three times those of each test structure, the upper explosive limit will be in the order of 2,700 to 3,600 kg (6,000 to 8,000 lbs) of H.E. when the explosive charge is located at the geometric center of the structure and the upper portions of the walls are supported with a system similar to the concrete aprons used in the tests. Belowground structures of similar design and with light frangible roofs will have explosive capacities in the same order of magnitude of those stated above. However belowground structures without the aprons and/or with multiple charges will have explosive capacities less than those stated above.

Recommendations

It is recommended that additional tests be performed to determine quantitative criteria for the design of reinforced concrete belowground structures and to develop other structural configurations of belowground structures for large explosive quantities.

REFERENCES

1. "Structures to Resist the Effects of Accidental Explosions, (with Addenda)", TM 5-1300/NAVFAC P-397/AFM 88-22, Department of the Army, the Navy and the Air Force, Washington, D.C., June 1969.
2. "Moisture - Density Relations of Soils Using 10-lb (4.5 kg) Hammer and 18 - in. (457 mm) Prop", American Society for Testing and Material, ASTM Designation D 1557-70, Annual Book of ASTM Standards, 1975.
3. Warnecke, C.H., "Support Test for Evaluation of a Belowground Cell", Document No. DPG-DR-C995A, U.S. Army Dugway Proving Ground, Dugway, Utah, December 1975.
4. "Overpressure Effects on Structures", HNDTR-75-23-ED-SR, U.S. Army Corps of Engineers, Huntsville Division, 1 February 1976.
5. Dobbs, N., et al, "Blast Capacity Evaluation of Single Revetted Barricades", Technical Report 5009, Picatinny Arsenal, Dover, New Jersey, September 1976.
6. "Safety Manual", Army Materiel Command Regulation AMCR 385-100 Headquarters, U.S. Army Materiel Command, Washington, D.C., April 1970 (with 14 October 1971 and 12 September 1974 changes).

Table 1
Charge properties and instrumentation

Test No.	Cell No.	Charge Wt. ^a		Full Scale Equivalent		Deflection Gages	Hand Measurements	Instrumentation		Camera Coverage	Still
		kg	lbs	kg	lbs			None	None		
1	1	0.9	2	24	54	Yes	None	None	None	None	Yes
2	1	2.7	6	73	162	Yes	None	None	None	None	Yes
3	1	2.7	6	73	162	Yes	None	None	None	None	Yes
4	1	11.2	25	302	675	Yes	Yes	Yes	Yes	Yes	Yes
5	1	19.5	43	527	1161	Yes	Yes	Yes	Yes	Yes	Yes
6	1	28.8	63	778	1701	Yes	Yes	Yes	Yes	Yes	Yes
7	1	36.9	81	996	2187	Yes	Yes	Yes	Yes	Yes	Yes
8	2	86.7	191 ^b	2341	5157	Yes	Yes	Yes	Yes	Yes	Yes
9	1	68.0	150 ^c	1836	4050	None	None	None	None	Yes	Yes
10	2	113.0	250 ^c	3051	6750	None	None	None	None	None	Yes

^aExcept as noted, each charge consists of Composition E and is cylindrical in shape with an aspect ratio of one.

^bTwo cylindrical Composition E charges placed side by side and weighing 43.4 kg (96 lbs) and 43.2 kg (95 lbs).

^cComposition C-4 blocks arranged in a cube.

^dAssuming test cells were one-third scale models.

Table 2
Summary of permanent deflections
(hand measurement)

Location	Test Number 4 ^b				Test Number 5				Test Number 6				Test Number 7				Test Number 8 ^c			
	North Wall	South Wall	West Wall	North Wall	North Wall	South Wall	West Wall	North Wall	South Wall	West Wall	North Wall	South Wall	West Wall	North Wall	South Wall	West Wall	North Wall	South Wall	West Wall	
A-1	3	2	2	6	8	3	-6	13	-3	-3	22	25	19	29	22	13	32	64	124	
B-1	0	10	3	13	10	30	16	38	60	57	64	60	41	38	45	156	118	187		
C-1	14	13	10	10	10	16	32	22	38	64	54	60	41	35	41	46	149	140	219	
D-1	10	10	11	3	13	30	25	25	22	60	54	51	35	41	46	149	133	203		
E-1	0																			
A-2	2	5	2	-3	11	5	-3	13	0	3	22	25	19	29	29	51	13	32		
B-2	13	16	13	19	35	19	22	32	32	60	46	60	41	30	38	45	108	64	124	
C-2	25	27	19	43	52	38	46	60	60	51	48	67	51	35	41	46	156	118	187	
D-2	22	25	19	32	64	41	48	67	67	51	45	73	51	32	35	48	133	133	203	
E-2	13	16	13	19	54	41	45	73	73	51	45	73	51	32	35	48				
A-3	2	6	2	-2	13	8	-3	16	0	0	19	22	29	22	29	57	18	41		
B-3	14	18	13	24	35	16	22	38	38	60	45	60	41	48	48	108	73	149		
C-3	32	32	25	41	57	35	45	60	45	48	70	48	76	48	48	48	140	125	216	
D-3	25	32	21	41	67	45	48	70	48	76	45	76	48	35	38	48	140	149	241	
E-3	13	19	16	32	57	41	45	76	48	76	48	76	41	35	38	48	108	133	216	
A-4	3	5	3	-3	11	6	-3	16	-3	0	19	22	16	16	19	35	49	13	35	
B-4	16	19	13	19	32	19	25	38	38	64	48	64	41	35	38	48	140	97	113	
C-4	27	25	22	46	57	29	48	64	64	51	70	51	41	35	41	48	143	122	200	
D-4	22	24	25	41	57	32	51	64	64	41	64	41	38	41	48	143	143	229		
E-4	10	19	14	32	51	32	41	64	64	41	64	41	38	41	48	108	137	203		
A-5	0	5	2	-3	6	3	-10	10	-3											
B-5	6	6	6	16	25	13	29	29	29	51	35	51	38	35	45	32				
C-5	8	8	10	35	35	13	35	35	35	51	38	51	38	35	45	32				
D-5	6	13	8	16	19	10	10	10	10	41	38	41	38	29	29					
E-5	-3	13	3																	

^aPermanent deflection is the relative permanent deflection unless noted otherwise.
All deflections are given here in mm.

^bDeflections given are total permanent deflections up to and including Test No. 4.

^cThis is the first test in Cell No. 2 and therefore deflections given are the total deflections.

Table 3
Summary of maximum and permanent deflections

Test No.	Gage No. ^a	Gage Measurements		Hand Measurements ^b		Remarks
		Maximum Deflections	Permanent Deflections	Permanent Deflections	Hand Measurements	
		in.	in.	in.	in.	
1 thru 3	all					
	1	14	0.53	14	0.53	10
	2	14	c	c	16	0.39
	3		c	c	17	0.63
	4		c	c	31	0.67
	5	45	1.79	24	0.95	1.22
	6	39	1.52	19	0.76	0.75
4	7		c	c	18	0.71
	1				17	0.67
	2	66	c	c		
	3	40	2.60	58	2.30	1.59
	4		1.58	40	1.58	1.06
	5	86	c	c	30	1.18
	6	44	3.38	55	41	1.61
5	7	60	1.75	44	2.17	1.14
	1				29	1.54
	2				39	1.38
	3				35	
	4					
	5					
	6					
6	7					
	1		c	c	13	0.51
	2		c	c	32	1.26
	3		c	c	33	1.30
	4		c	c	46	1.81
	5	65	2.57	29	1.15	1.77
	6		c	c	45	1.77
7	7	69	2.70	61	2.40	1.81
	1					
	2	26	1.01	d	15	0.59
	3	27	1.07	d	20	0.79
	4	33	1.30	d	20	0.79
	5	57	2.24	d	40	1.57
	6	36	c	c	32	1.26
7	7	50	1.42	c	33	1.30
					35	1.38

Gage Numbers 8 and 9 were not used in any test. bHand measurements can vary by ± 1 mm ($\pm 1/16$ in.). These measurements were obtained from deflection contours by interpolation at the locations of the gages. deflection fixture disconnected. Drive base was too short to give permanent deflection. Broken electrical connection. Gage not used.

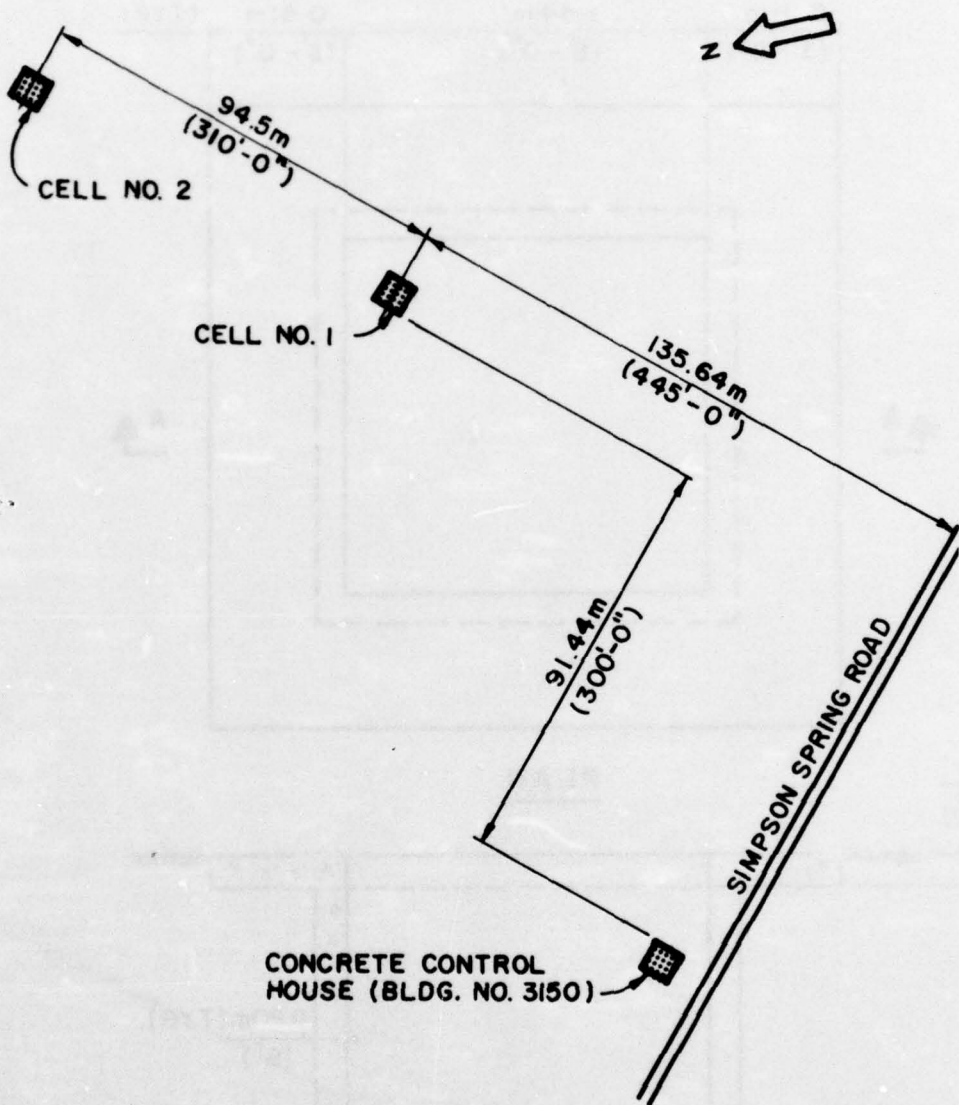


Fig 1 White Sage Flat Test Site

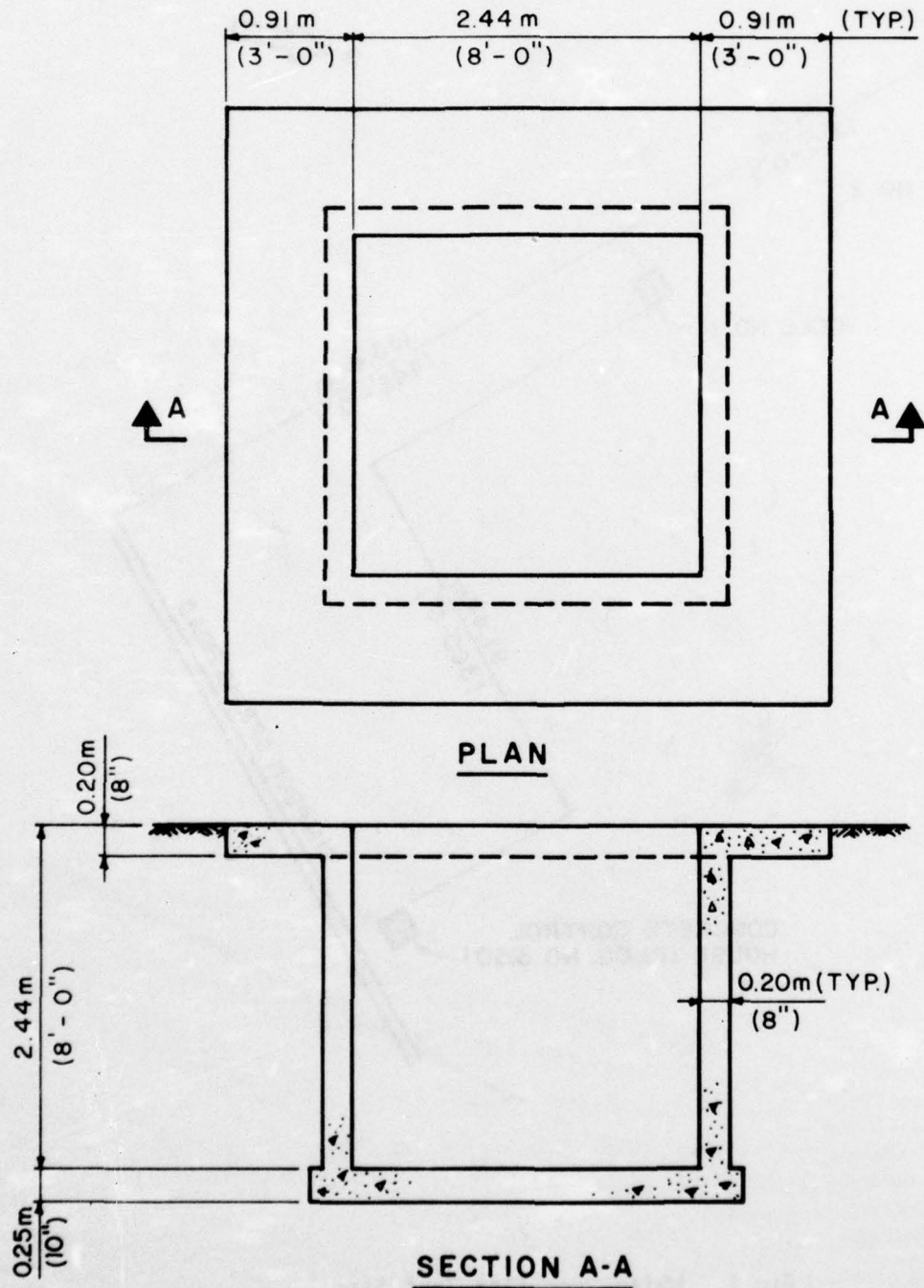


Fig 2 Test structures layout

BEST AVAILABLE COPY

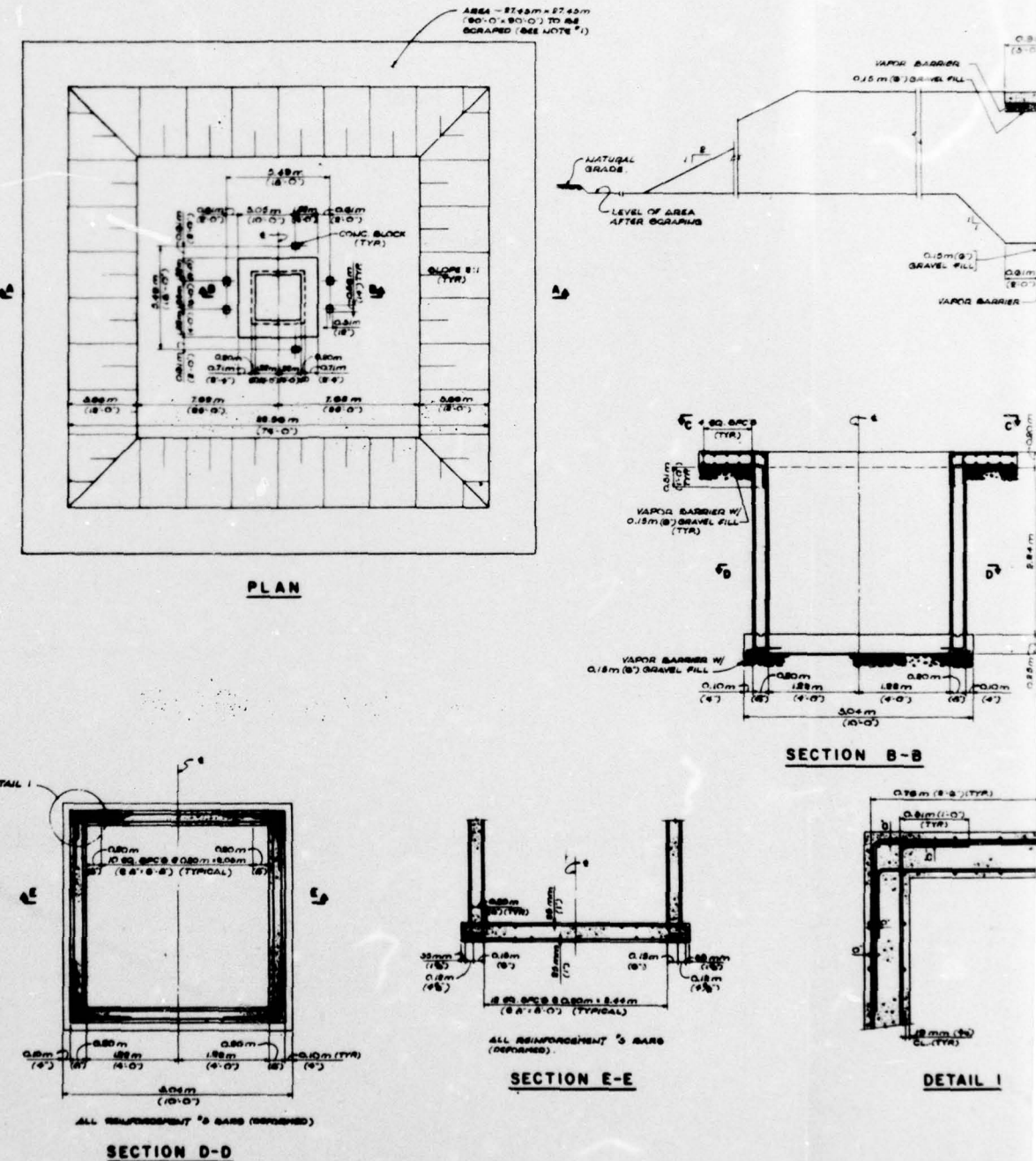
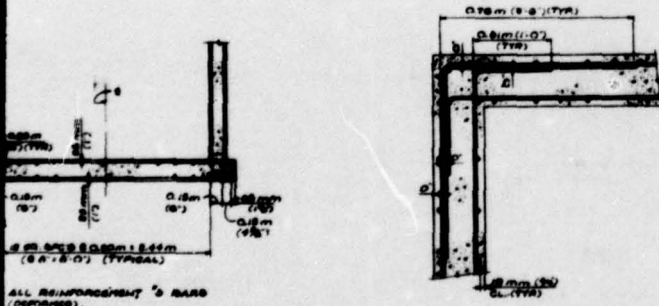
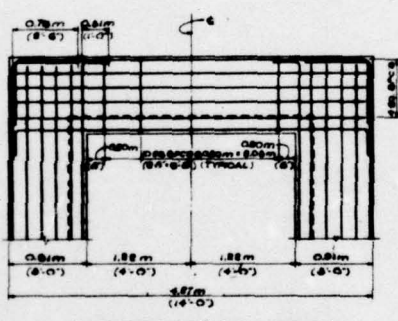
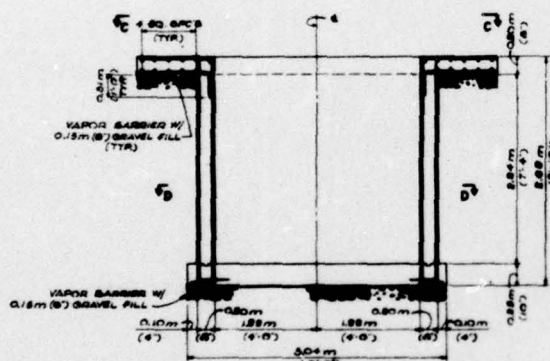
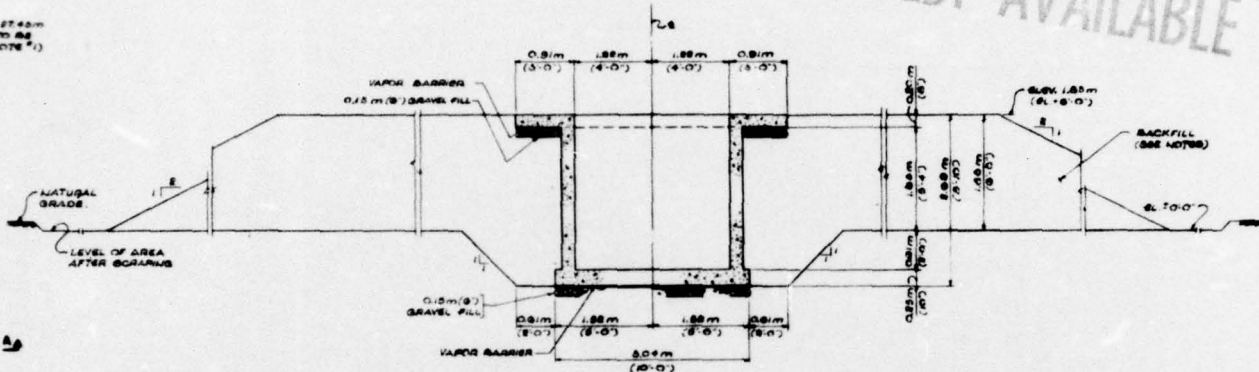


Fig 3 Structural details of test struct

BEST AVAILABLE COPY



DETAIL I

NOTES:

1. AN AREA OF APPROXIMATELY 27.48m x 27.48m (90'x90') OF THE SITE SHALL BE STRIPPED OF ALL VEGETATION AND LOOSE SOIL, BY DORING AND THE SURFACE OF THE AREA.
2. BACKFILL SHALL BE A WELL GRADED SAND-GRAVEL MATERIAL WITH A MAXIMUM PARTICLE SIZE OF 51MM (2"). THE BACKFILL MATERIAL SHALL HAVE AT LEAST 95% RETAINED ON THE 1/4 INCH AND NO FINEER THAN 10%, PRACTICALLY THE '60 GRAVE'.
3. BACKFILL SHOULD BE PLACED IN UNIFORM LAYERS NOT MORE THAN 0.60m (2') IN THICKNESS AND COMPACTED TO AT LEAST 95% OF MAXIMUM DRY DENSITY AS DETERMINED BY ASTM C-167.
4. BACKFILL OPERATION IS TO BE COORDINATED WITH PLACEMENT OF INSTRUMENTATION AND TEST.
5. ALL REINFORCING BARS SHALL COMPLY TO SPECIFICATIONS FOR DEFORMED STEEL BARS, ASTM DESIGNATION A615, GRADE 60.

Fig 3 Structural details of test structures

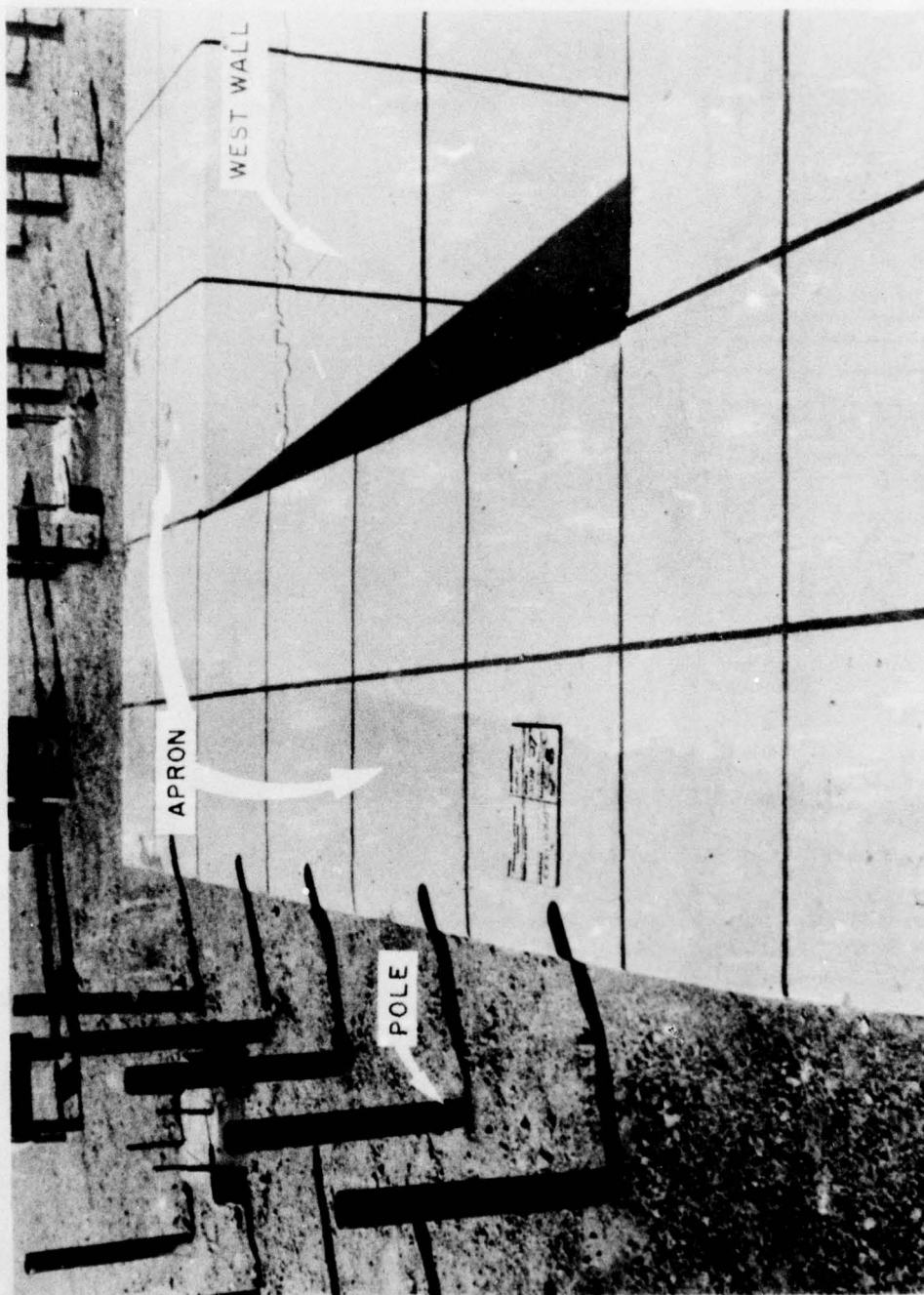


Fig 4 Top view of concrete apron

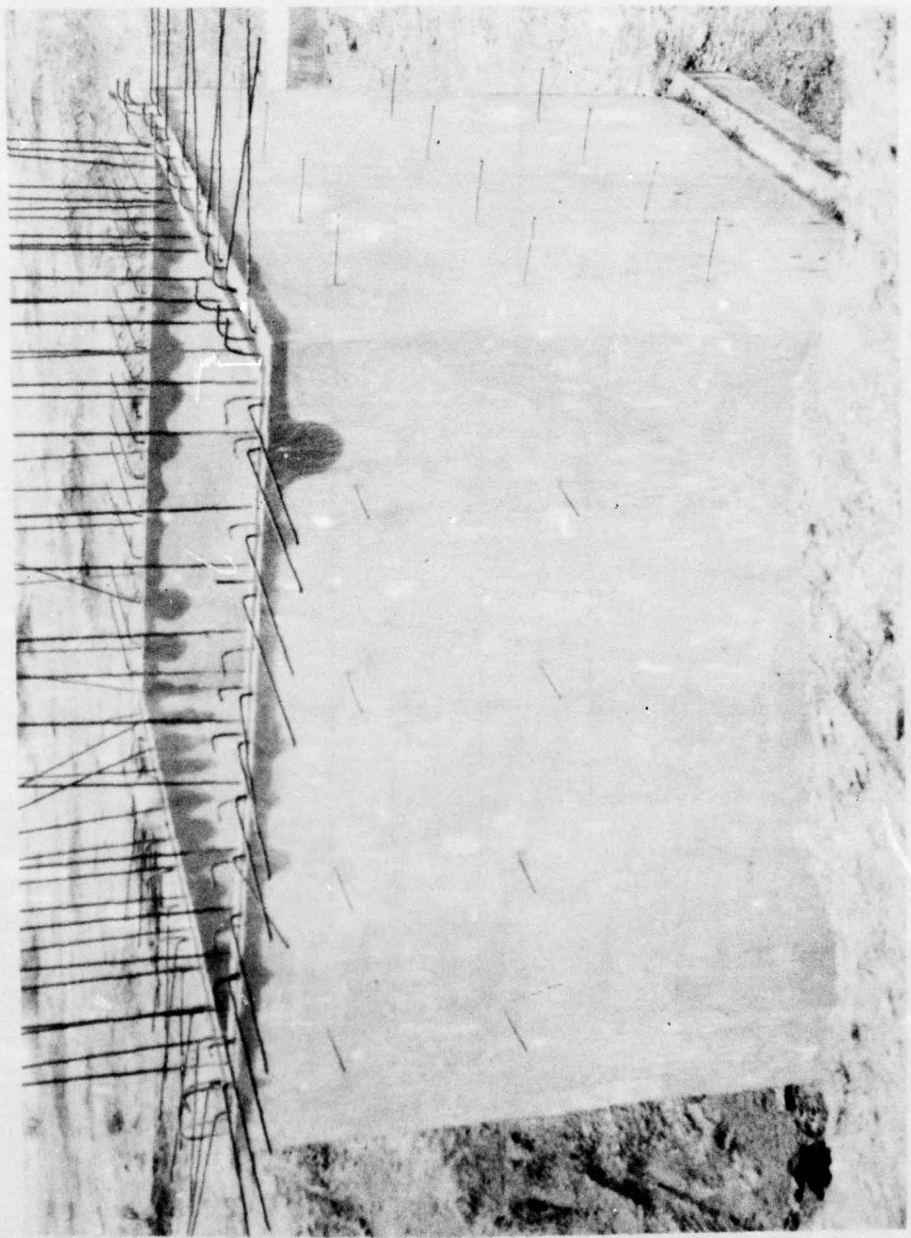
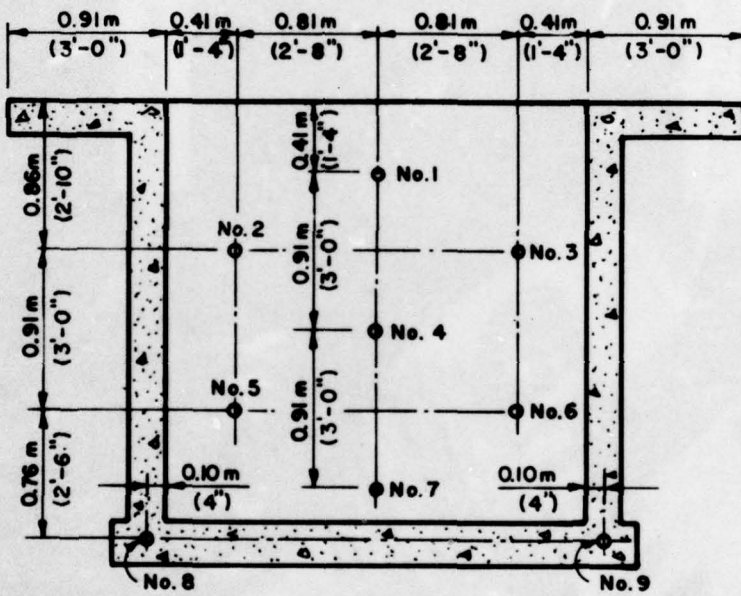


Fig 5 Construction phase of test structures



Fig 6 Typical setup for Composition C-4 charges



SECTIONAL ELEVATION - NORTH WALL

Fig 7 Attachment location of deflection gages

BEST AVAILABLE COPY

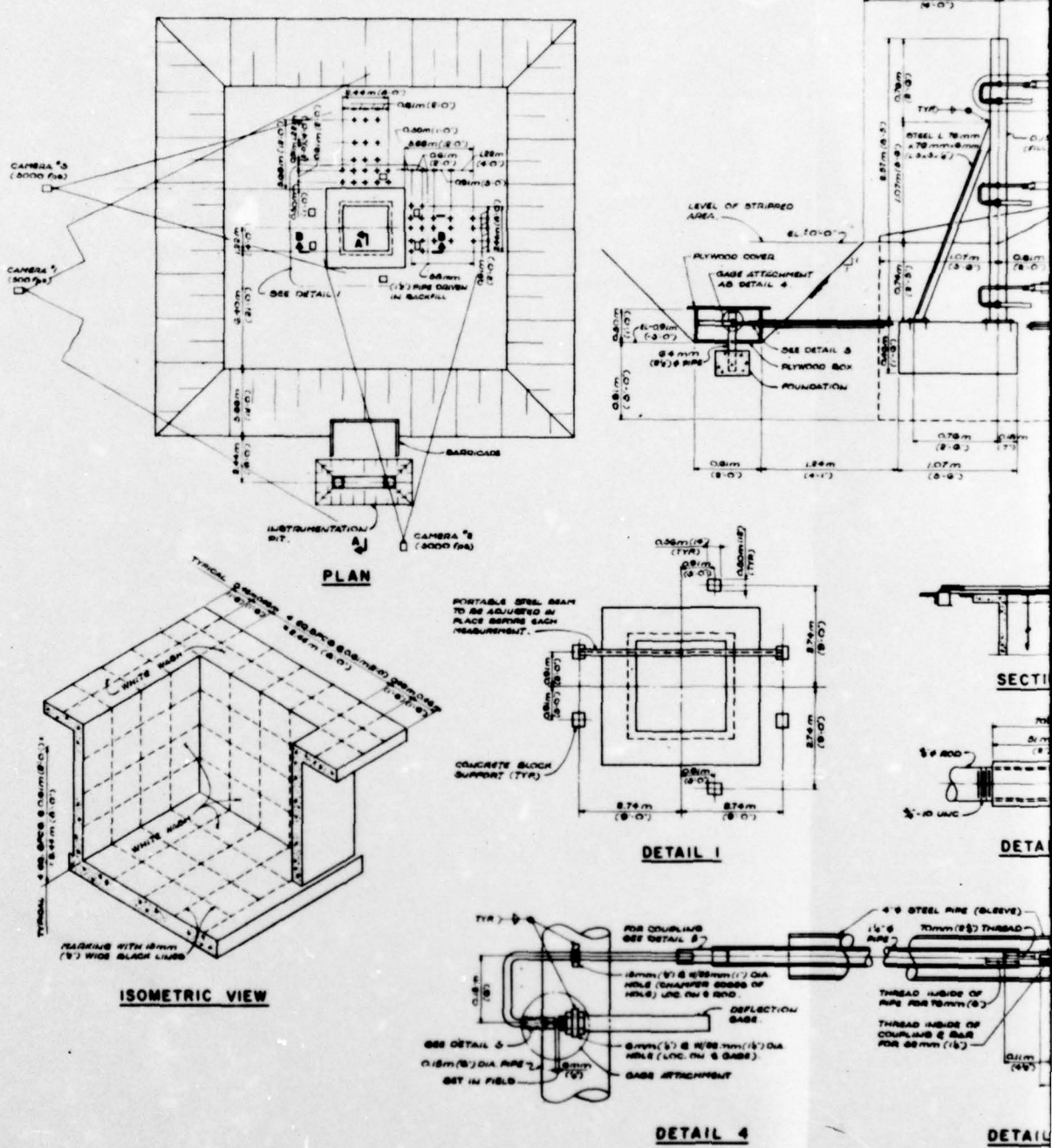


Fig 8 Instrumentation details

BEST AVAILABLE COPY

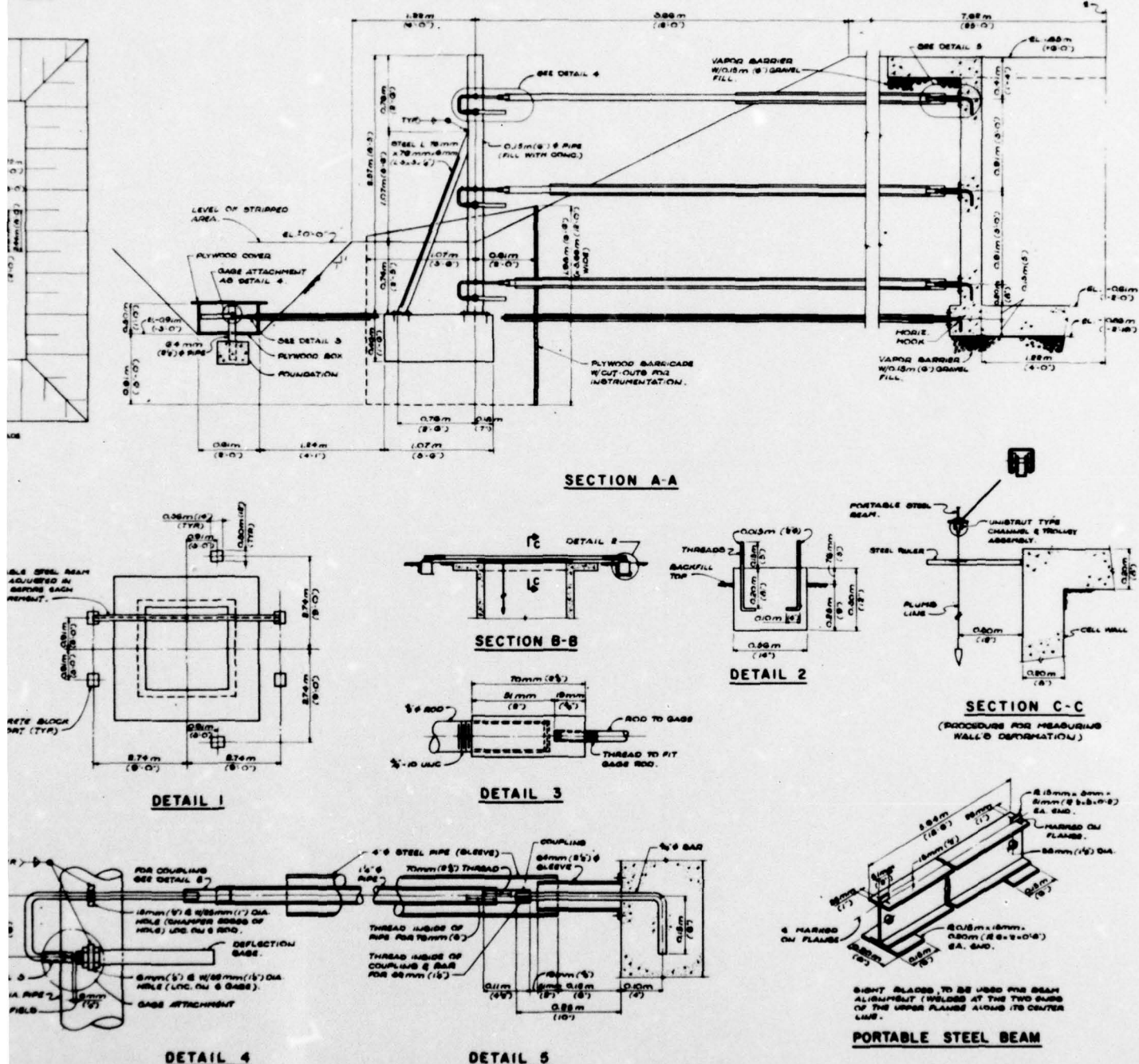
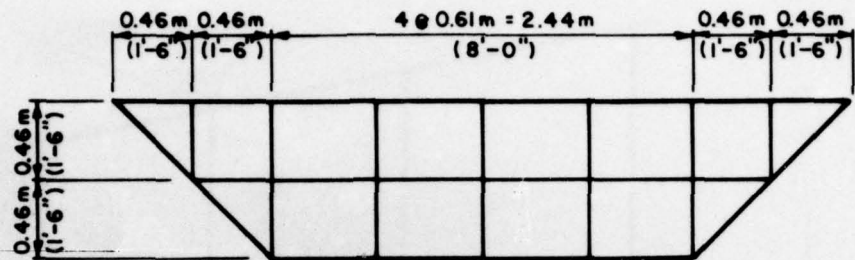
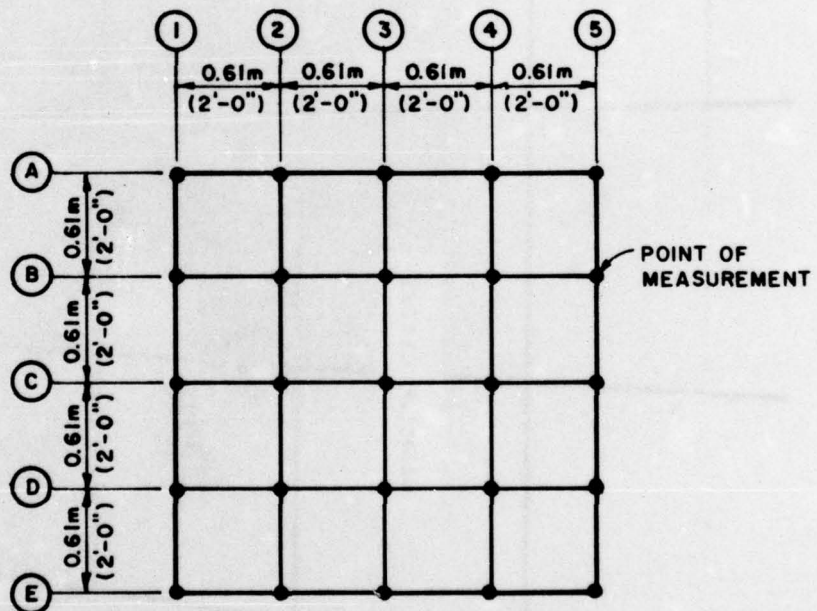


Fig 8 Instrumentation details



APRON PLAN



INTERIOR WALL ELEVATION

Fig 9 Hand measurement and damage survey grid

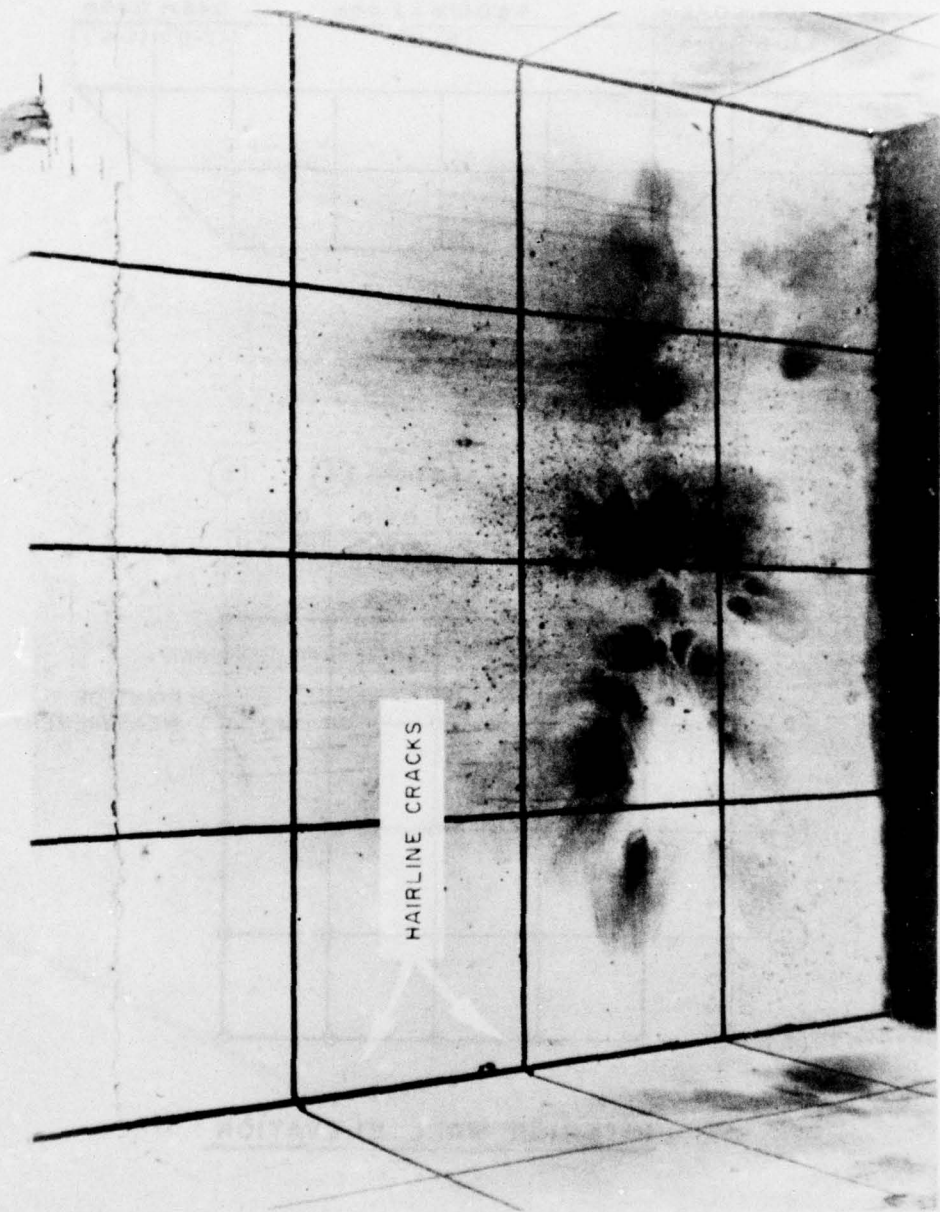


Fig 10 Post-test view of Cell No. 1 west wall (Test No. 2)

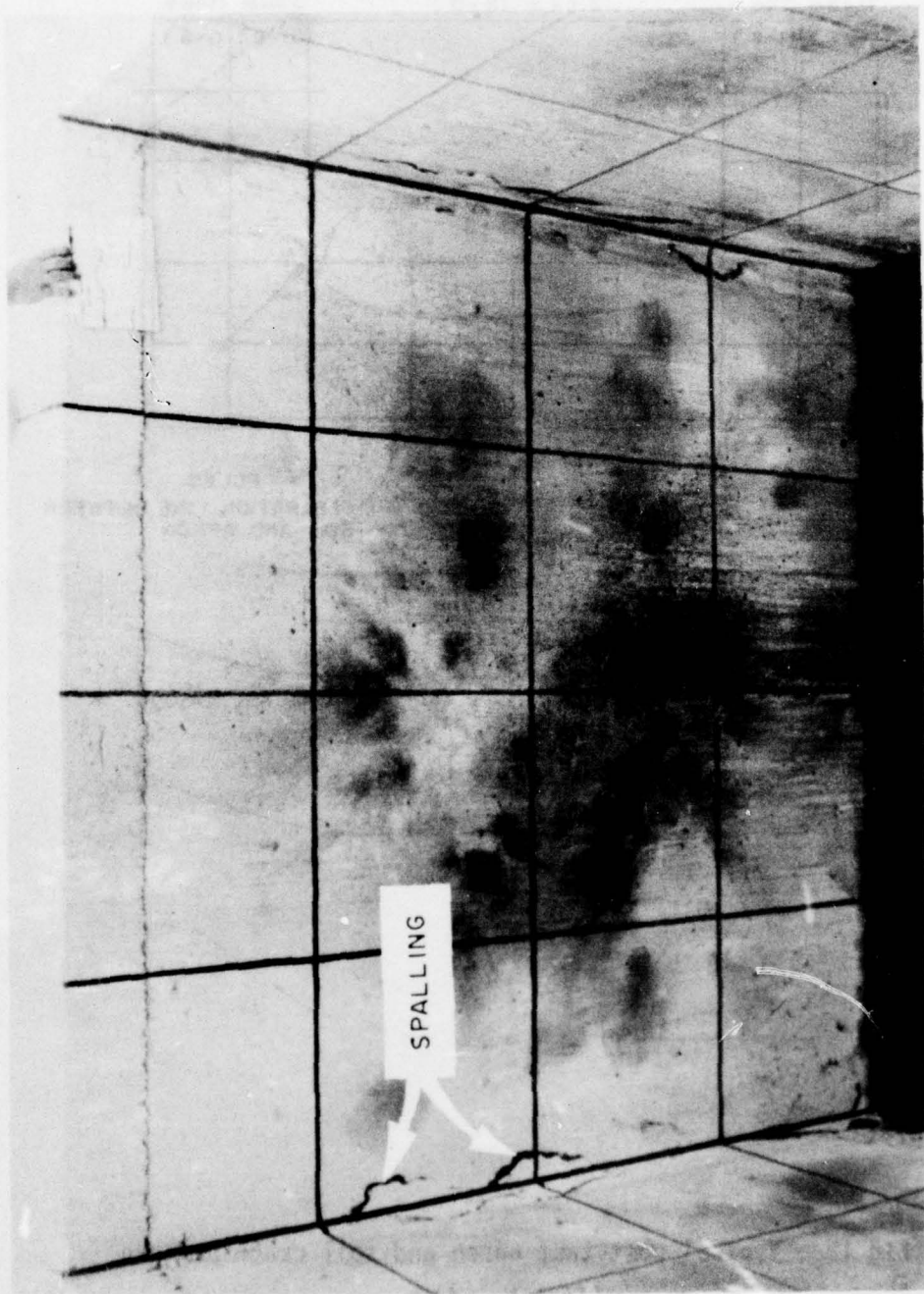


Fig 11 Post-test view of Cell No. 1 west wall (Test No. 3)

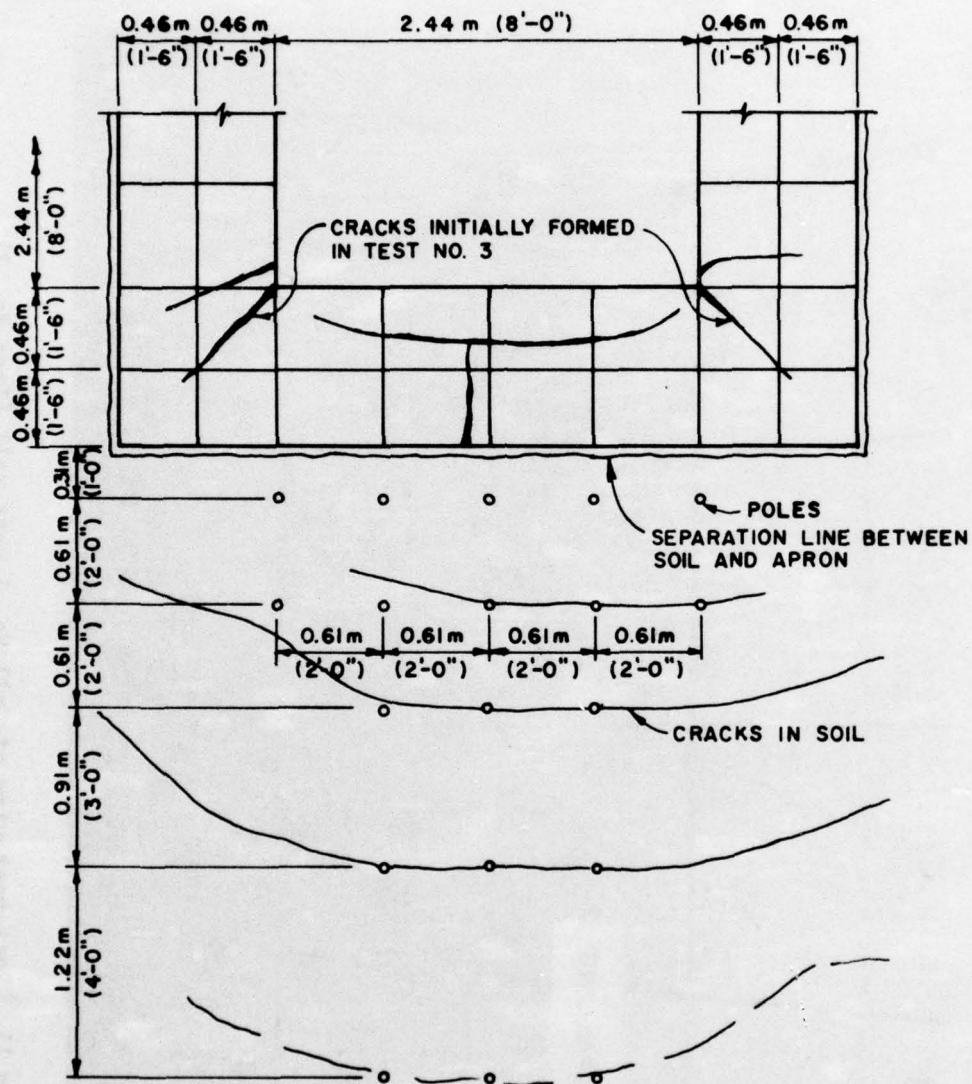


Fig 12 Typical post-test apron and soil crack pattern
(Test No. 4)



Fig 13 Post-test damage to Cell No. 1 east wall (Test No. 4)

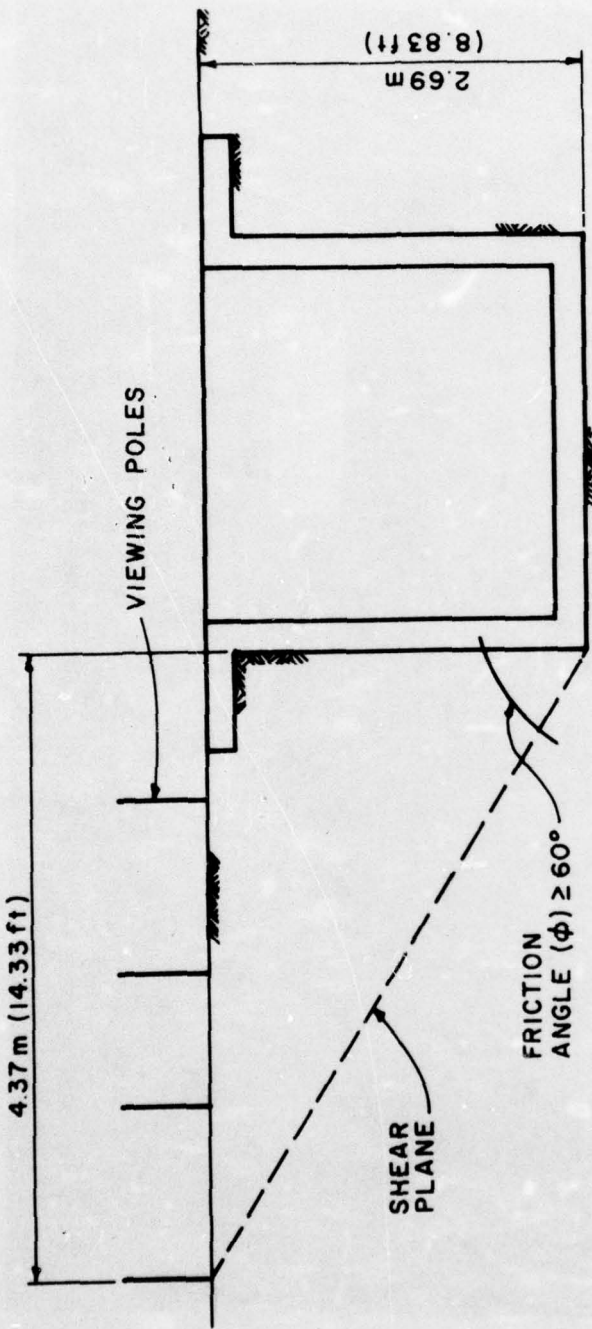


Fig 14 Shear plane in soil

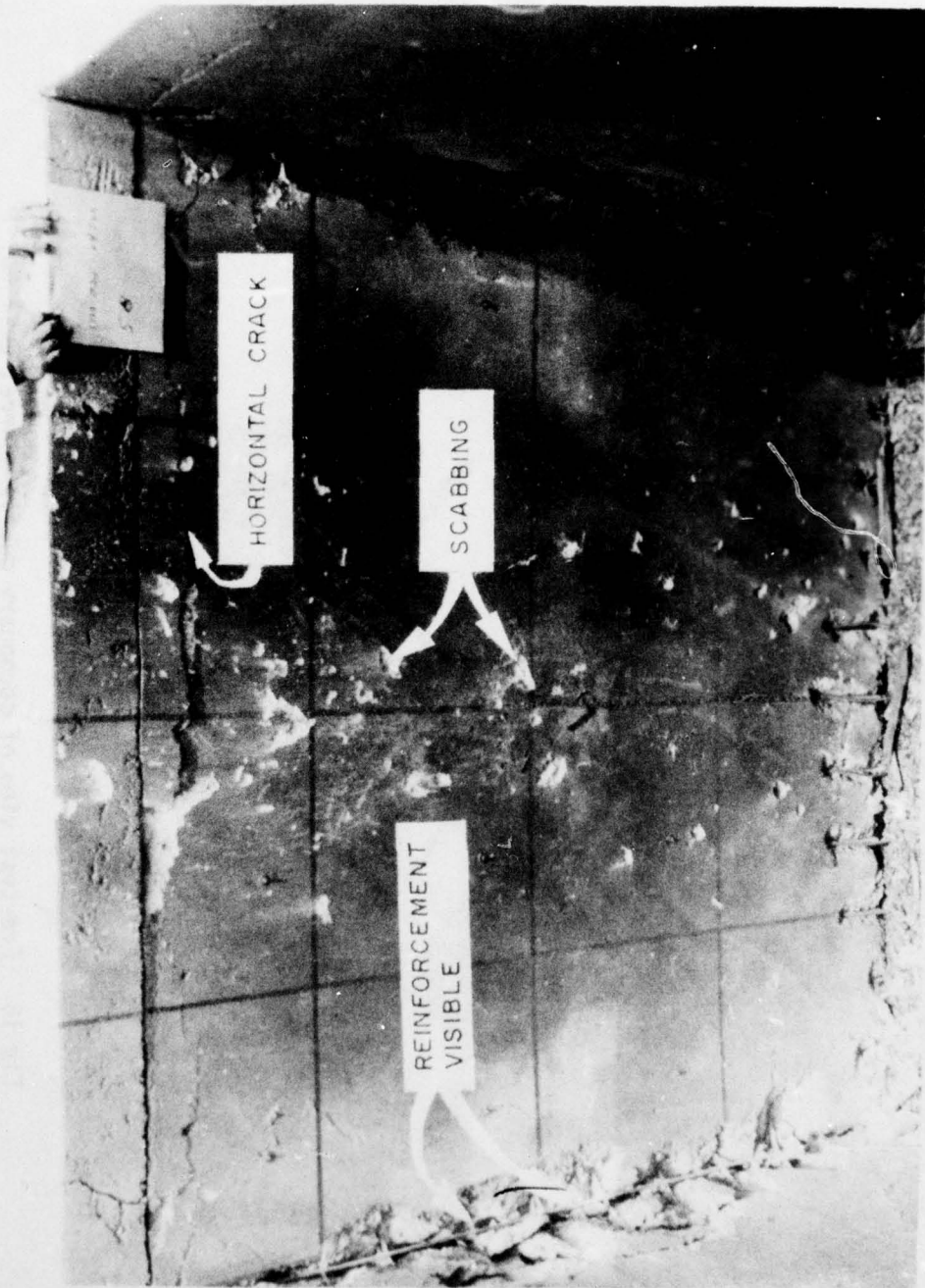


Fig 15 Post-test damage to Cell No. 1 east wall (Test No. 5)

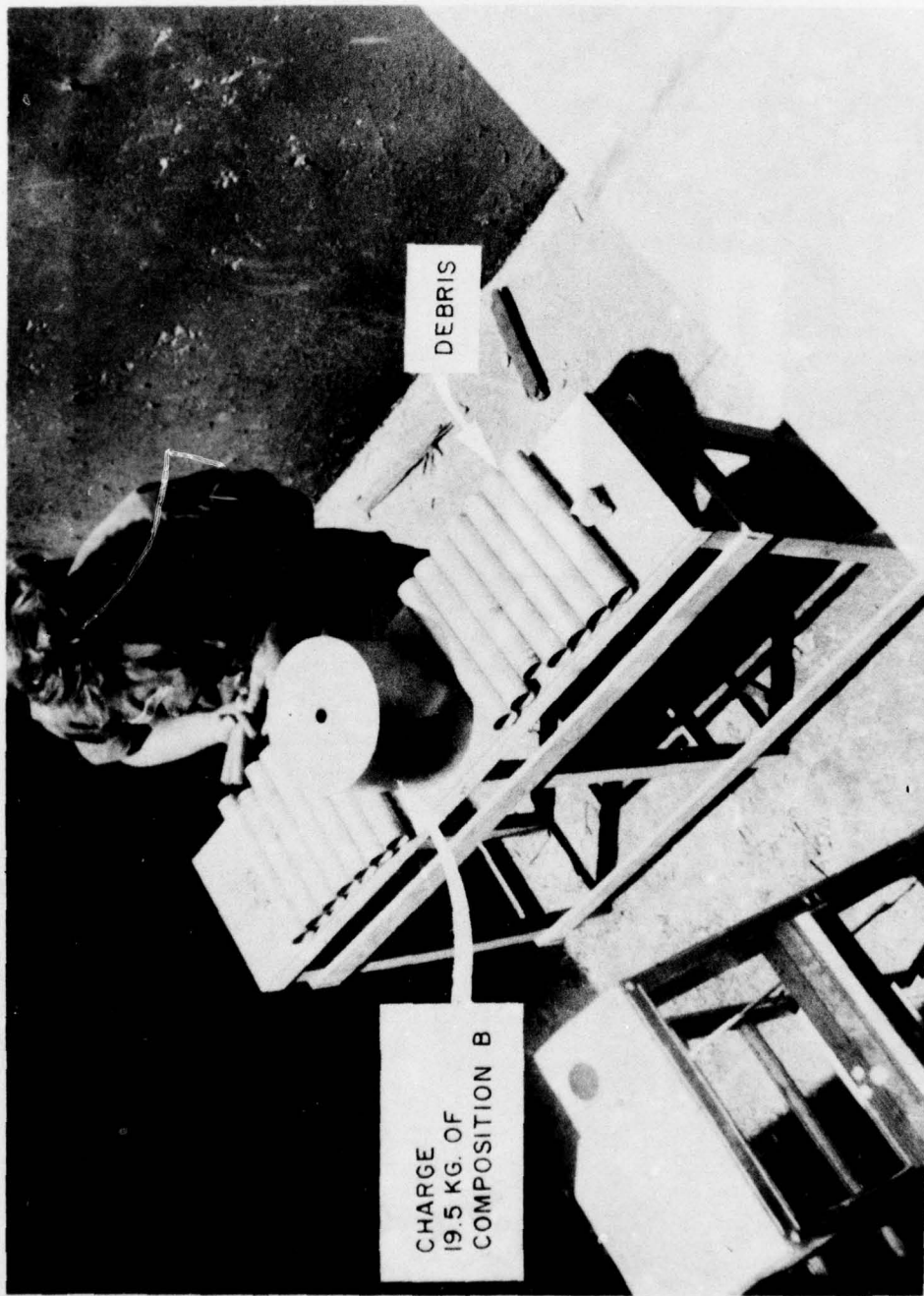


Fig 16 Pre-test view of secondary debris source, Cell No. 1
(Test No. 5)



Fig 17 Post-test damage to Cell No. 1 apron (Test No. 5)

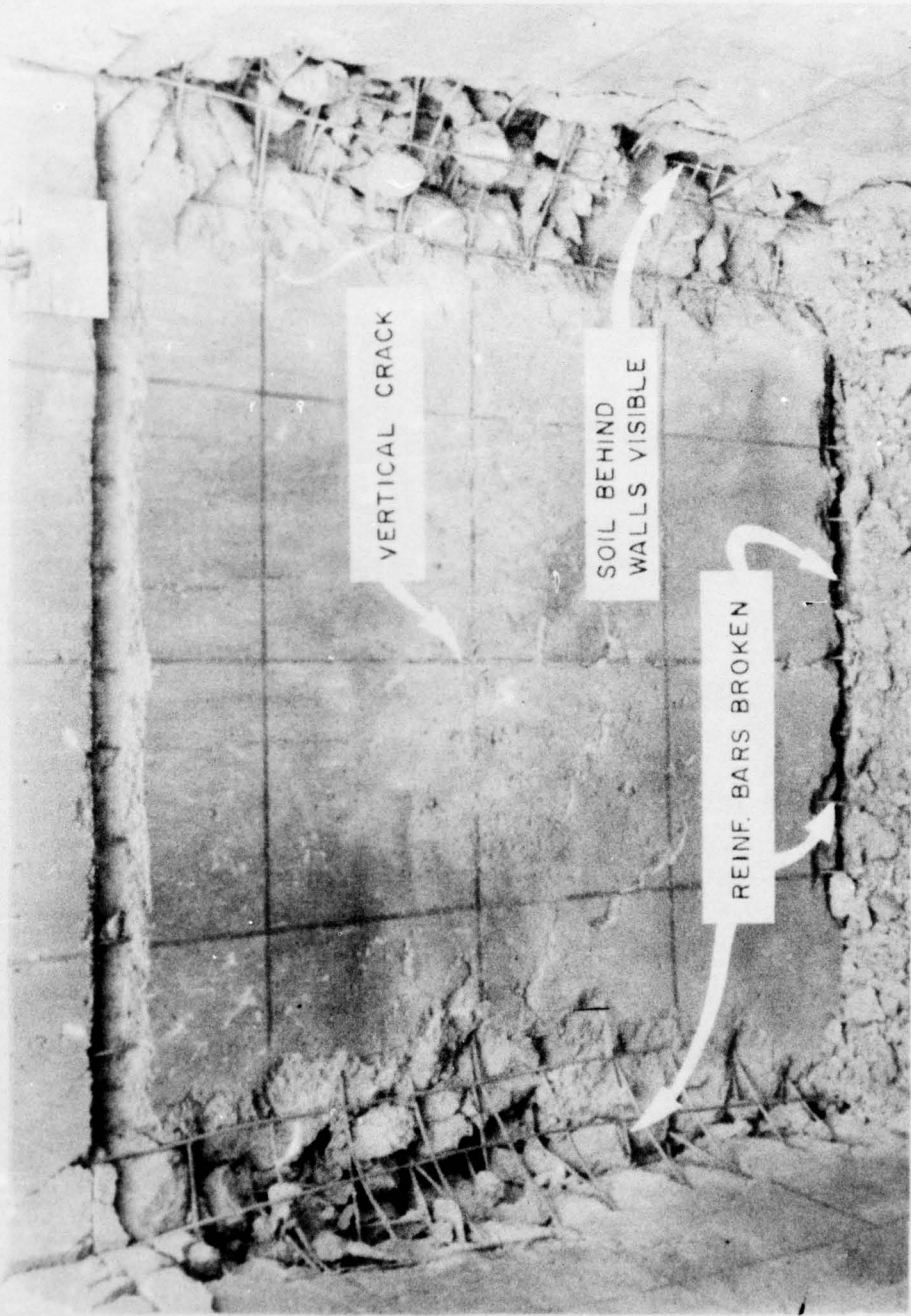


Fig 18 Post-test damage to Cell No. 1 north wall (Test No. 6)

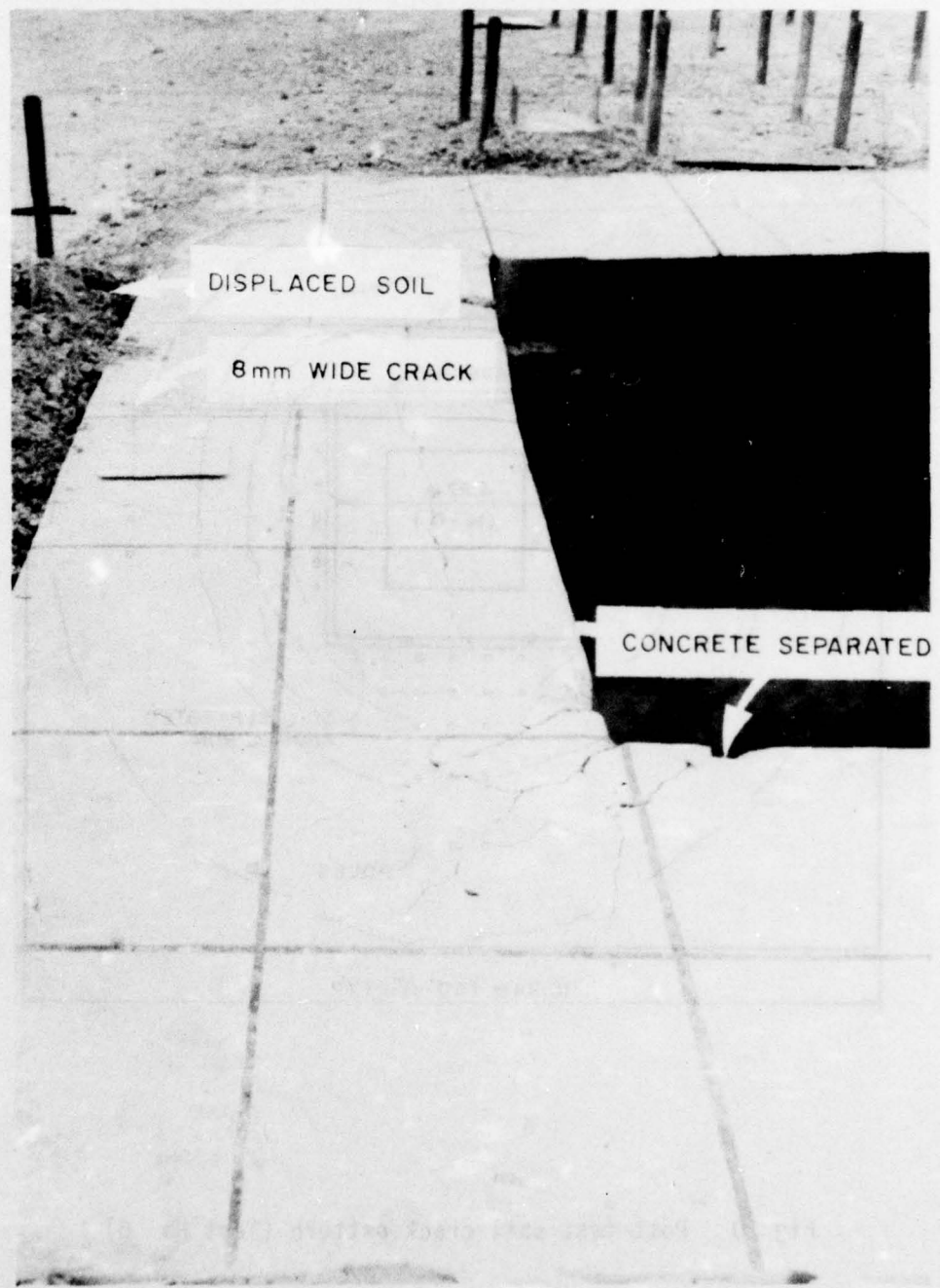


Fig 19 Post-test damage to Cell No. 1 apron (Test No. 6)

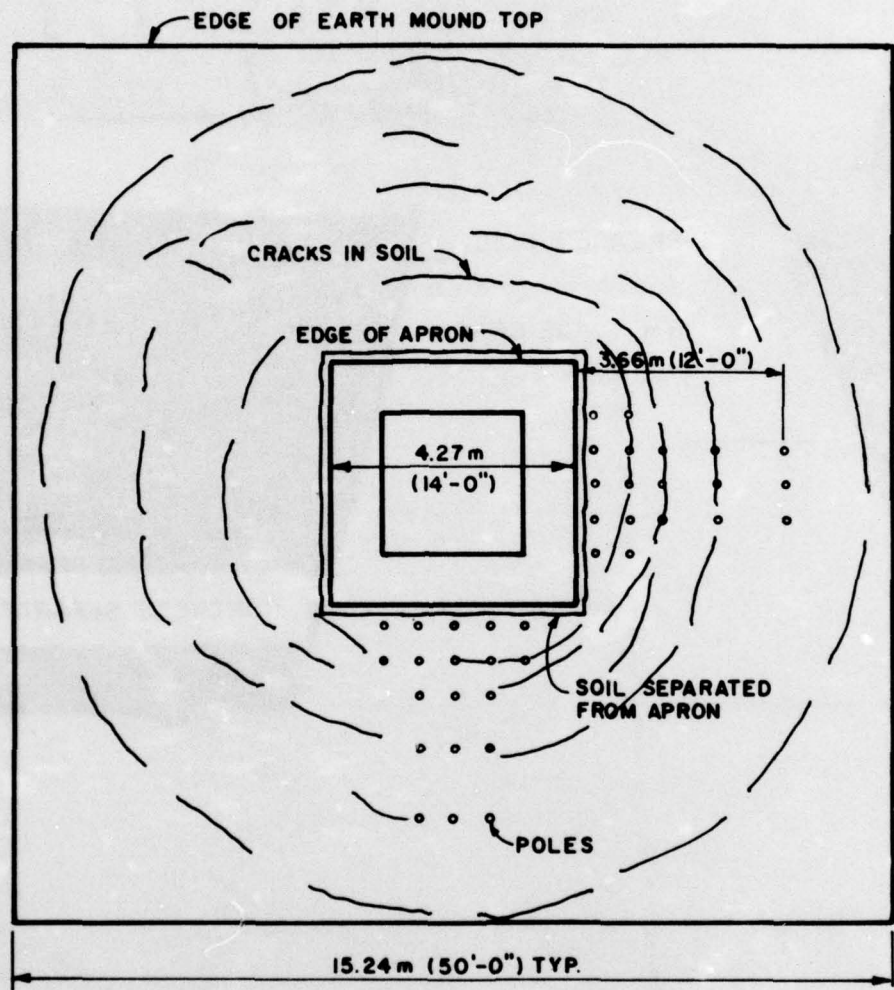
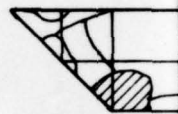
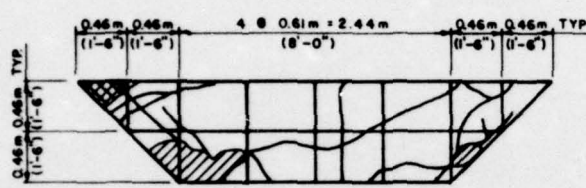


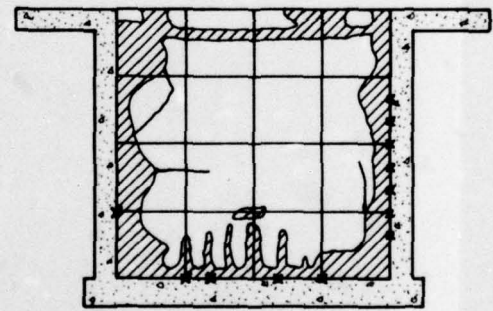
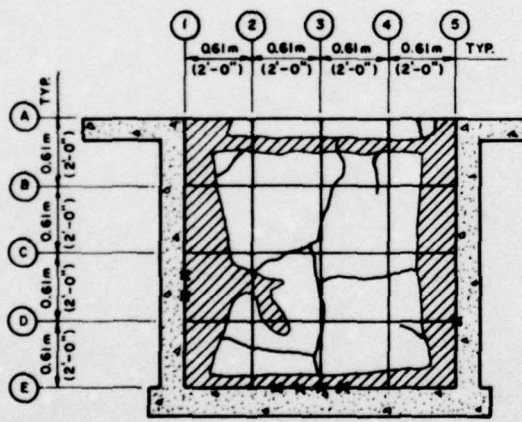
Fig 20 Post-test soil crack pattern (Test No. 6)



Fig 21 Post-test exterior view of Cell No. 1 (Test No. 7)



APRON PLAN



NORTH

EAST

WALL ELEVATIONS

Fig 22 Post-test damage to Cell No. 1 (Test No. 1)

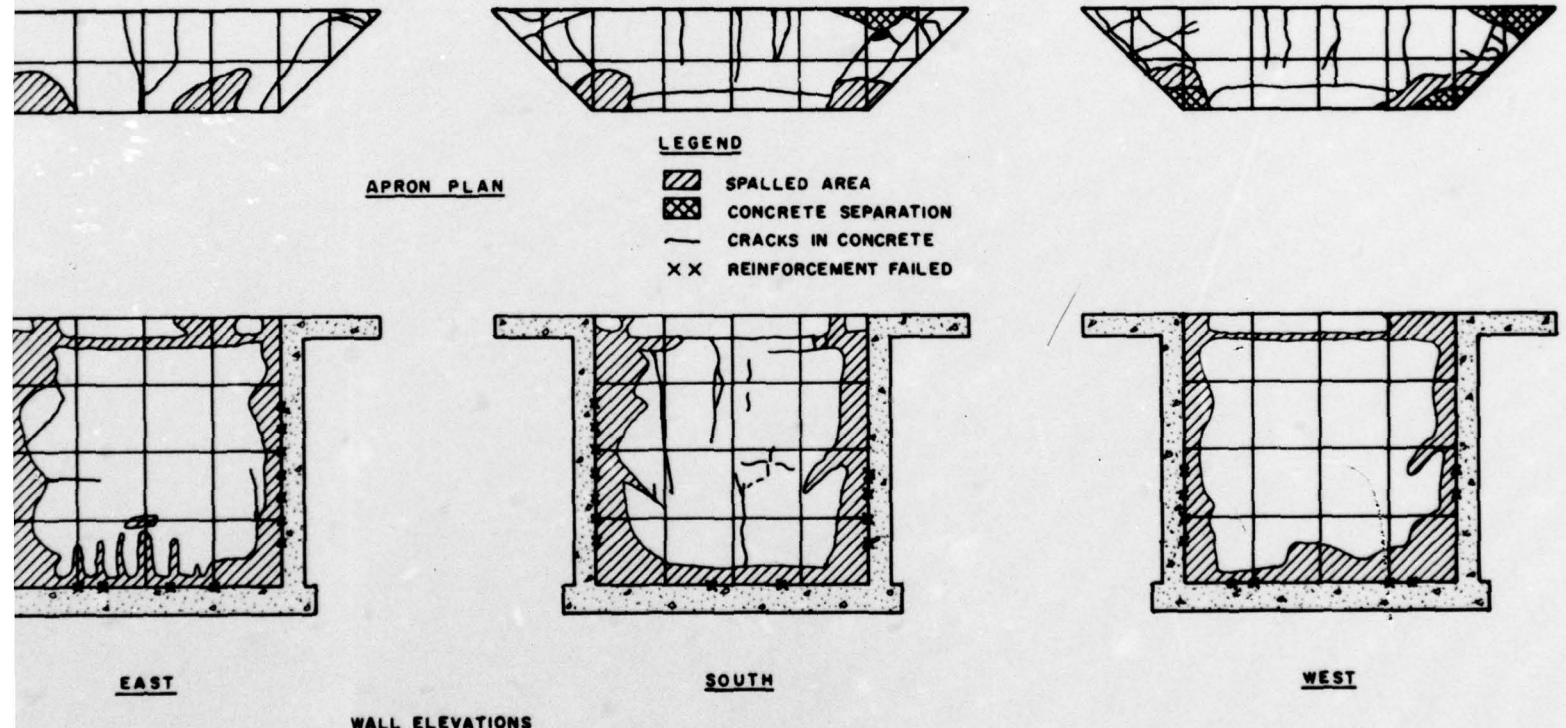


Fig 22 Post-test damage to Cell No. 1 (Test No. 7)

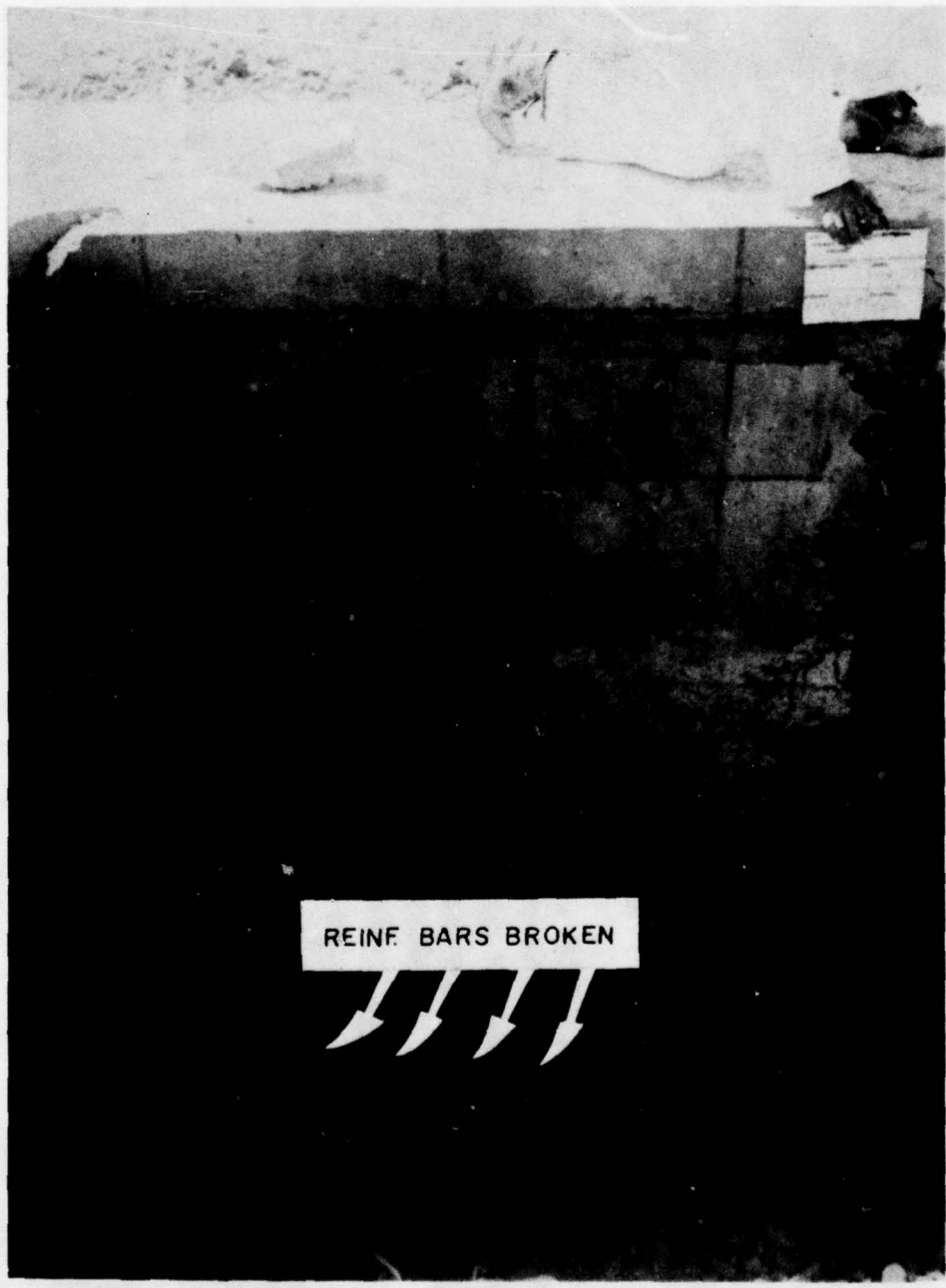


Fig 23 Post-test damage to Cell No. 1 north wall (Test No. 7)

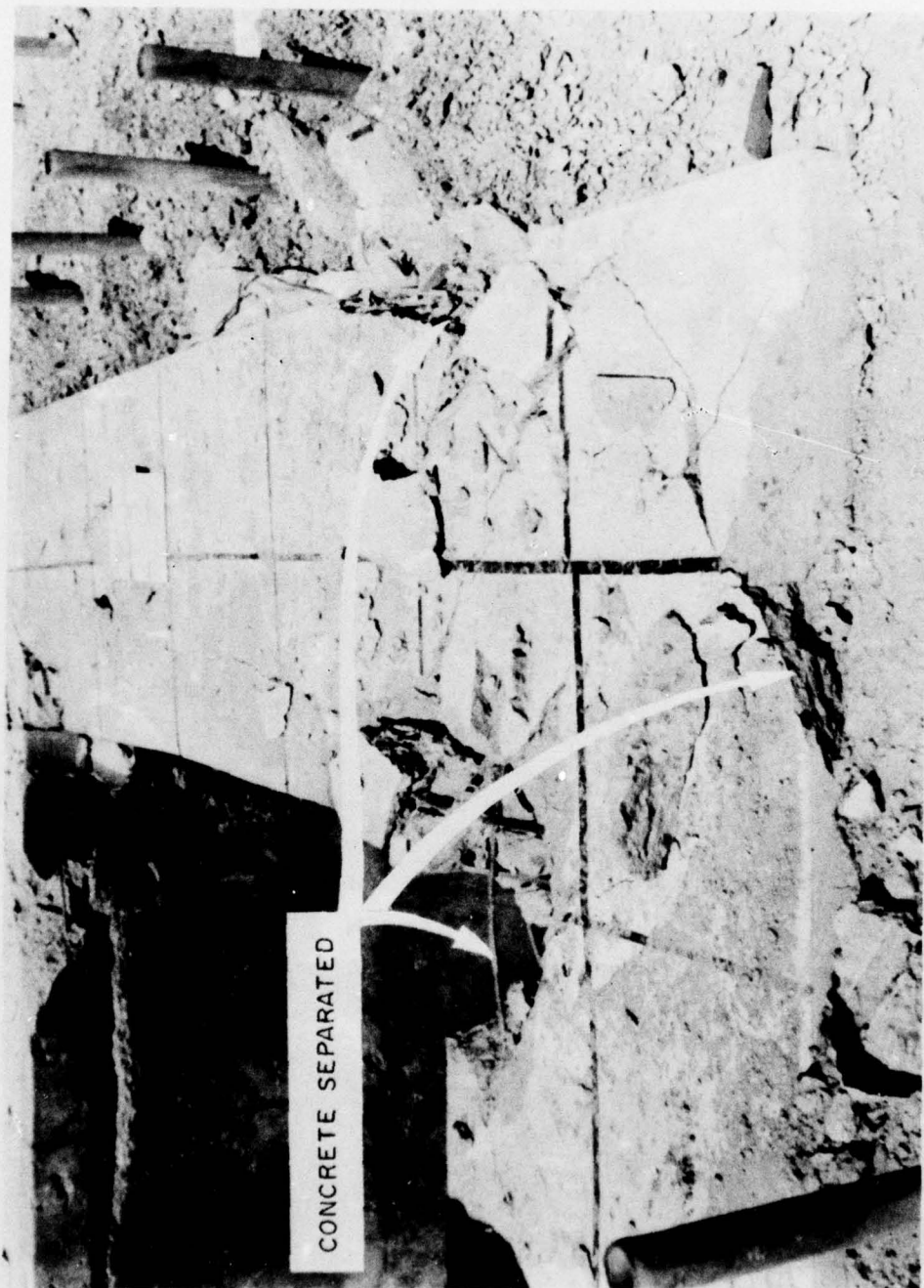
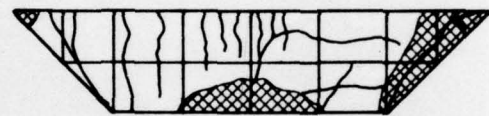
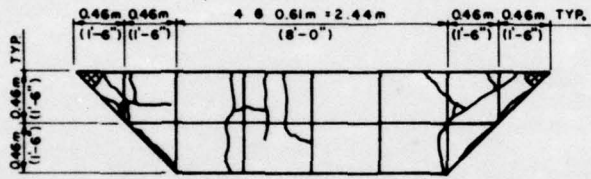
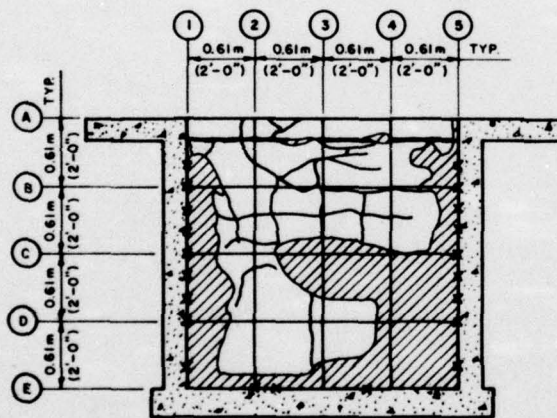


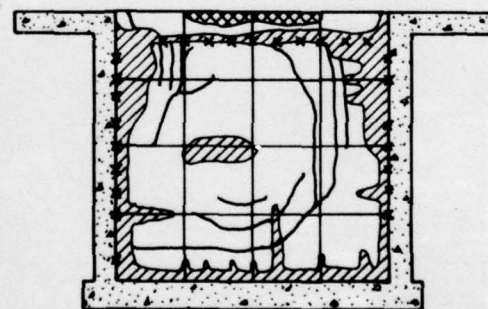
Fig 24 Break-up of Cell No. 1 concrete apron (Test No. 7)



APRON PLAN



NORTH



EAST

WALL ELEVATIONS

Fig 25 Post-test damage to Cell No. 2 (Te)

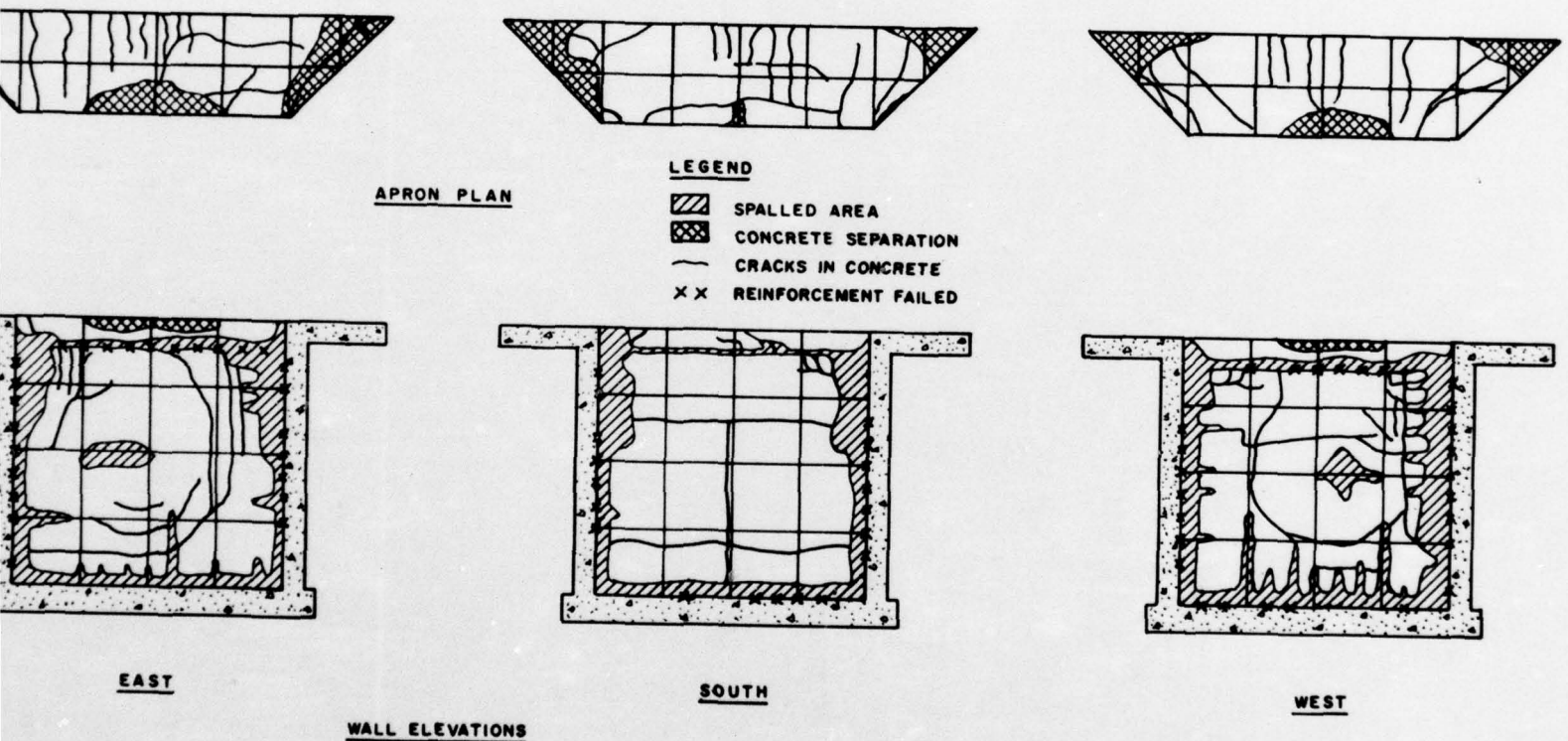


Fig 25 Post-test damage to Cell No. 2 (Test No. 8)

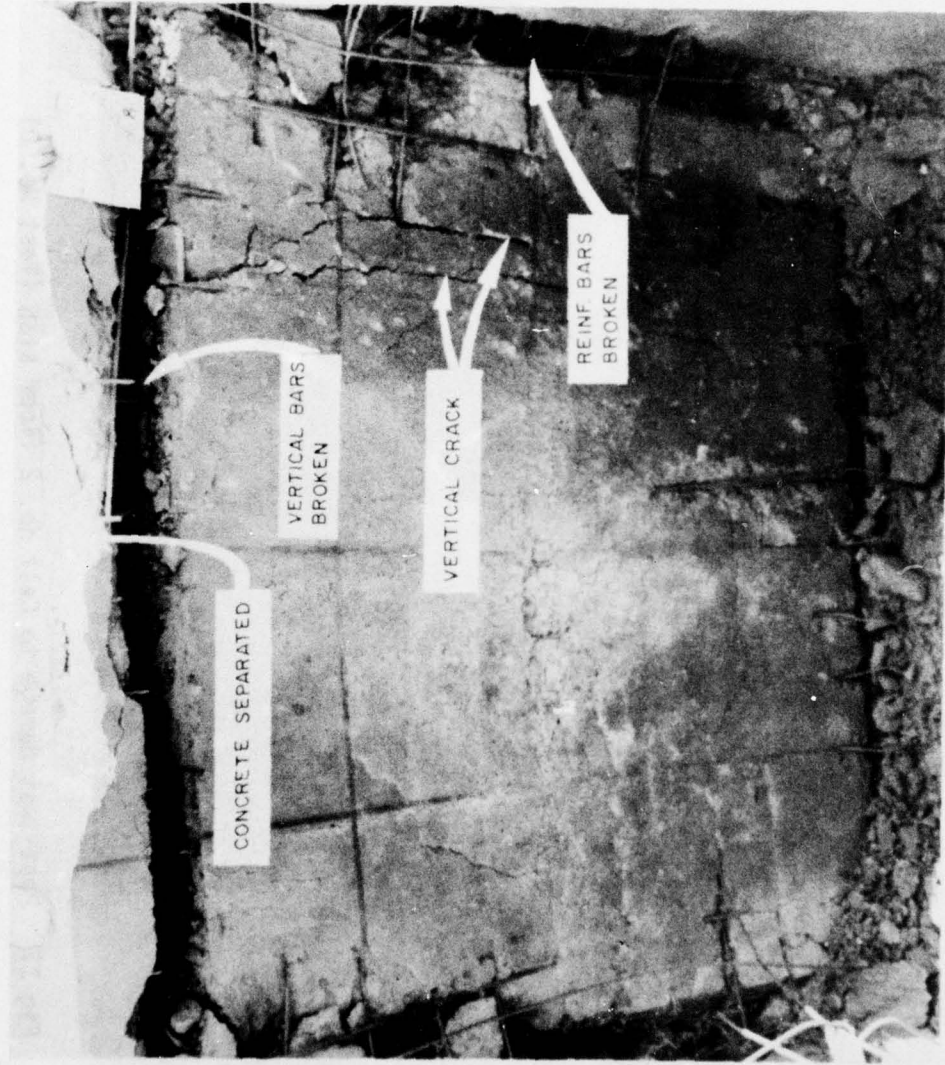


Fig 26 Post-test damage to Cell No. 2 east wall
(Test No. 8)

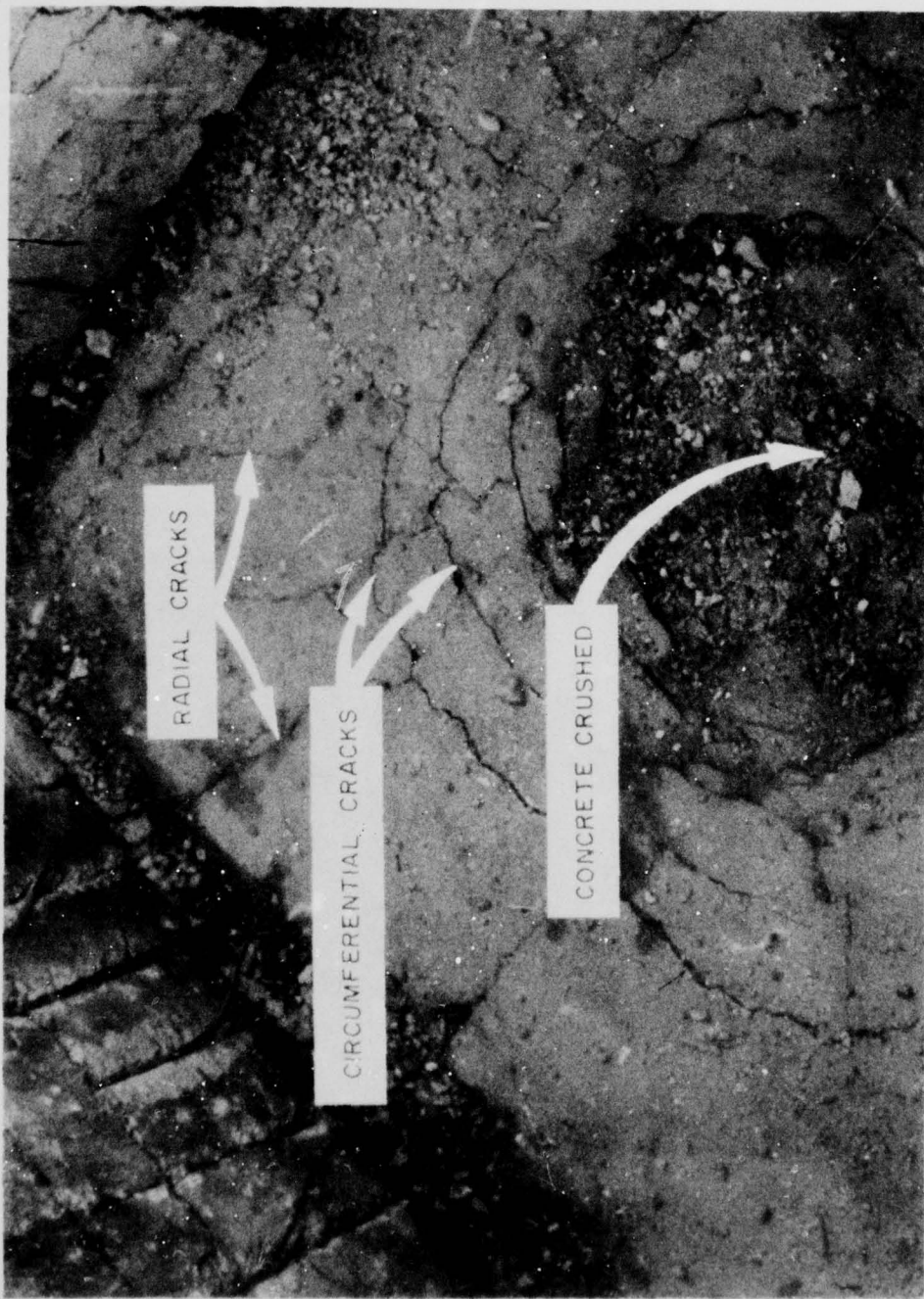
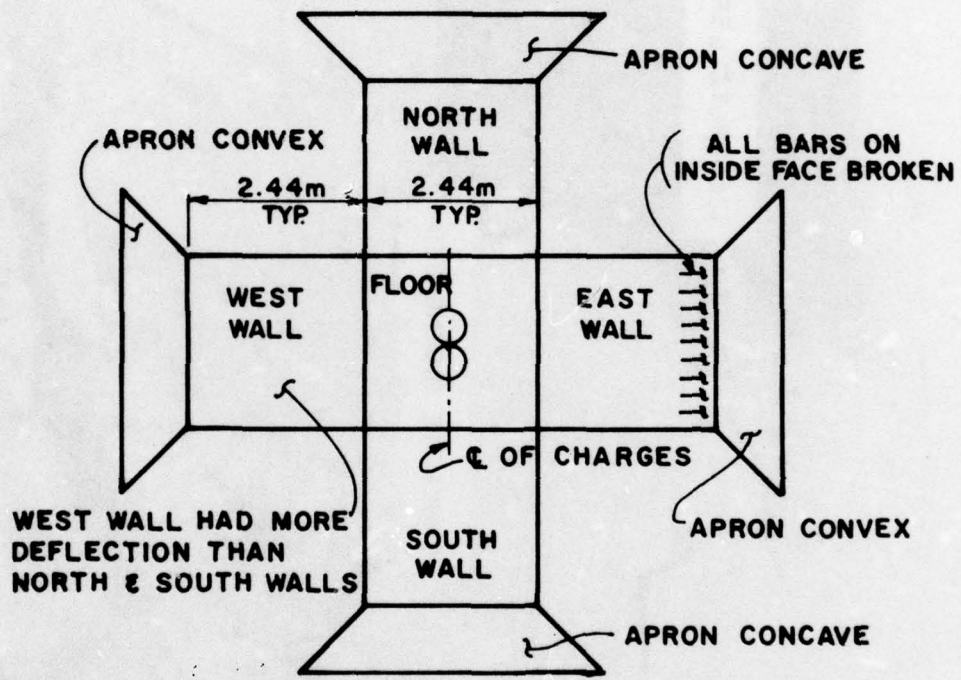


Fig 27 Post-test damage to Cell No. 2 floor slab (Test No. 8)



NOTE: CHARGES LOCATED AT MID. HEIGHT OF CELL

Fig 28 Location of charges and damage to Cell No. 2 (Test No. 8)

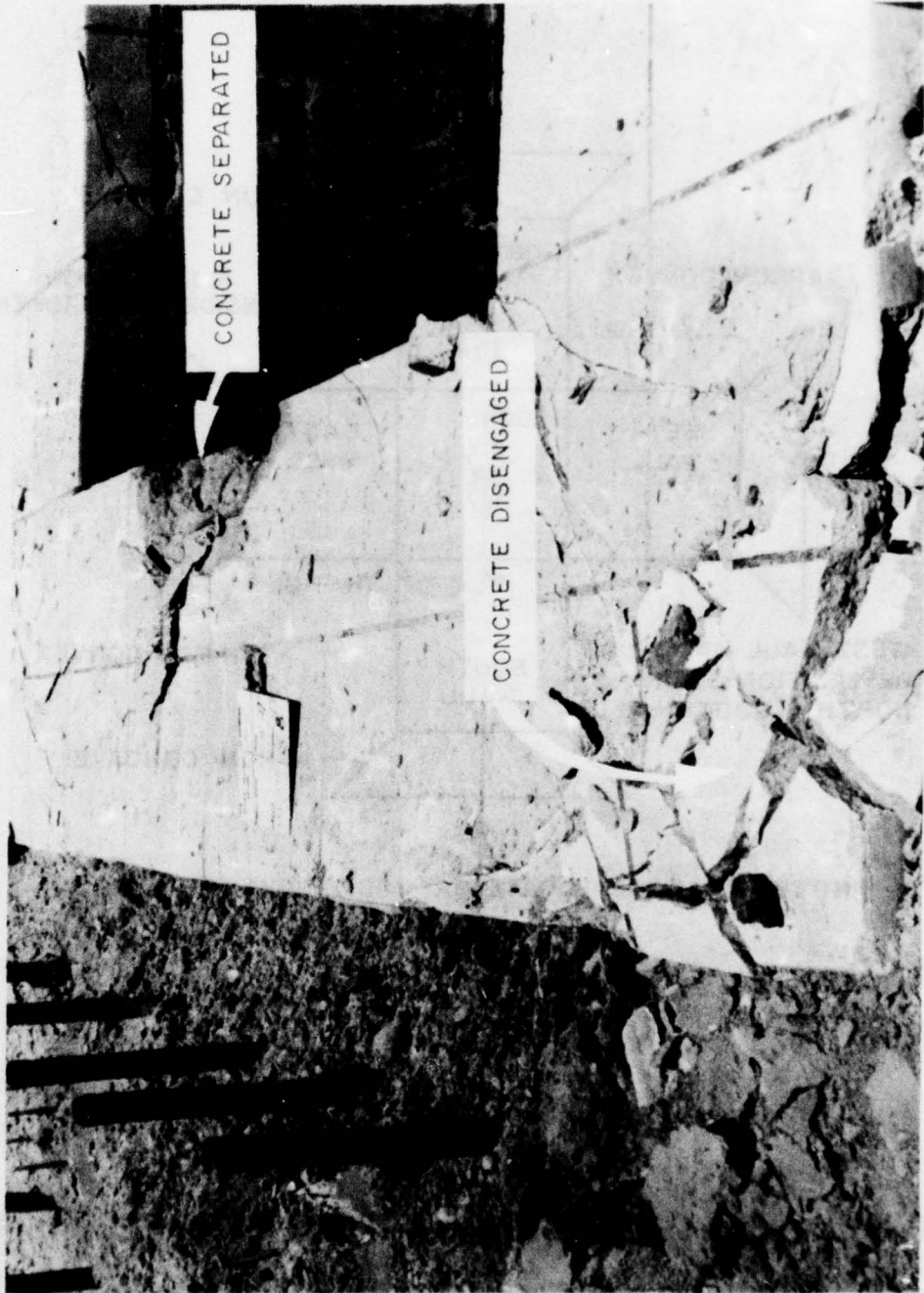


Fig 29 Post-test damage to Cell No. 2 concrete apron
(Test No. 8)

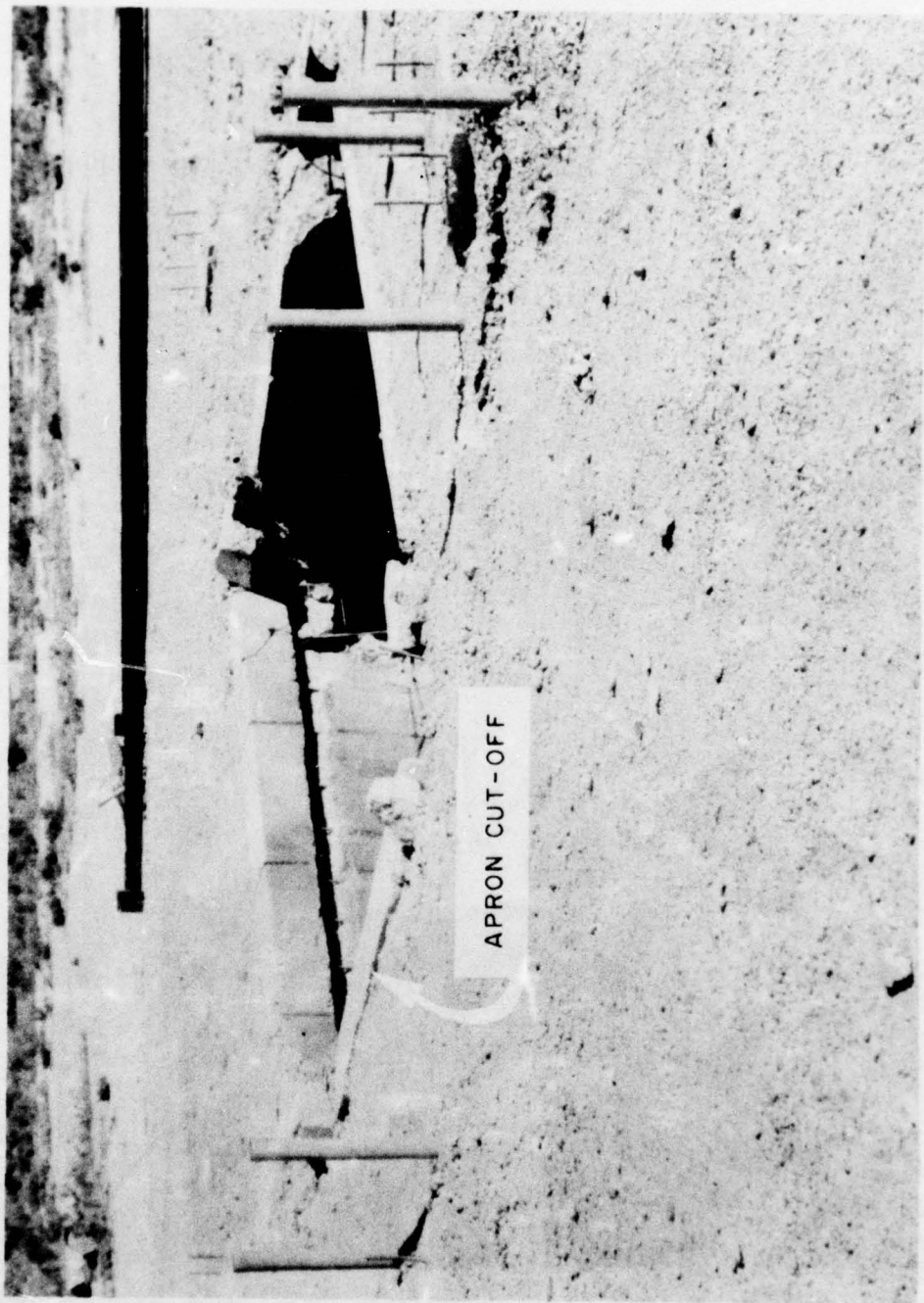
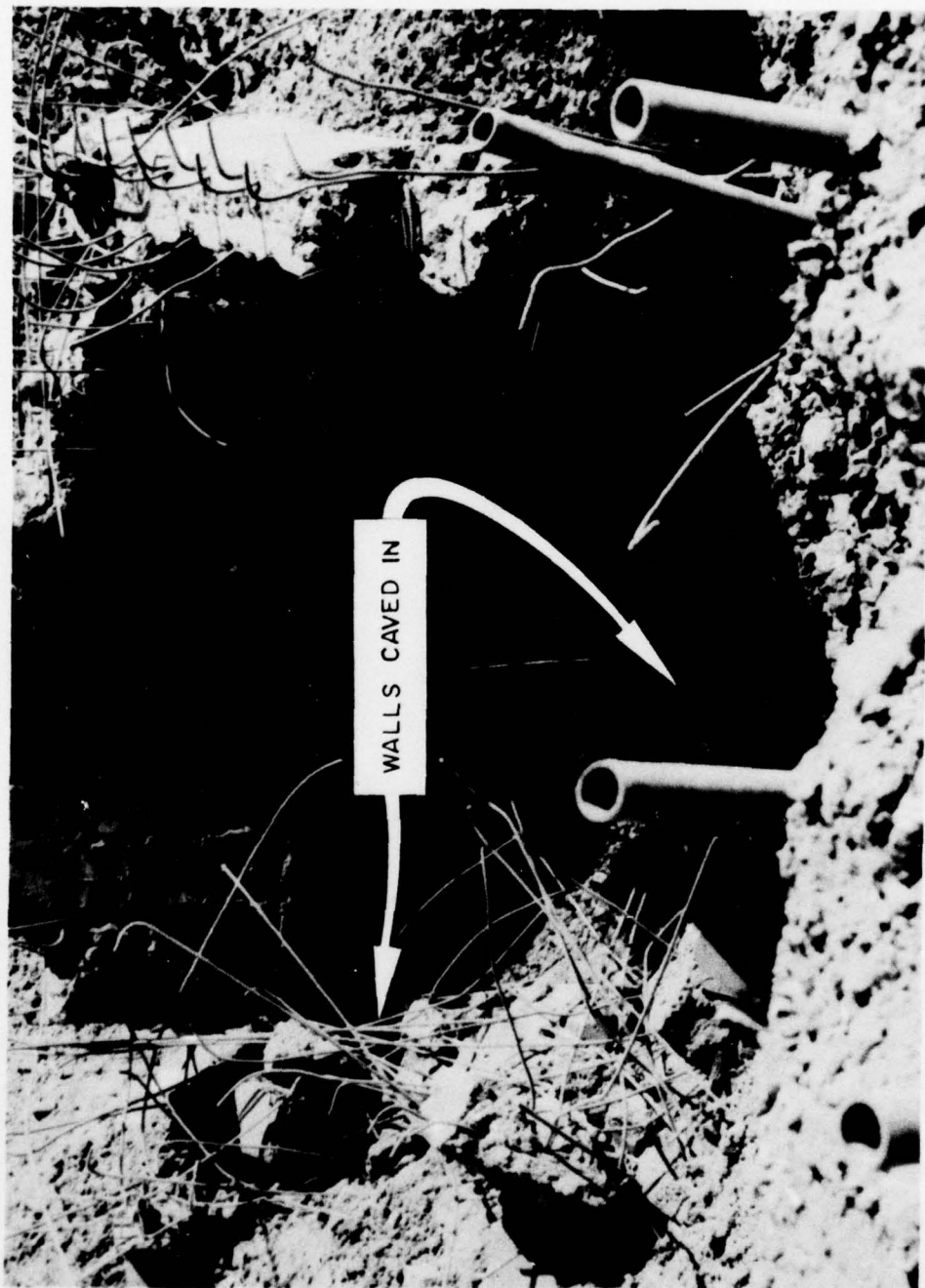


Fig 30 Cell No. 1 after removal of apron

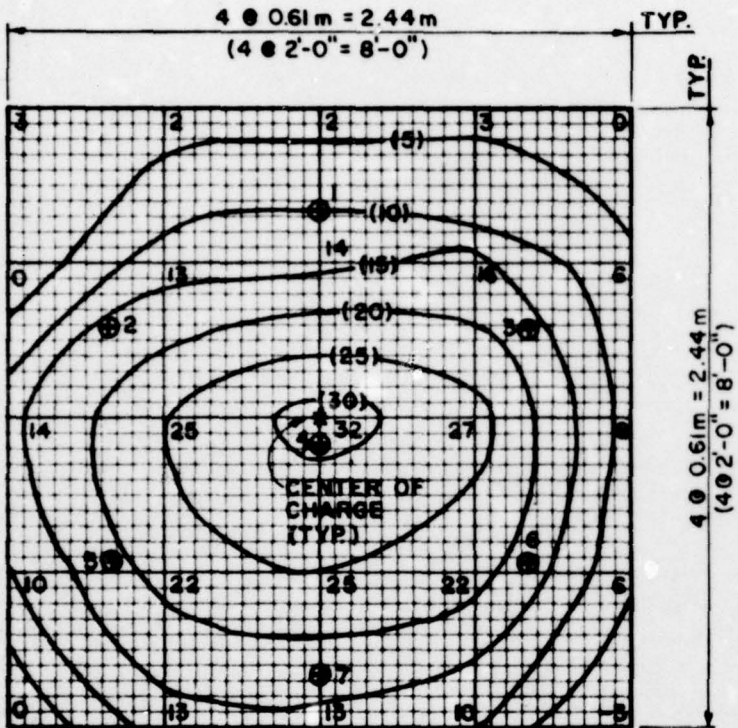


Fig 31 Post-test damage to Cell No. 1 north wall
(Test No. 9)

Fig 32 Post-test damage to Cell No. 2 (Test No. 10)

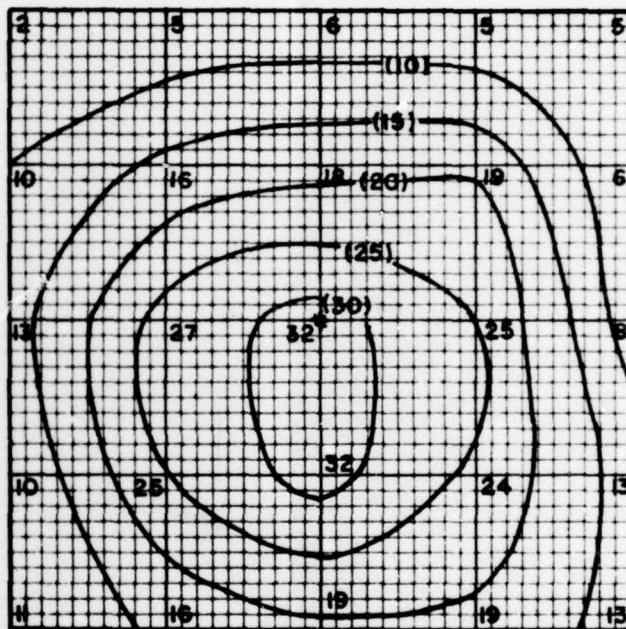


BEST AVAILABLE COPY



NORTH

NOTE: DISPLACEMENT MEASUREMENTS IN MILLIMETRES



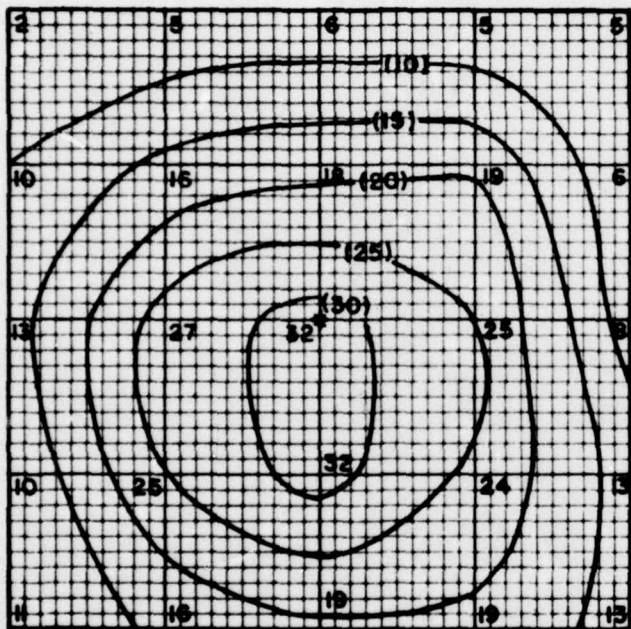
SOUTH

INTERIOR WALL ELEVATIONS

Fig 33 Permanent deflection contours, Cell No. 1 (Test

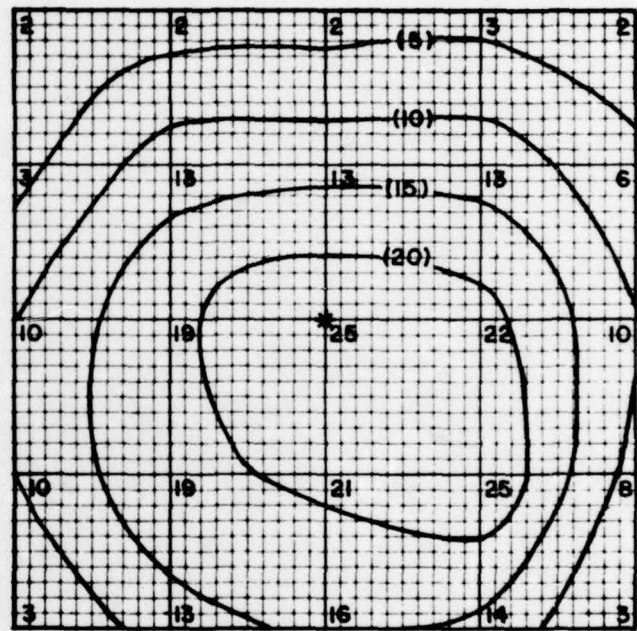
PRECEDING PAGE BLANK - NOT FILMED

BEST AVAILABLE COPY



SOUTH

INTERIOR WALL ELEVATIONS

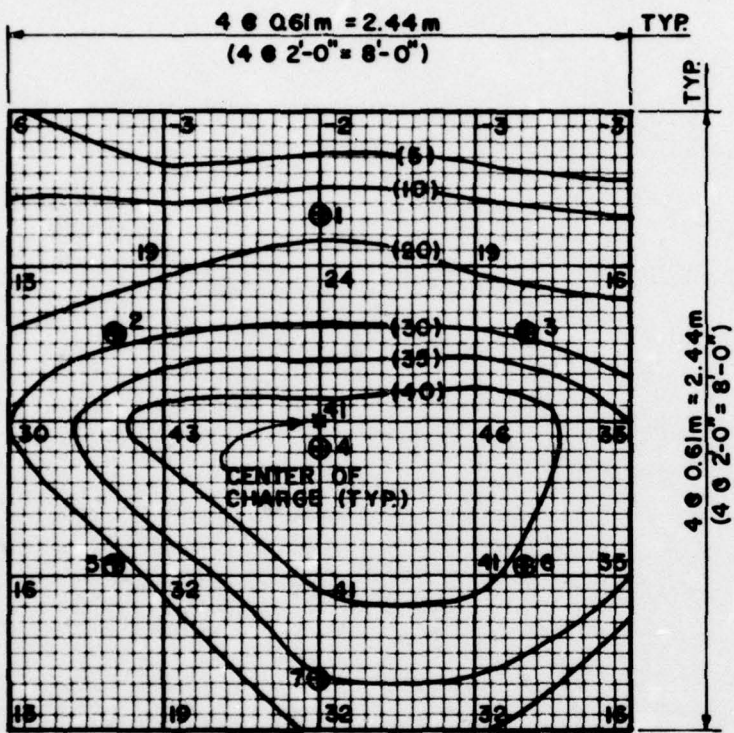


WEST

⊕ LOCATION OF DEFLECTION GAGE

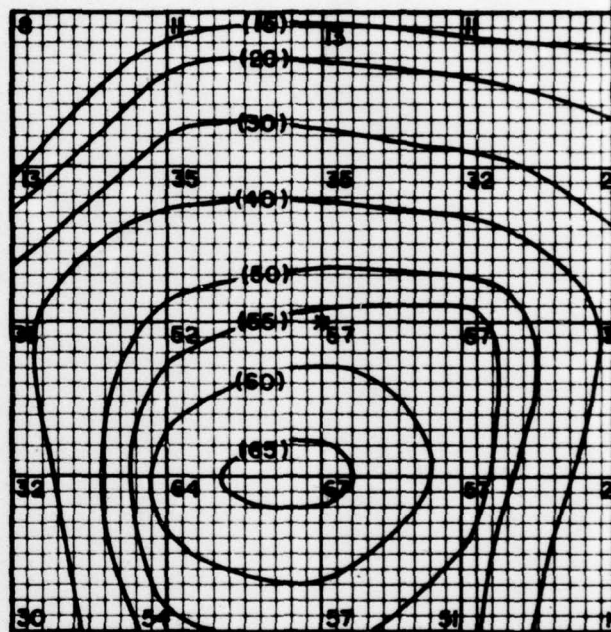
Fig 33 Permanent deflection contours, Cell No. 1 (Test No. 4)

BEST AVAILABLE COPY

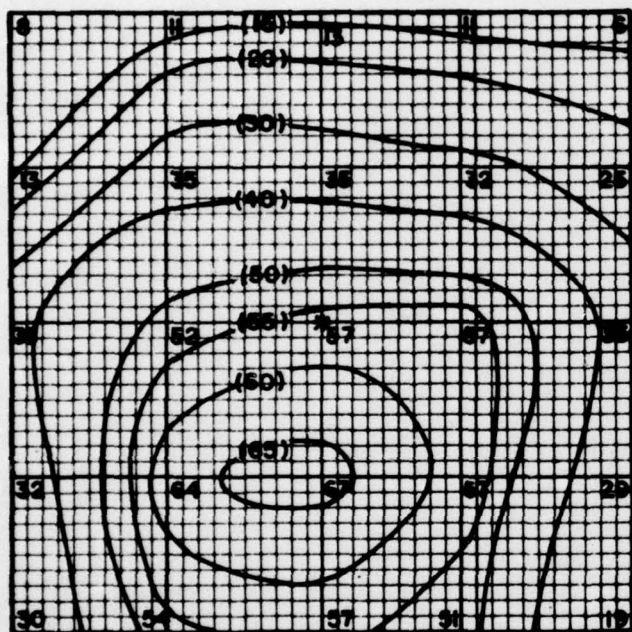


NORTH

NOTE: DISPLACEMENT MEASUREMENTS IN MILLIMETRES

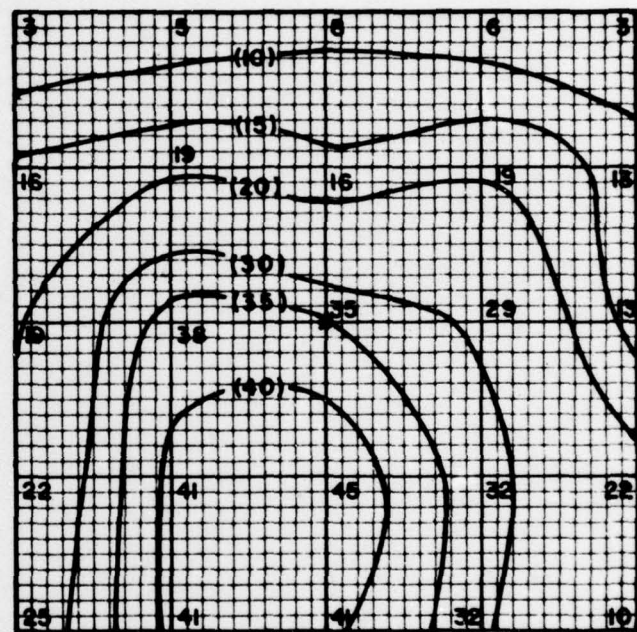


BEST AVAILABLE COPY



SOUTH

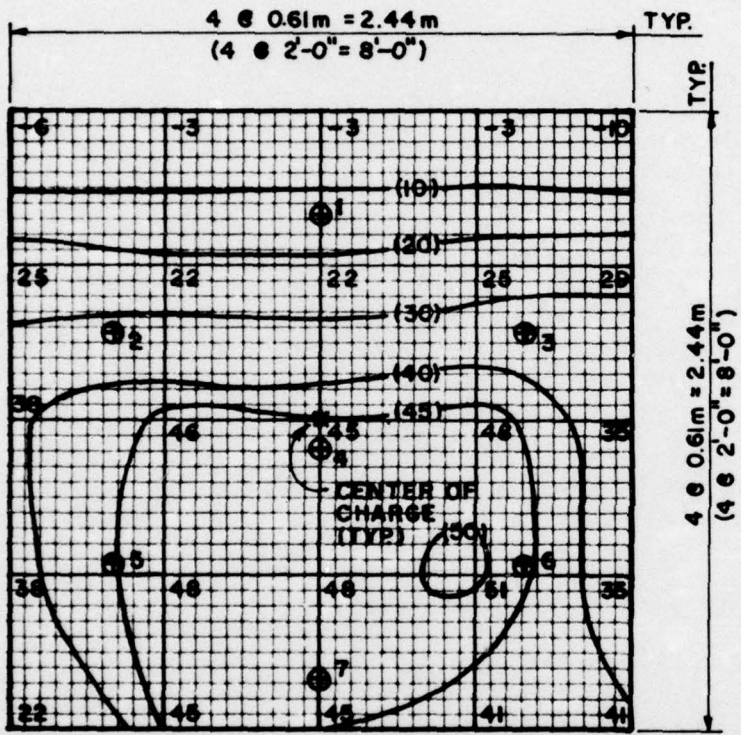
INTERIOR WALL ELEVATIONS



WEST

⊕ LOCATION OF DEFLECTION GAGE

34 Permanent deflection contours, Cell No. 1 (Test No. 5)



NOTE: DISPLACEMENT MEASUREMENTS IN MILLIMETRES

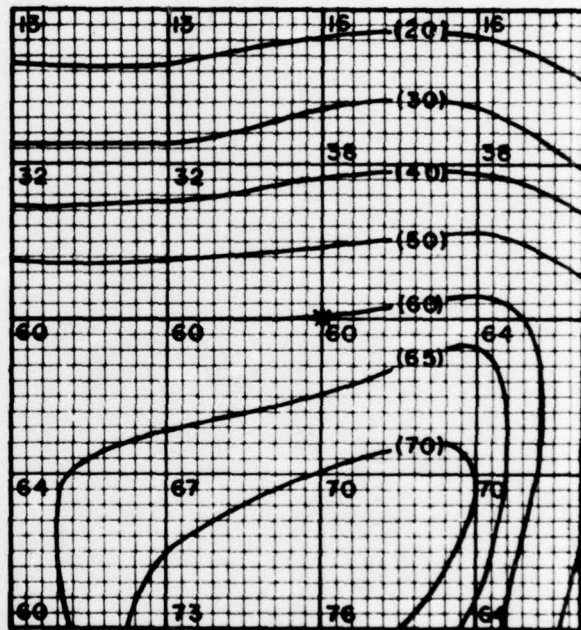
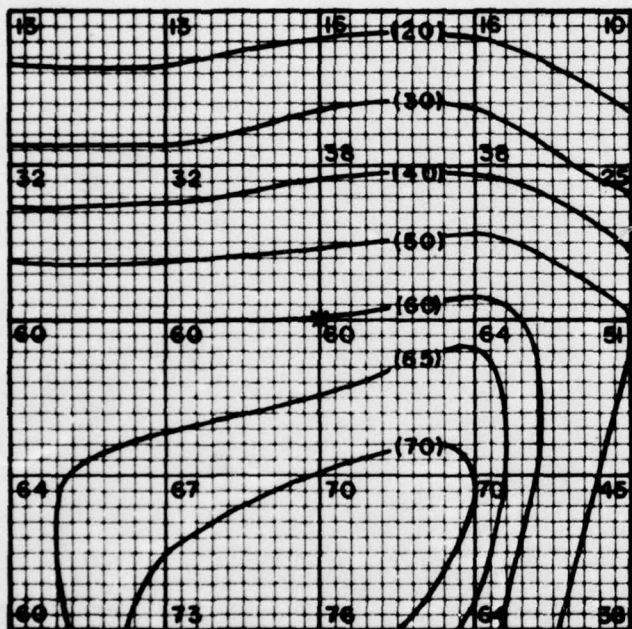


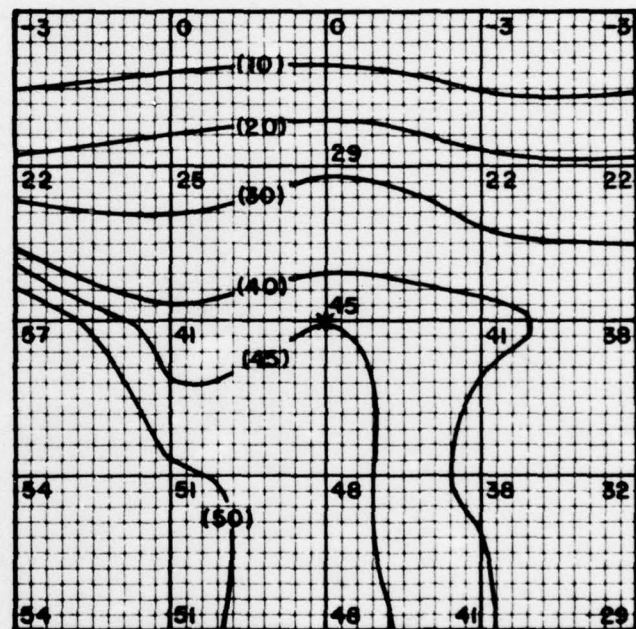
Fig 35 Permanent deflection contours, Cell No. 1

BEST AVAILABLE COPY



SOUTH

INTERIOR WALL ELEVATIONS



WEST

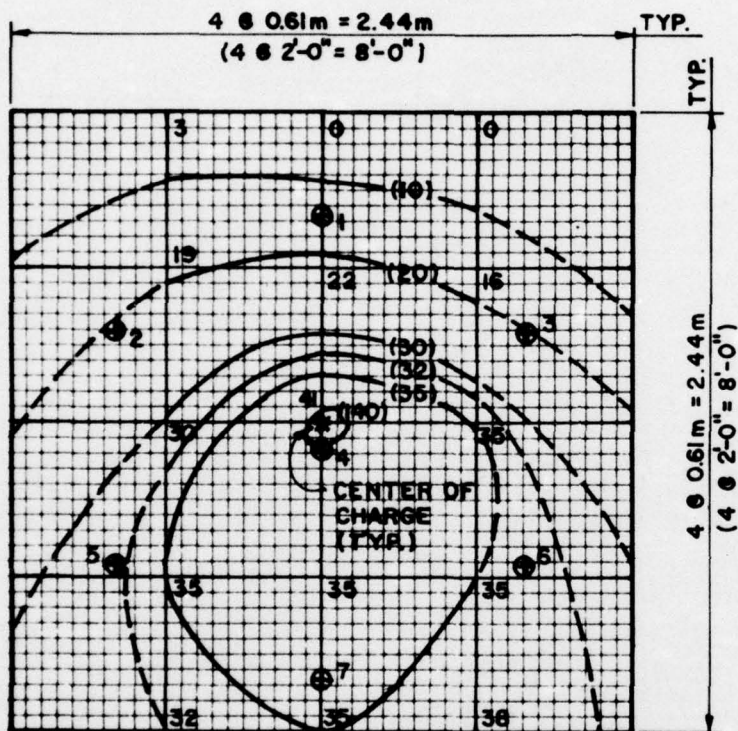
⊕ LOCATION OF DEFLECTION GAGE

Fig 35 Permanent deflection contours, Cell No. 1 (Test No. 6)

BEST AVAILABLE COPY

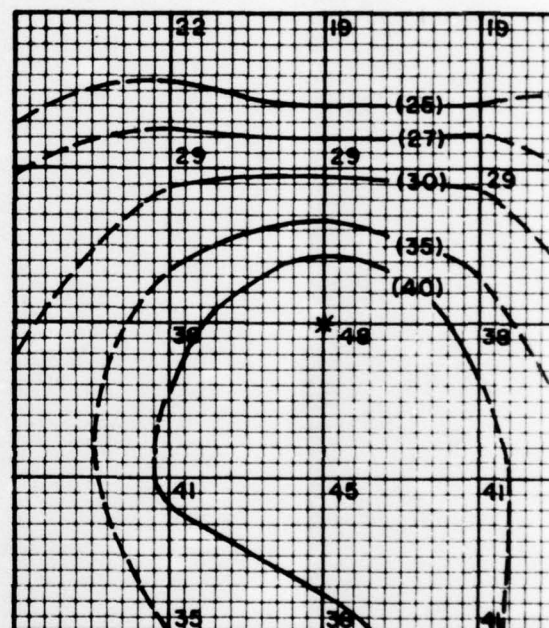
2

COPY



NORTH

NOTE: DISPLACEMENT MEASUREMENTS IN MILLIMETRES



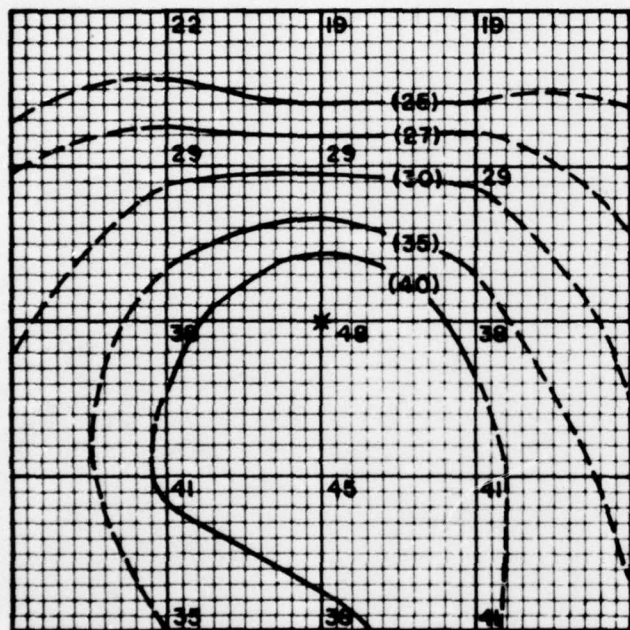
SOUTH

INTERIOR WALL ELEVATION

Fig 36 Permanent deflection contours, Cell No. 1

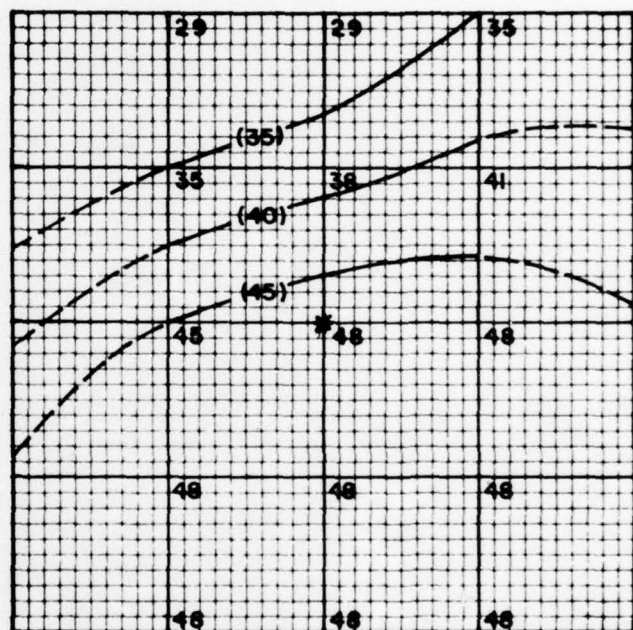
BEST AVAILABLE COPY

72



SOUTH

INTERIOR WALL ELEVATIONS

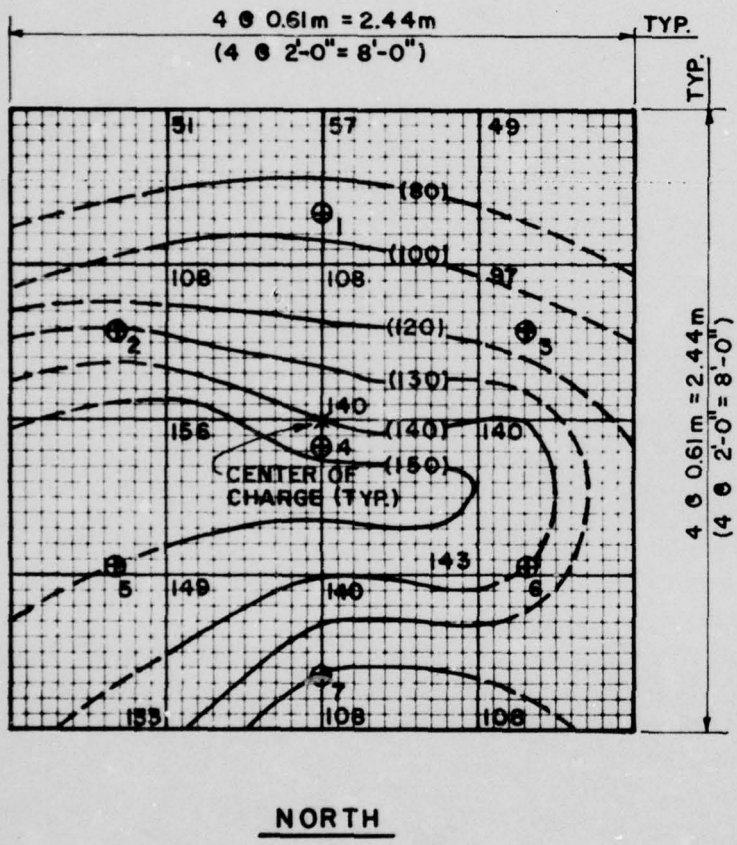


WEST

--- CURVES EXTRAPOLATED
⊕ LOCATION OF DEFLECTION GAGE

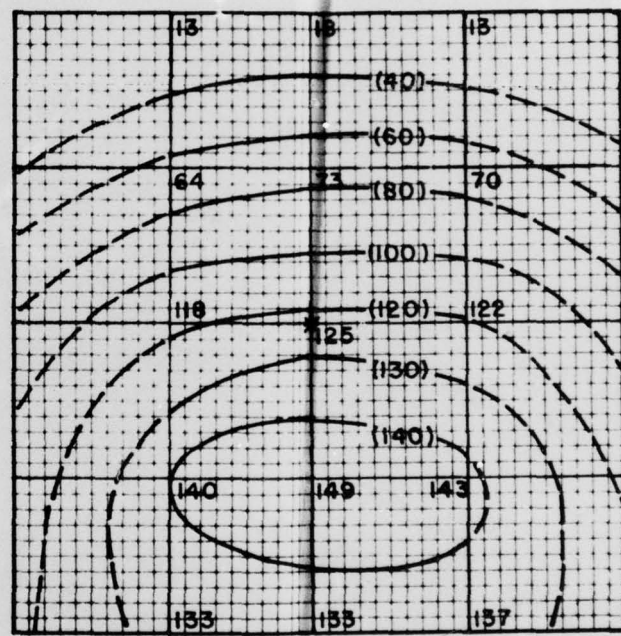
Fig. 36 Permanent deflection contours, Cell No. 1 (Test No. 7)

BEST AVAILABLE COPY



NORTH

NOTE: DISPLACEMENT MEASUREMENTS IN MILLIMETRES

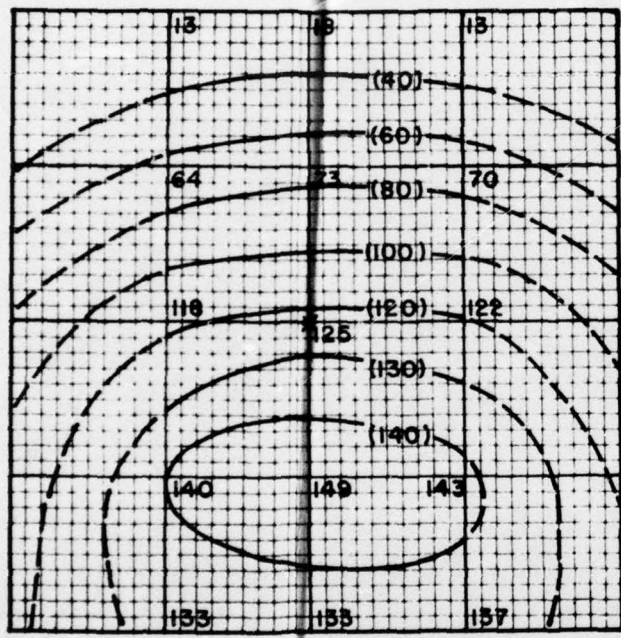


SOUTH

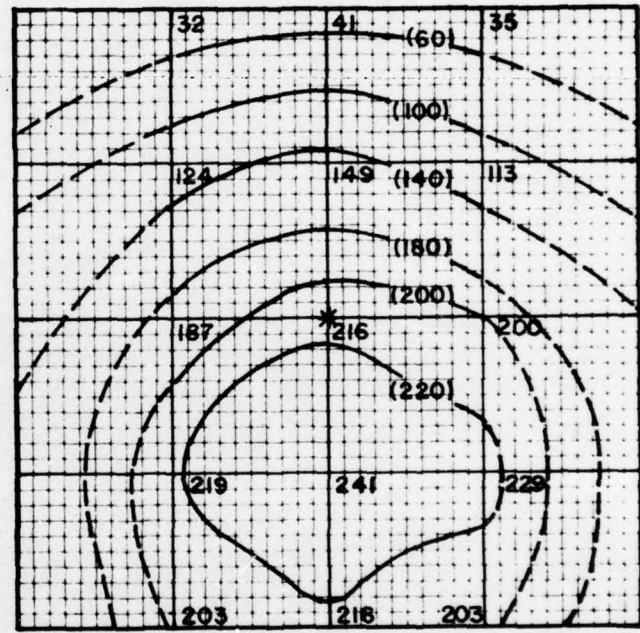
INTERIOR WALL ELEVATIONS

Fig 37 Permanent deflection contours, Cell No. 2 (Test No.

BEST AVAILABLE COPY



INTERIOR WALL ELEVATIONS



— CURVES EXTRAPOLATED
⊕ LOCATION OF DEFLECTION GAGE

Fig 37 Permanent deflection contours, Cell No. 2 (Test No. 8)

BEST AVAILABLE COPY

D

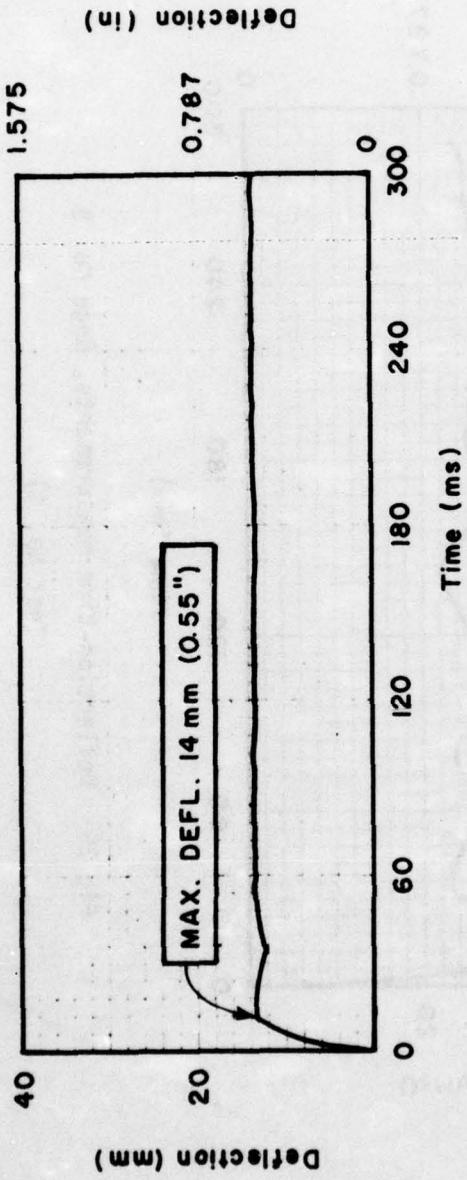


Fig 38 Deflection-time measurements, Gage No. 2
(Test No. 4)

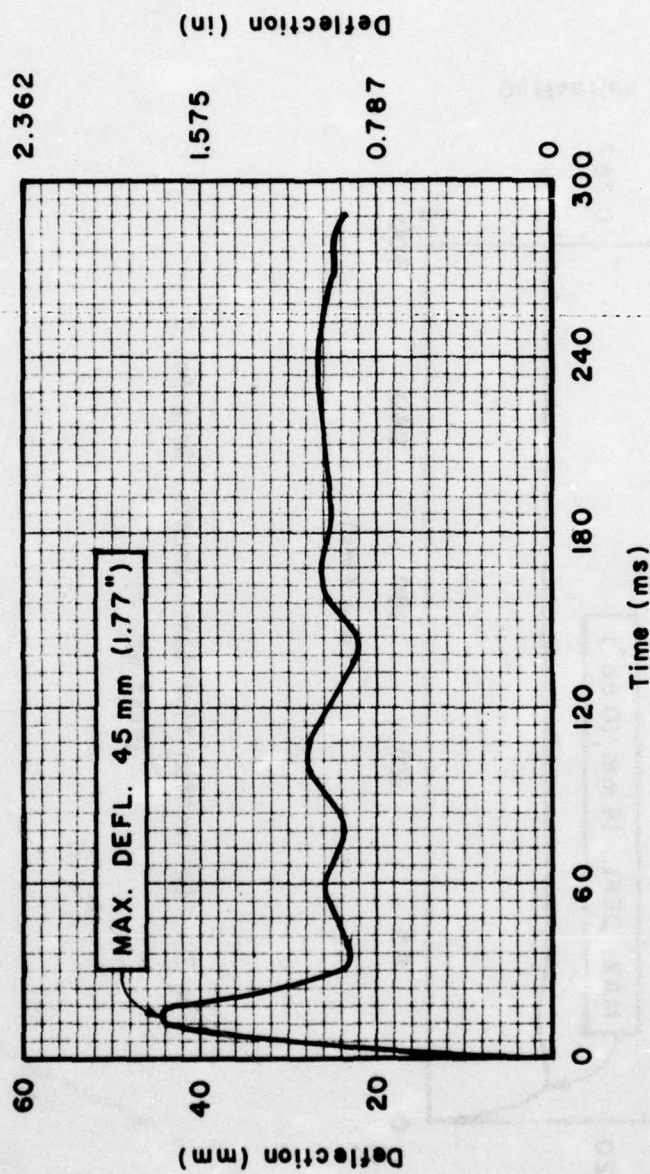


Fig 39 Deflection-time measurements, Gage No. 5
(Test No. 4)

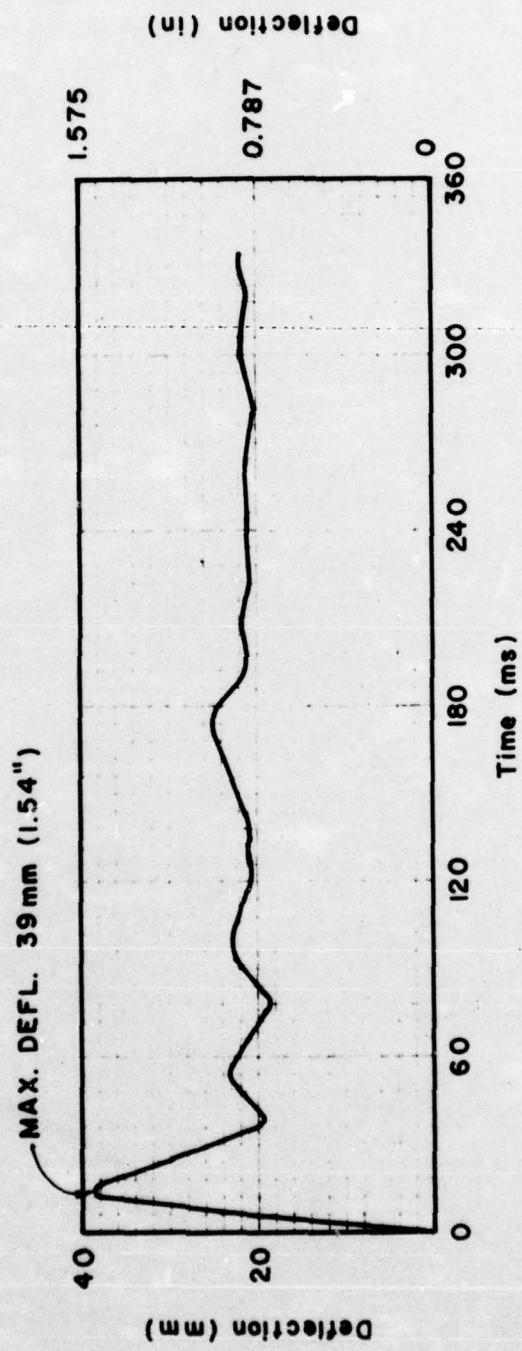


Fig 40 Deflection-time measurements, Gage No. 6
(Test No. 4)

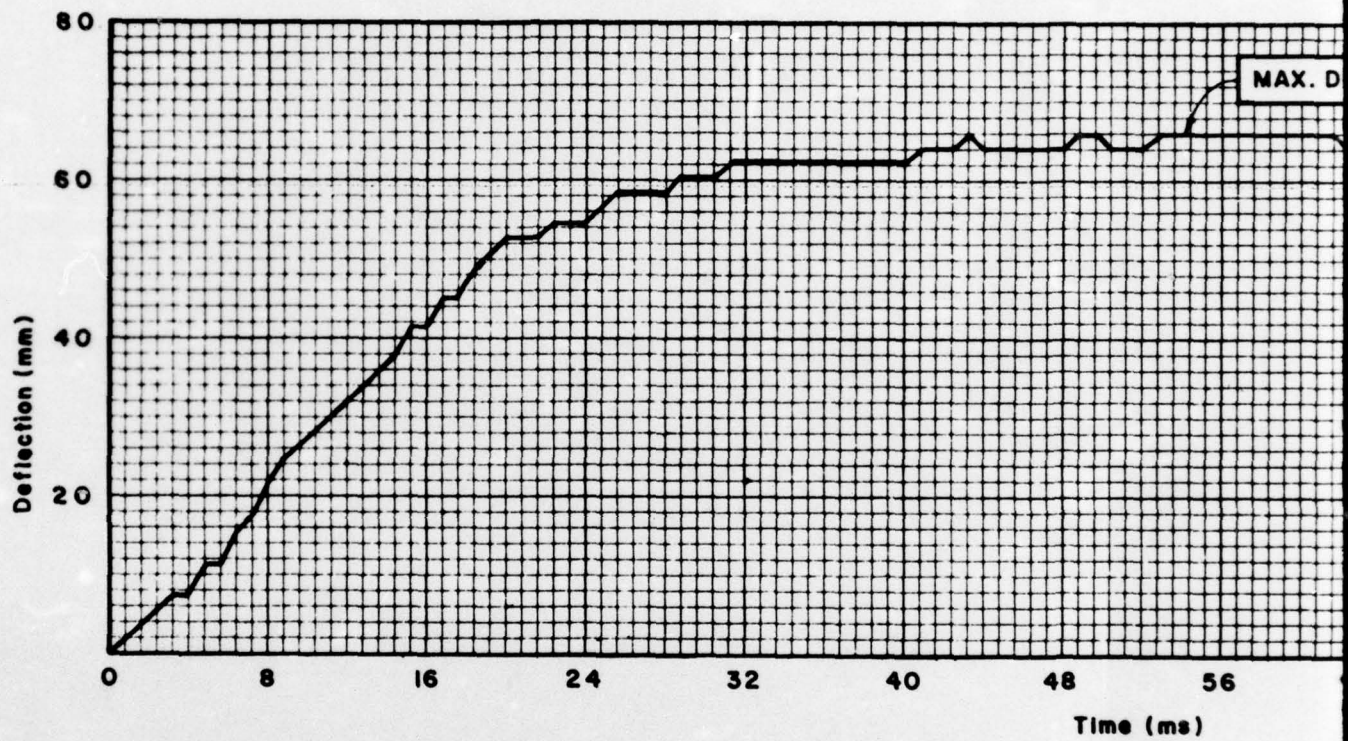


Fig 41 Deflection-time measurements, Gage No

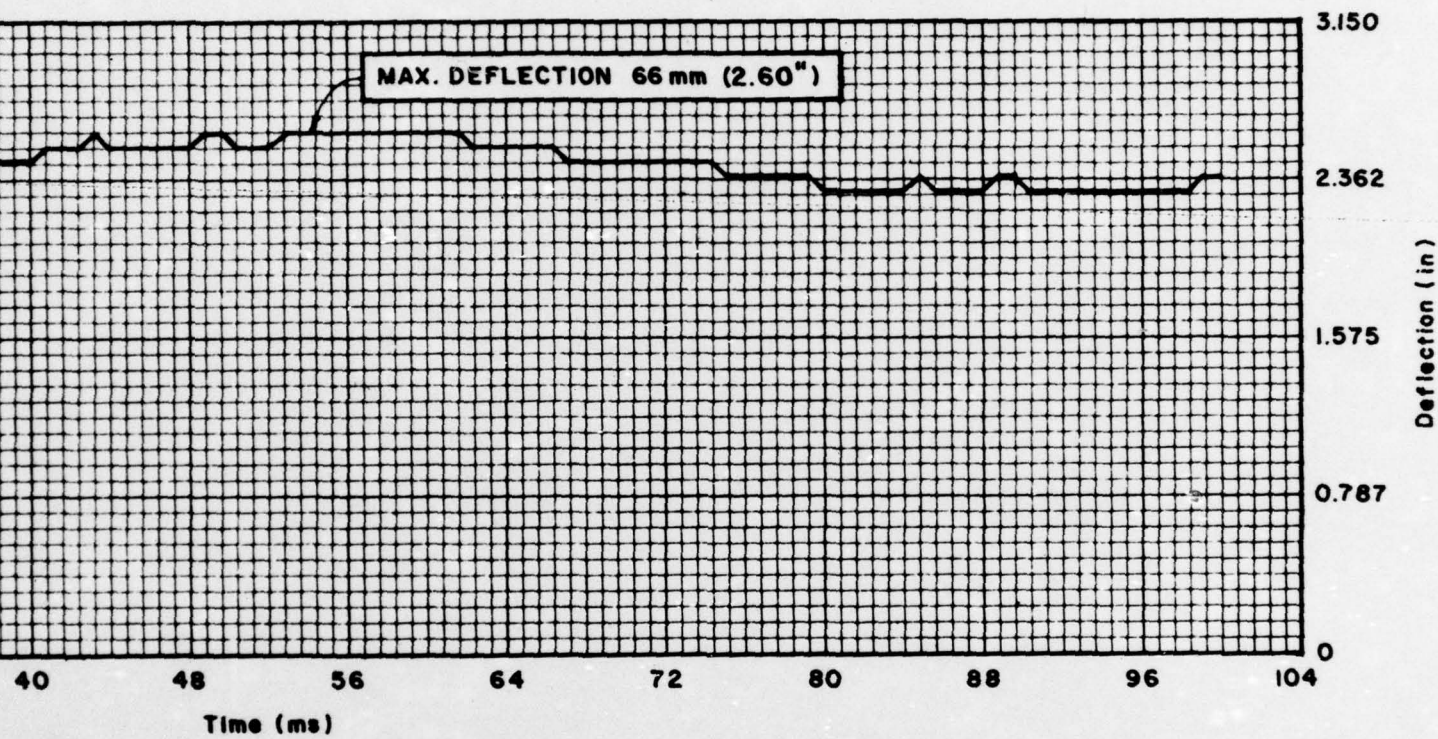


Fig 41 Deflection-time measurements, Gage No. 2 (Test No. 5)

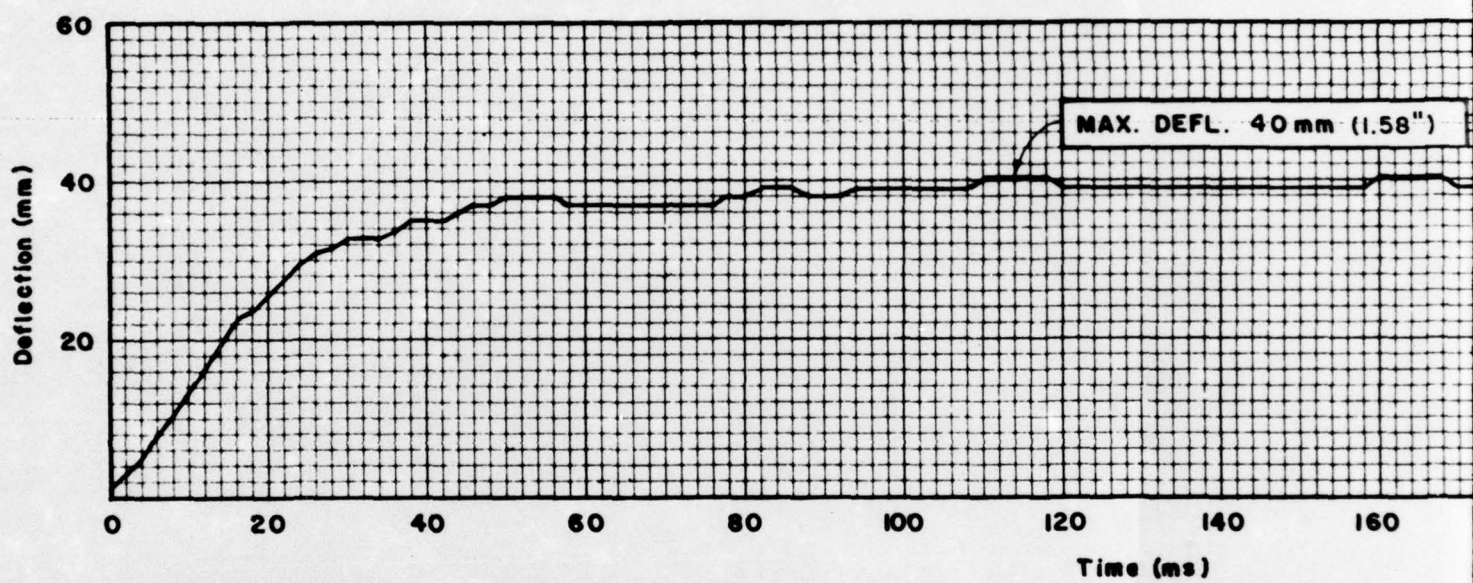


Fig 42 Deflection-time measurements, Gage No. 3 (Test

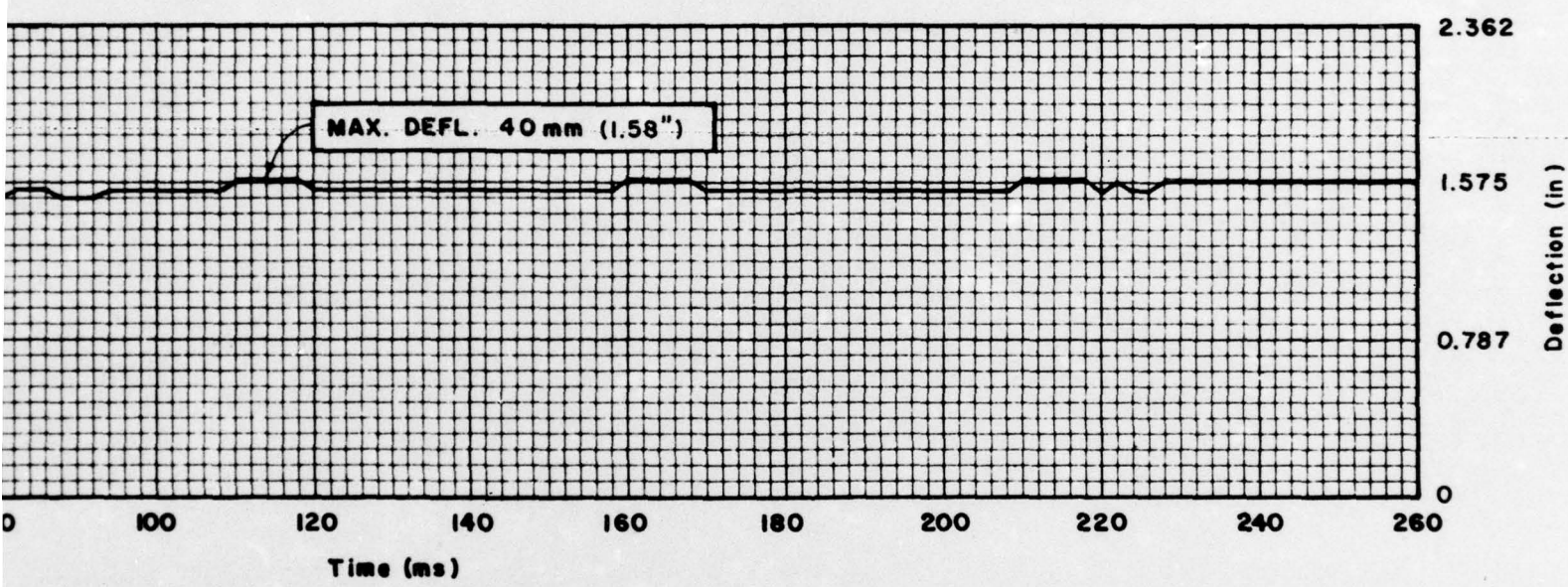


Fig 42 Deflection-time measurements, Gage No. 3 (Test No. 5)

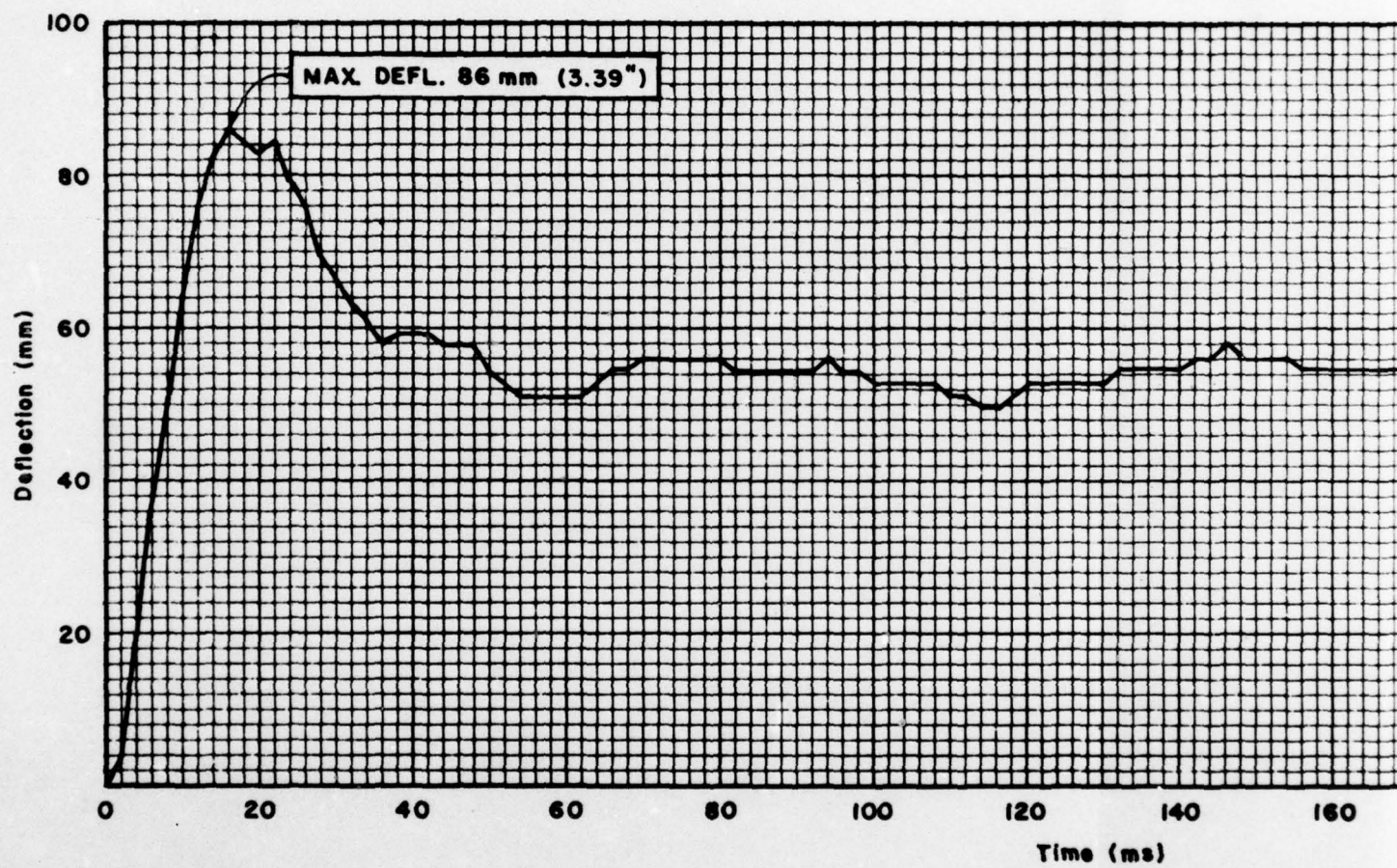
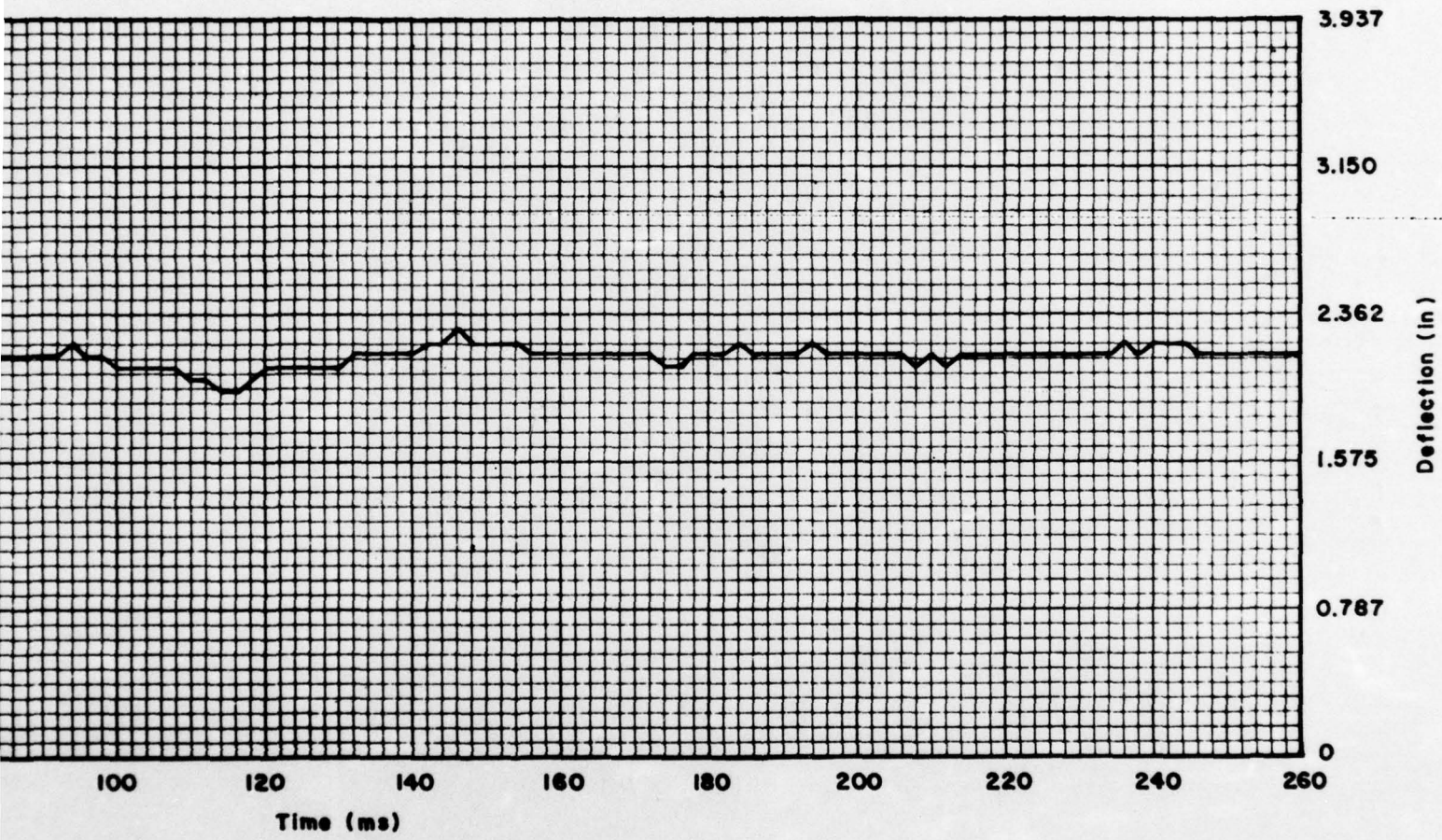


Fig 43 Deflection-time measurements, Gage No. 5 (Test



43 Deflection-time measurements, Gage No. 5 (Test No. 5)

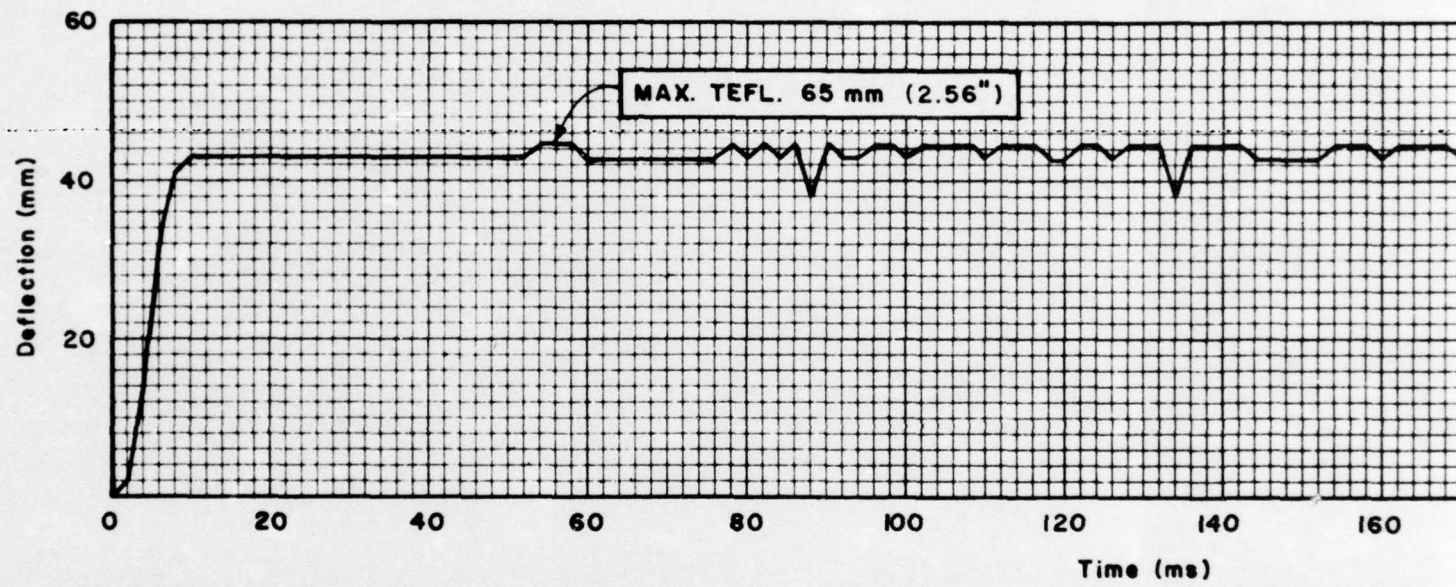


Fig 44 Deflection-time measurements, Gage No. 6 (Test

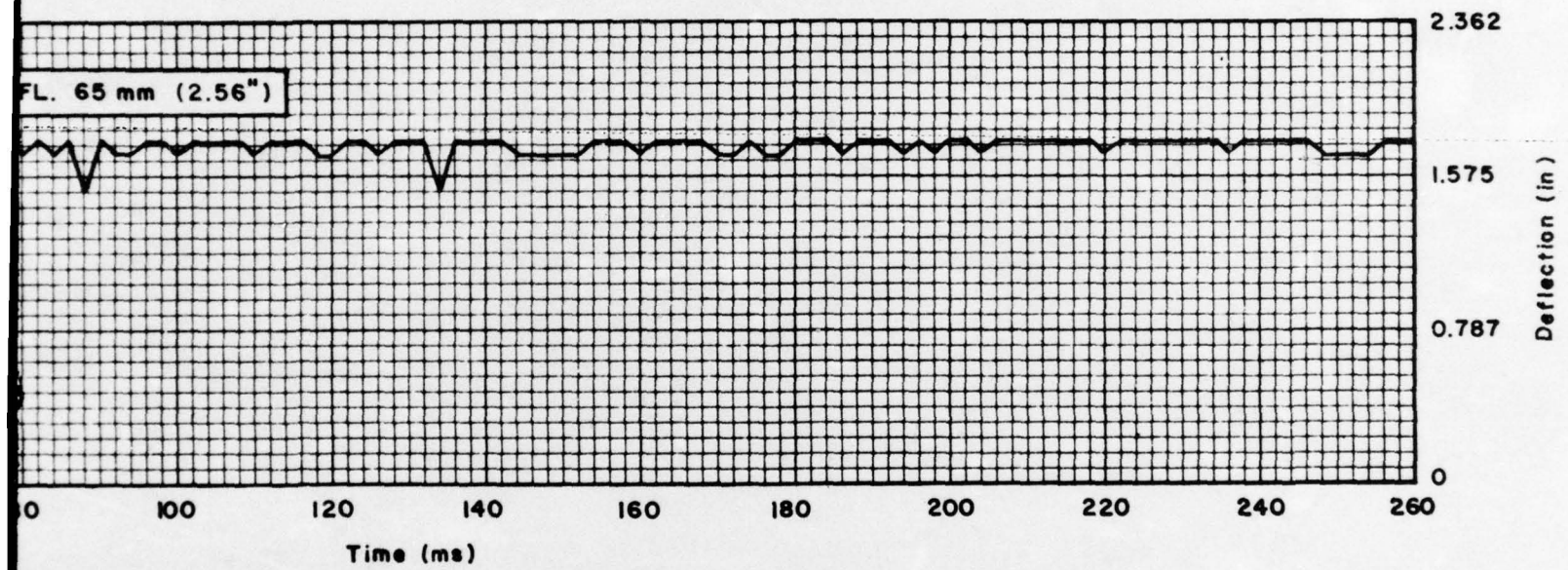


Fig 44 Deflection-time measurements, Gage No. 6 (Test No. 5)

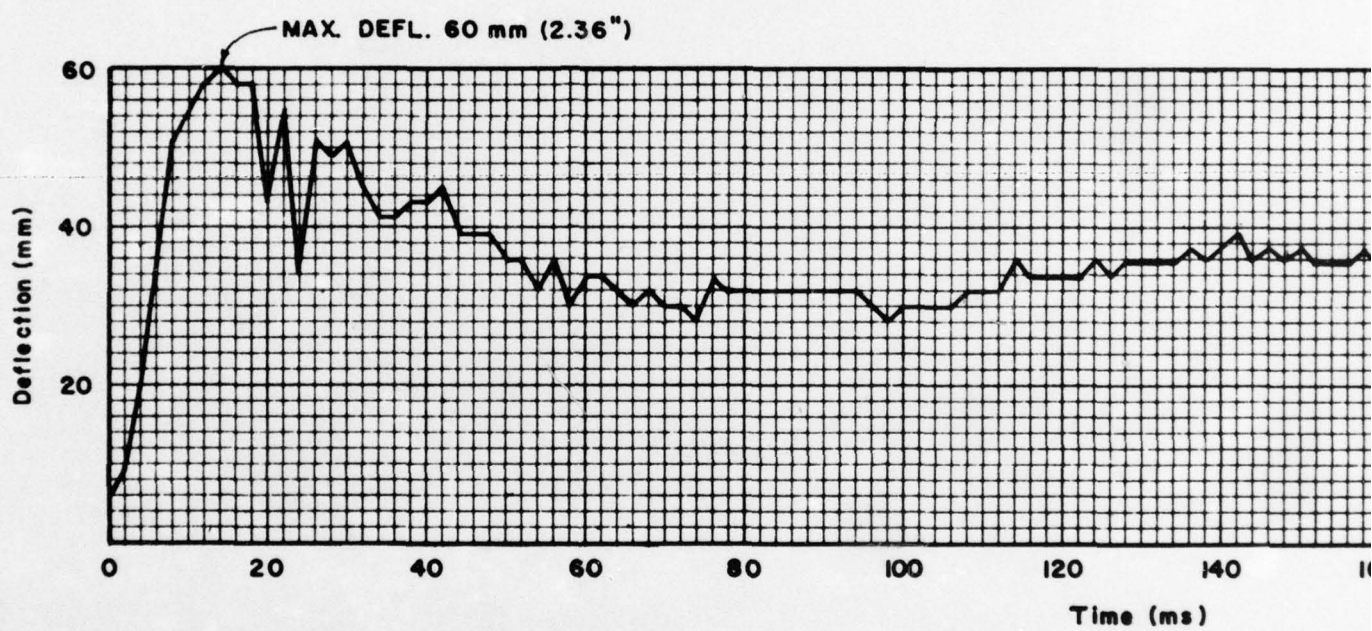


Fig 45 Deflection-time measurements, Gage No. 7

AD-A040 137

AMMANN AND WHITNEY NEW YORK
BLAST CAPACITY EVALUATION OF BELOWGROUND STRUCTURES. (U)

MAY 77 R ARYA, A AMMAR, S WEISSMAN, N DOBBS DAAA21-76-C-0125

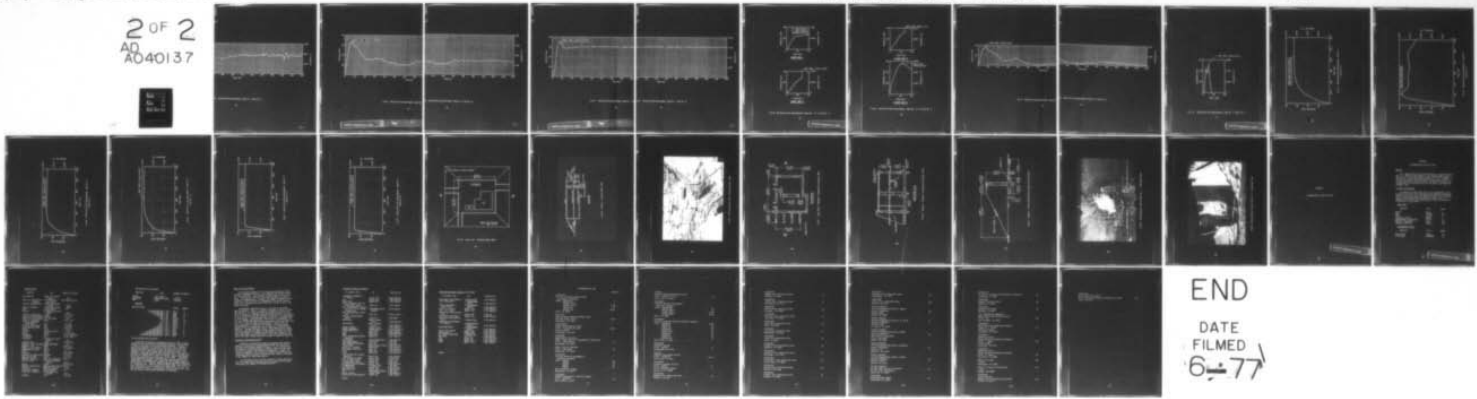
ARLCD-CR-77006

F/G 19/4

REF UNCLASSIFIED

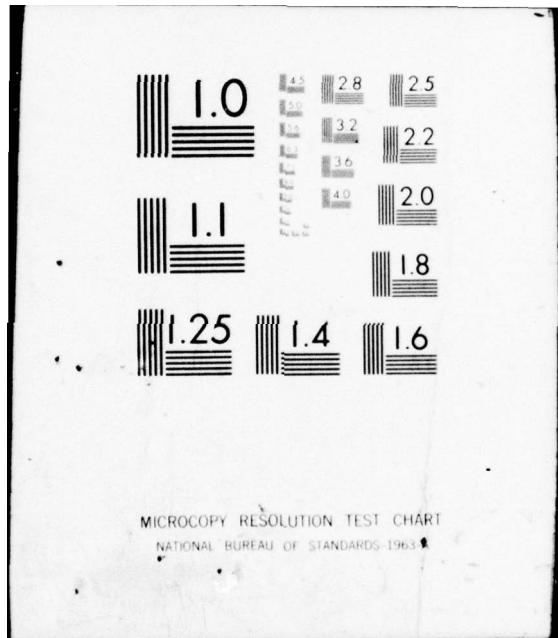
NL

2 OF 2
AD-A040137

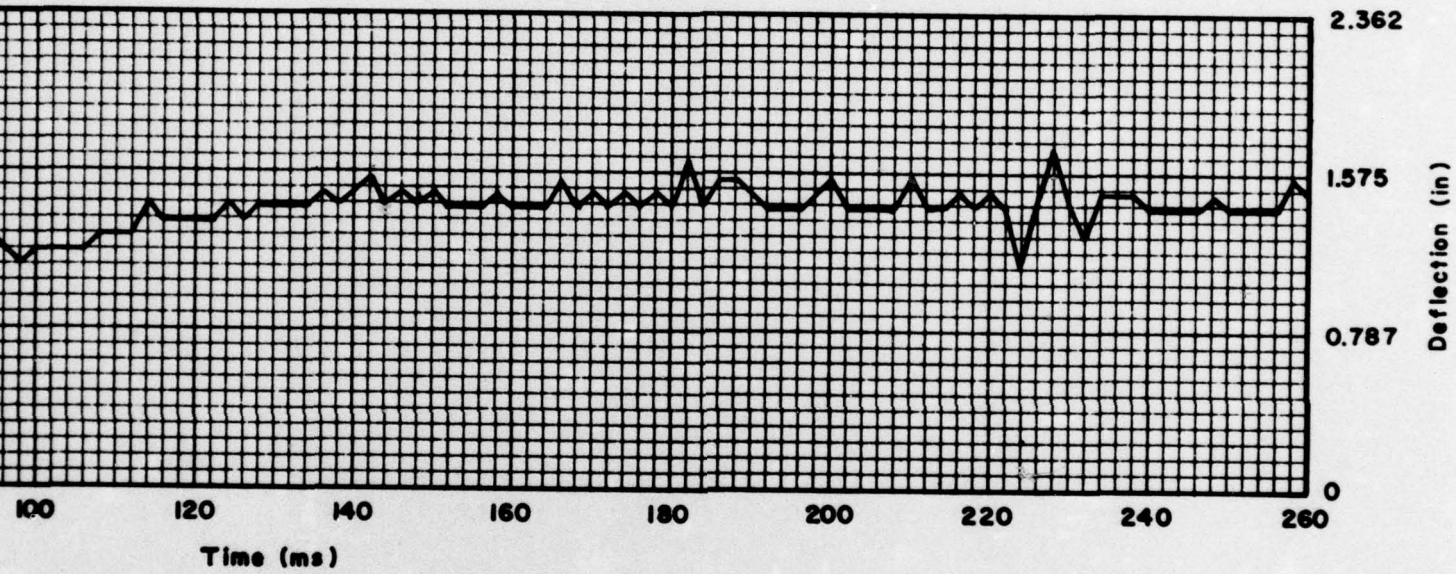


END

DATE
FILMED
6-77



MICROCOPY RESOLUTION TEST CHART
NATIONAL BUREAU OF STANDARDS-1963



45 Deflection-time measurements, Gage No. 7 (Test No. 5)

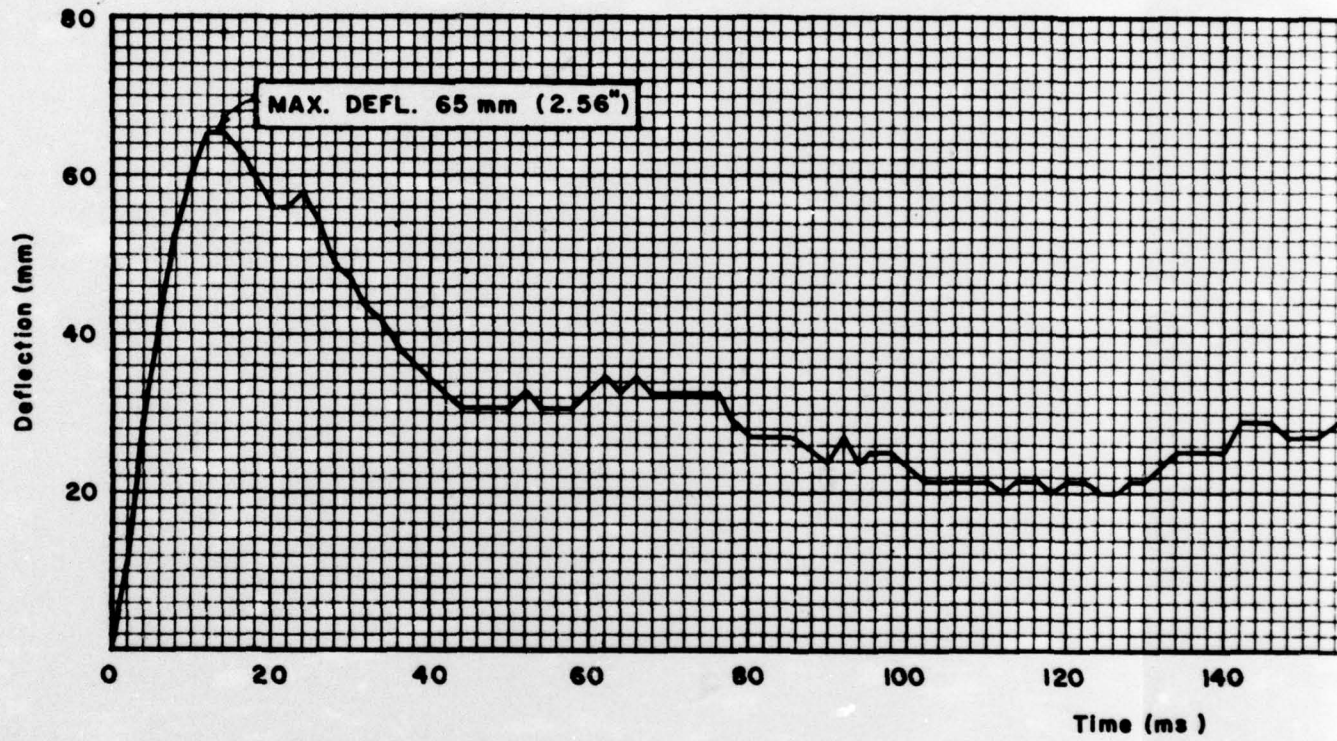
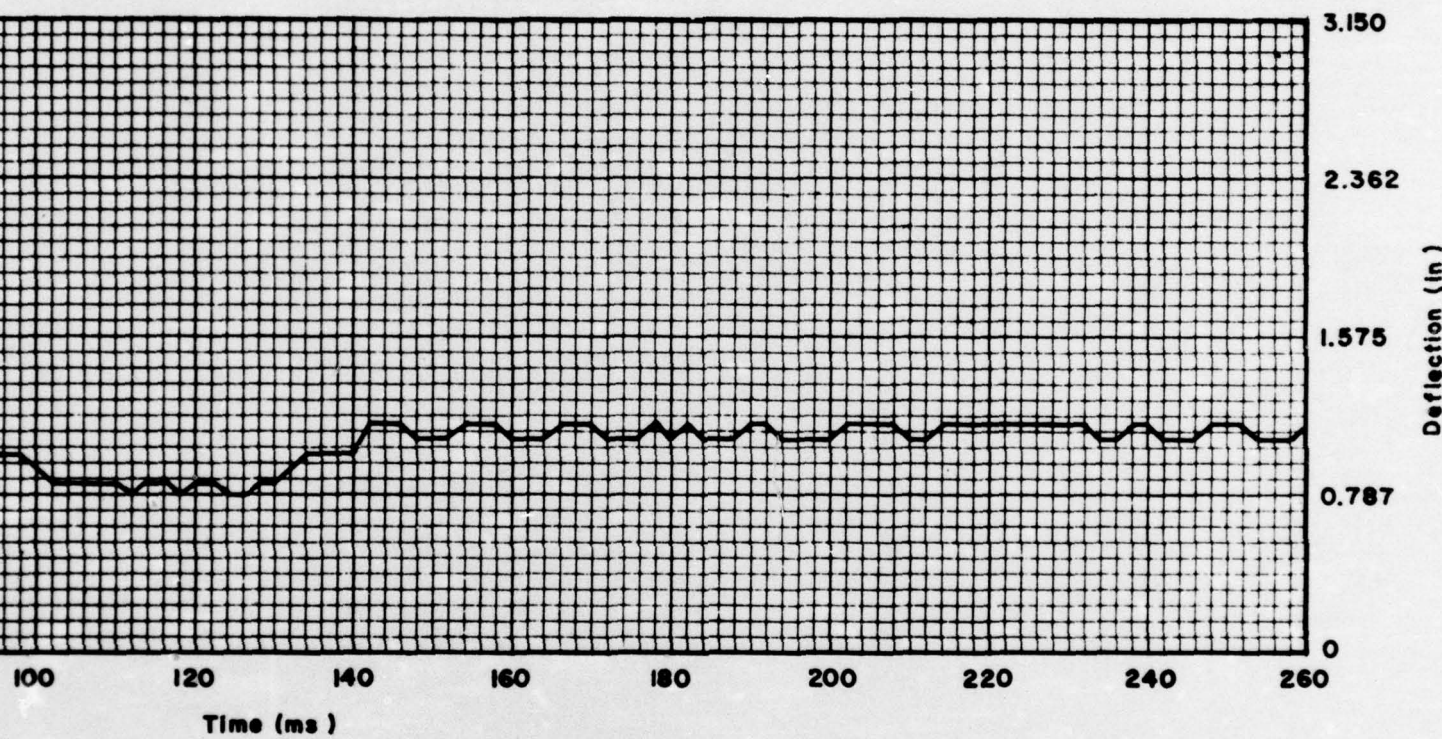


Fig 46 Deflection-time measurements, Gage No.



46 Deflection-time measurements, Gage No. 5 (Test No. 6)

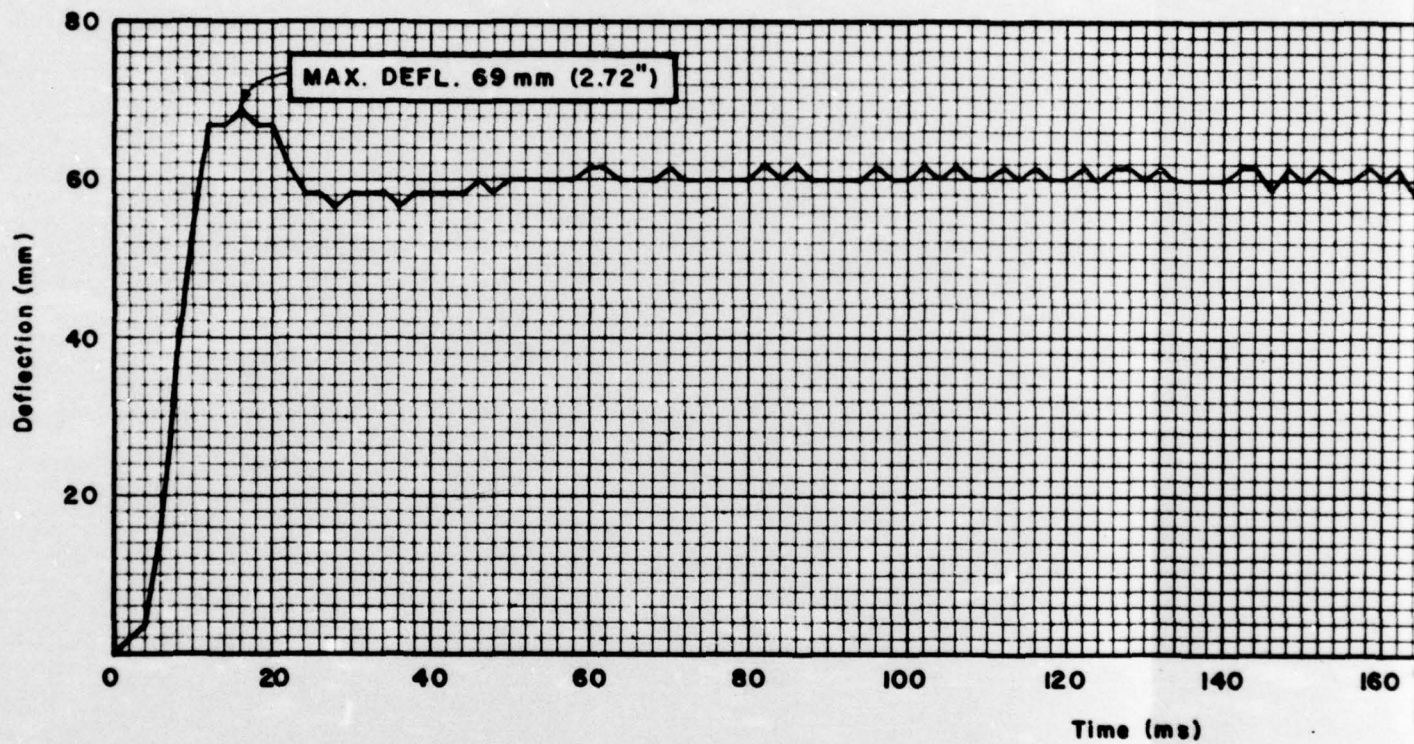


Fig 47 Deflection-time measurements, Gage No. 7 (T)

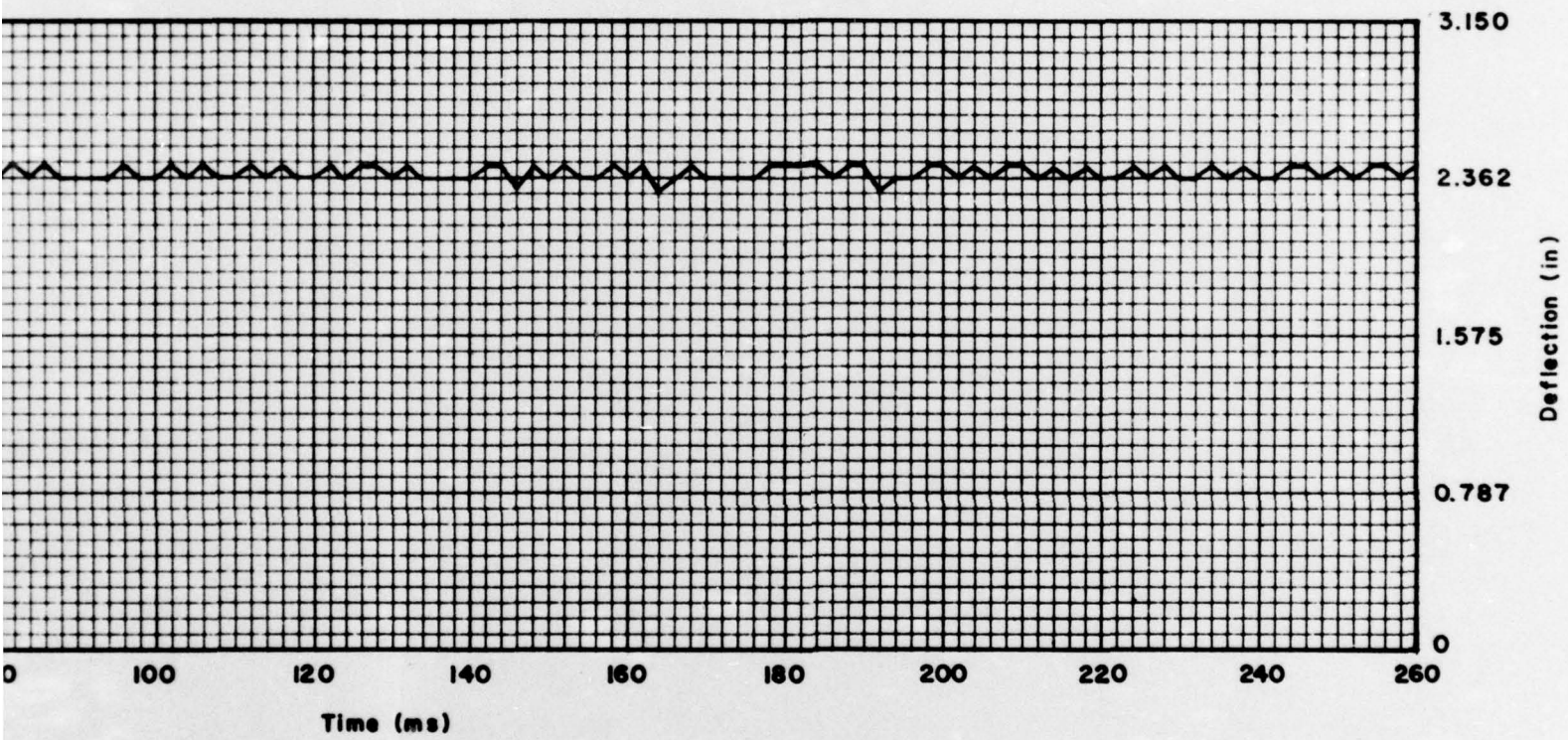


Fig 47 Deflection-time measurements, Gage No. 7 (Test No. 6)

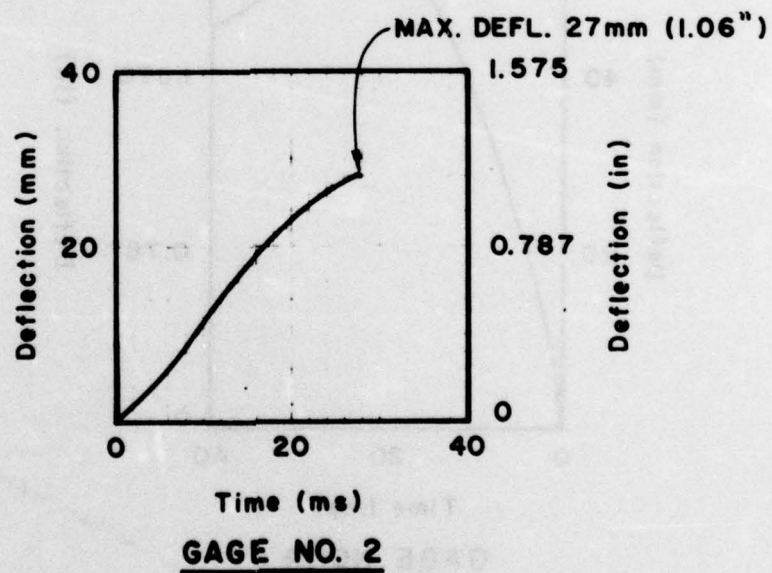
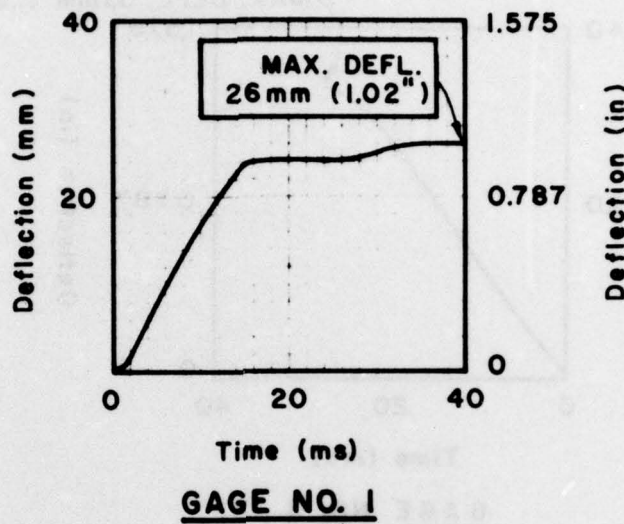


Fig 48 Deflection-time measurements, Gage Nos. 1 & 2 (Test No. 7)

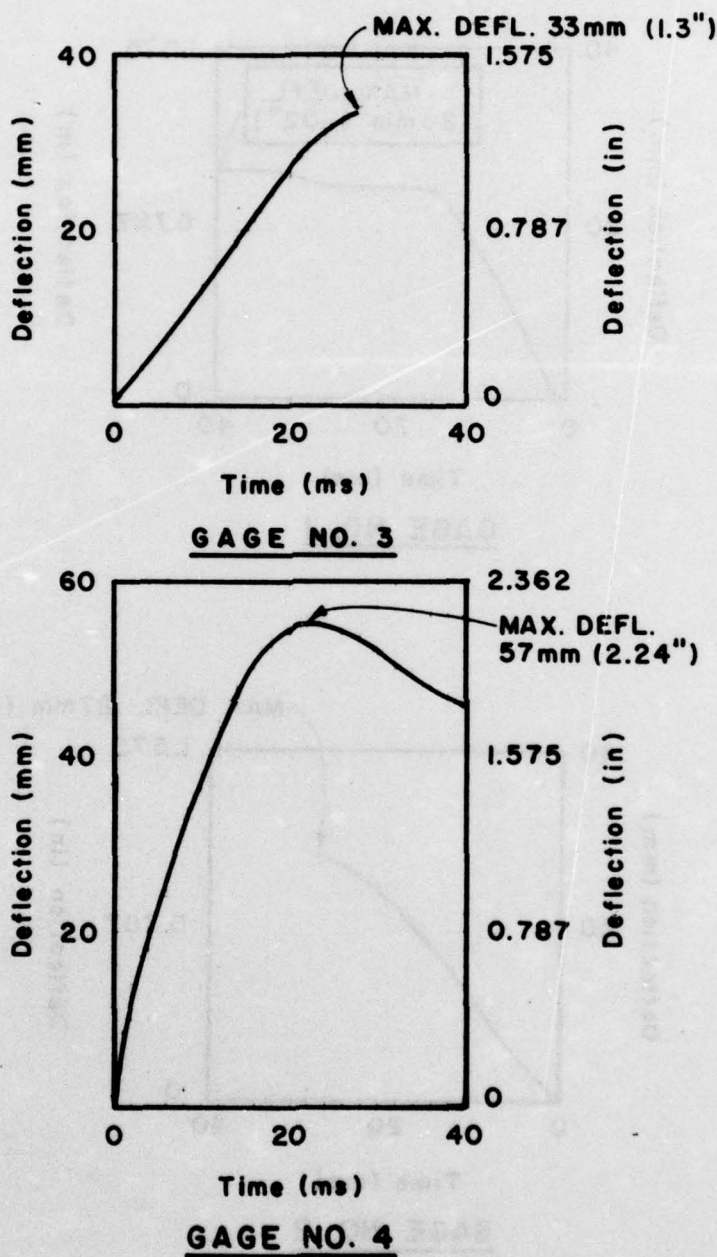


Fig 49 Deflection-time measurements, Gage Nos. 3 & 4 (Test No. 7)

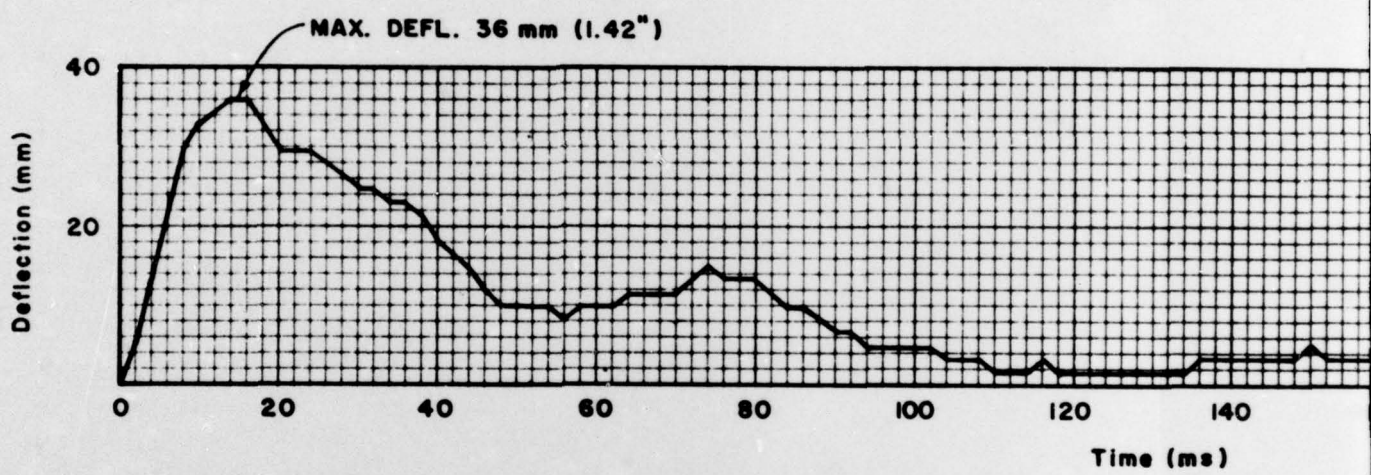
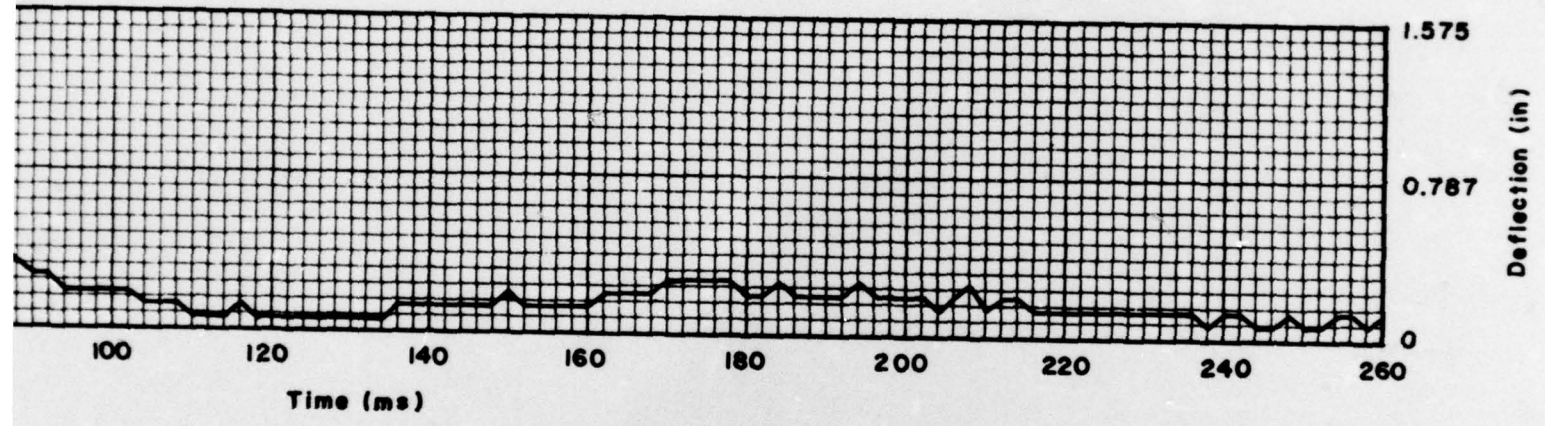


Fig 50 Deflection-time measurements, Gage No. [illegible]



Deflection-time measurements, Gage No. 6 (Test No. 7)

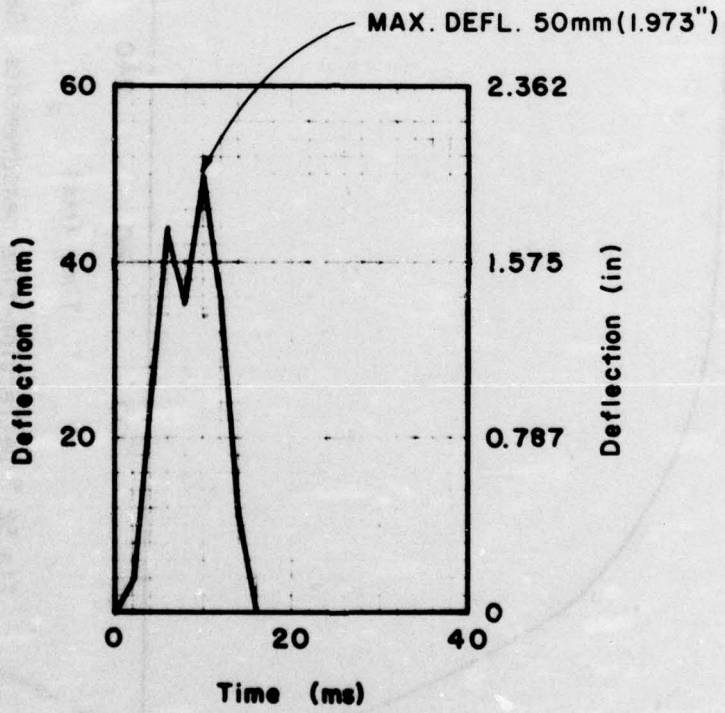


Fig 51 Deflection-time measurements, Gage No. 7 (Test No. 7)

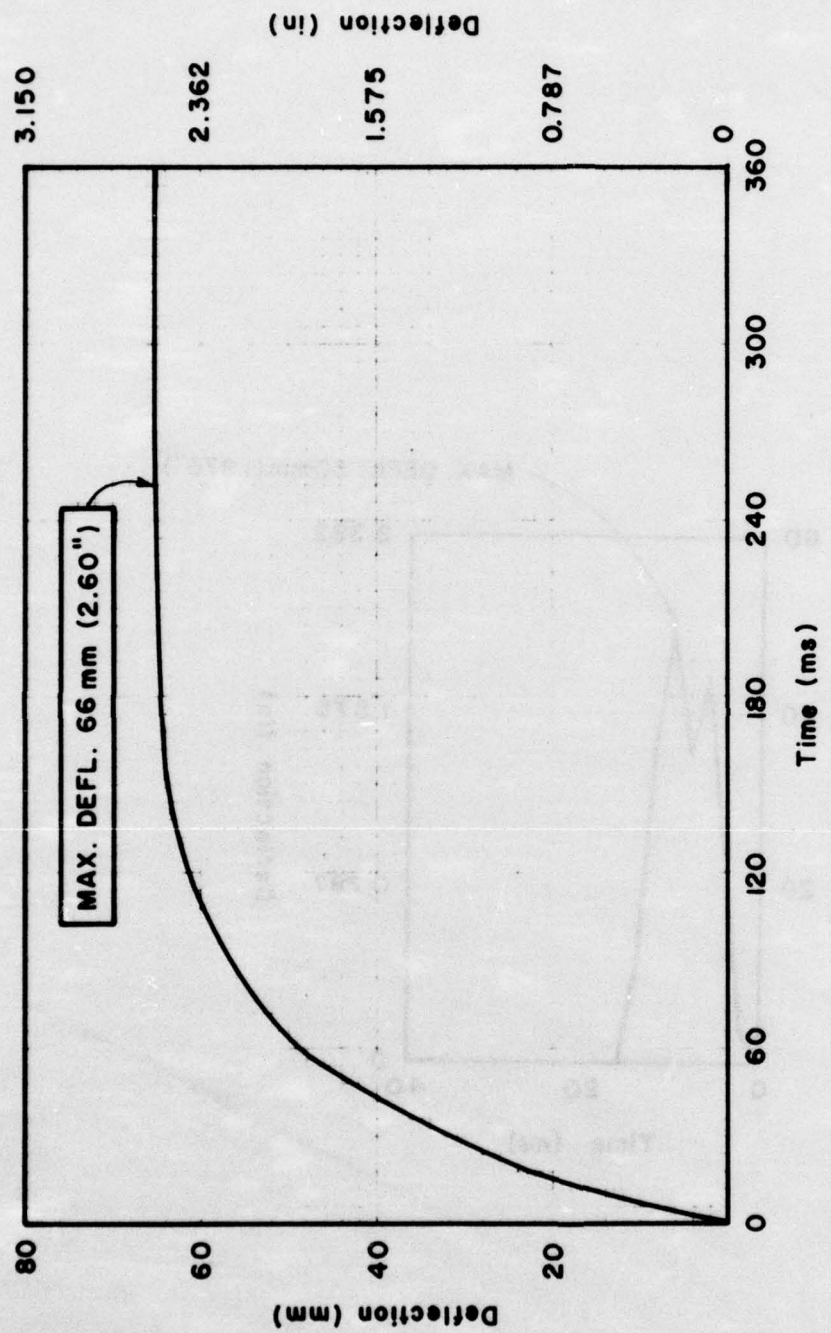


Fig 52 Deflection-time measurements, Gage No. 1
(Test No. 8)

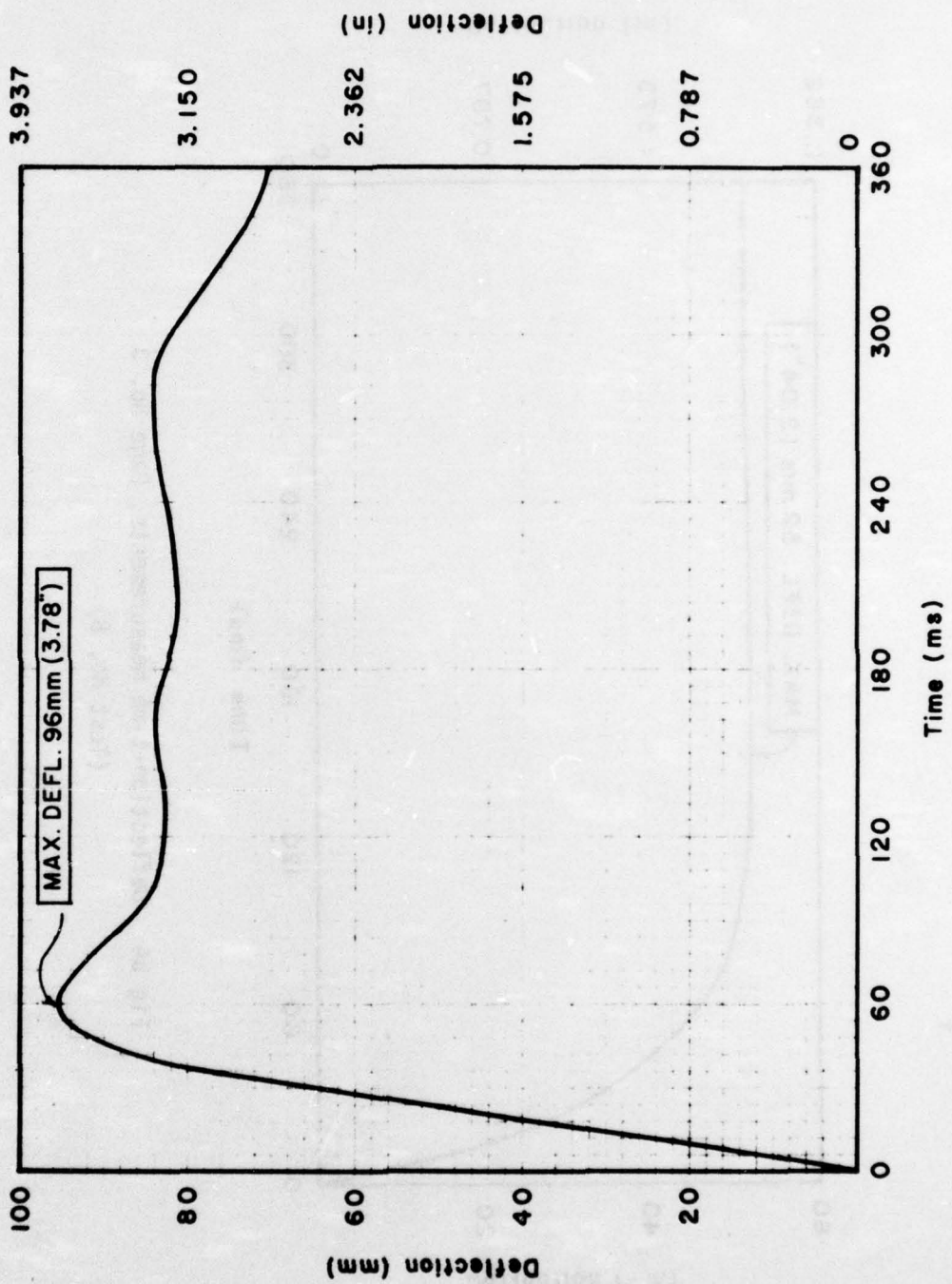


Fig 53 Deflection-time measurements, Gage No. 2
(Test No. 8)

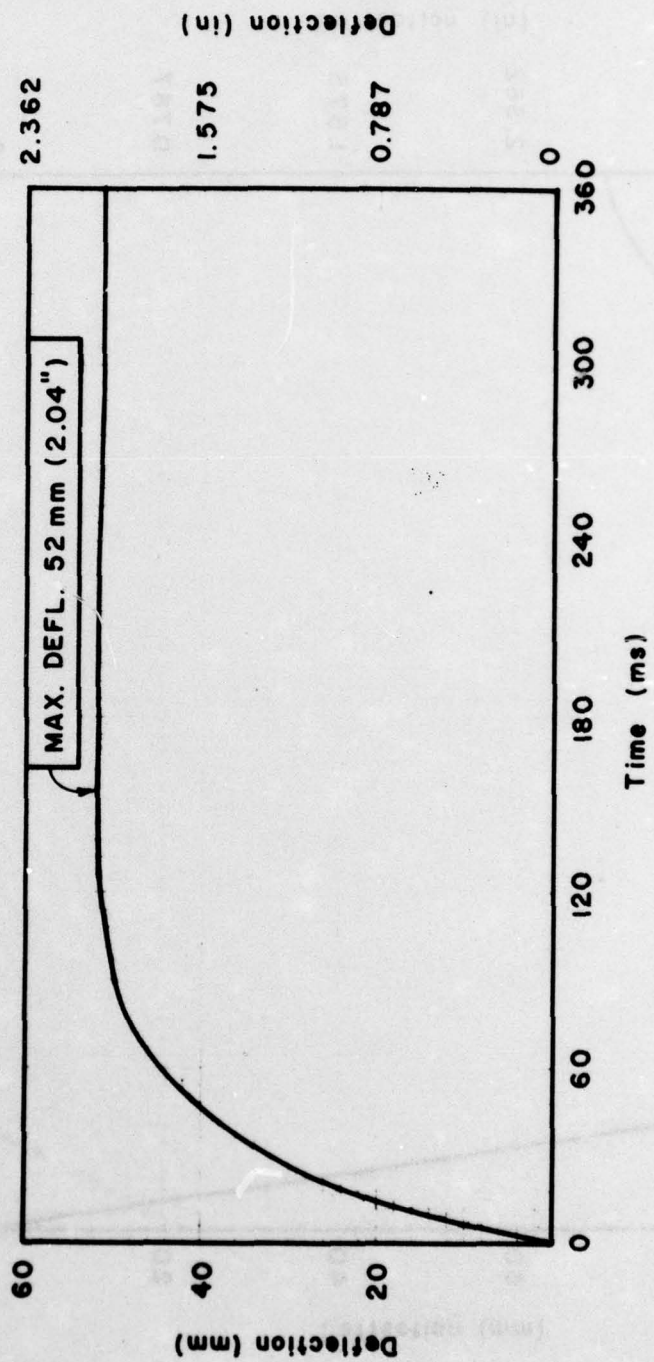


Fig 54 Deflection-time measurements, Gage No. 3
(Test No. 8)

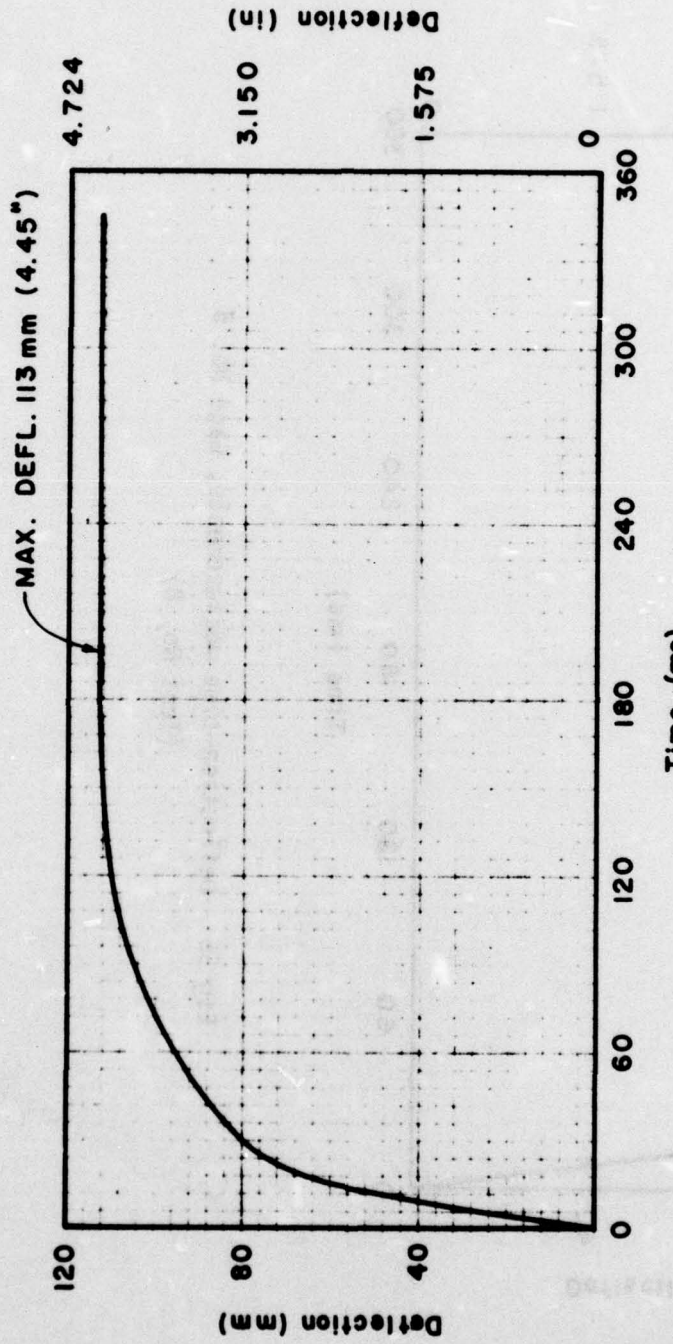


Fig 55 Deflection-time measurements, Gage No. 4
(Test No. 8)

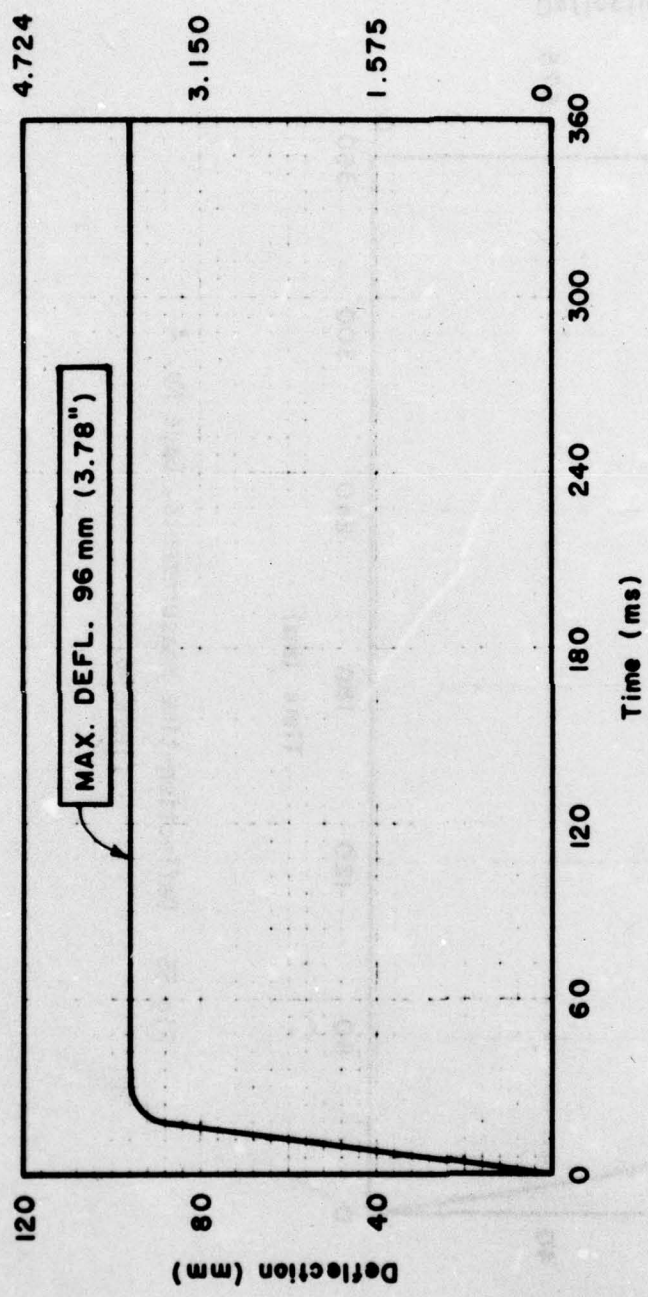


Fig 56 Deflection-time measurements, Gage No. 5
(Test No. 8)

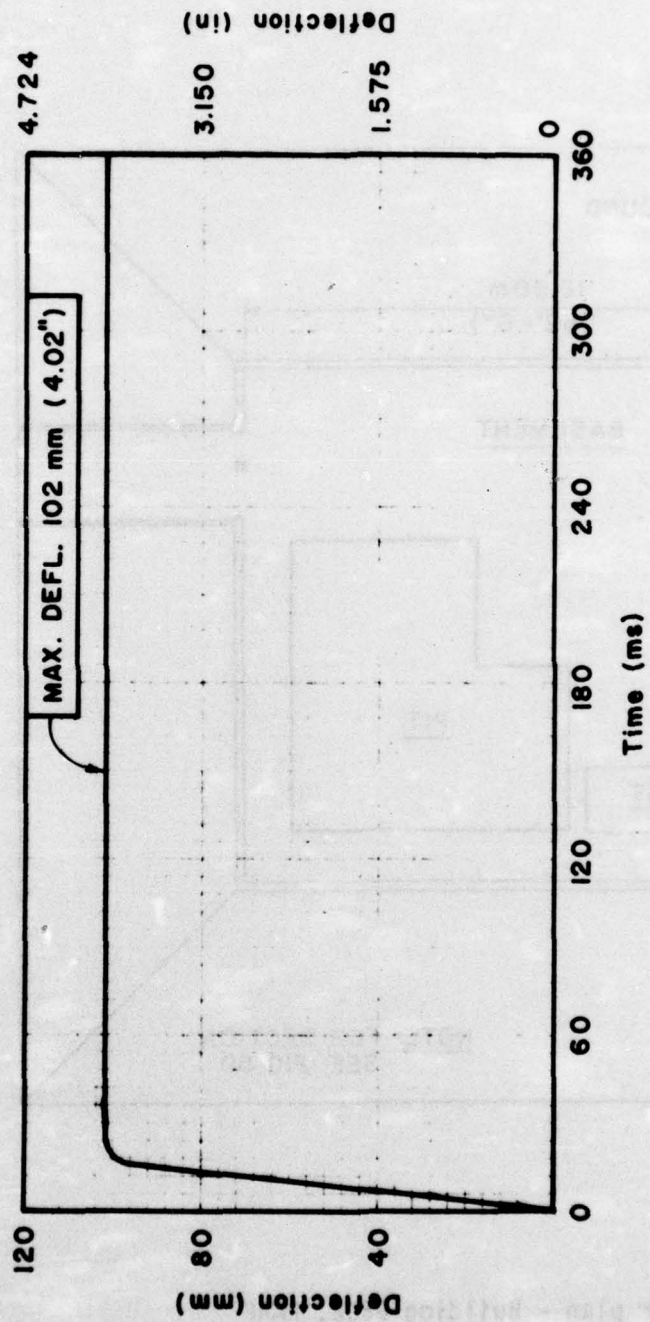


Fig 57 Deflection-time measurements, Gage No. 6
(Test No. 8)

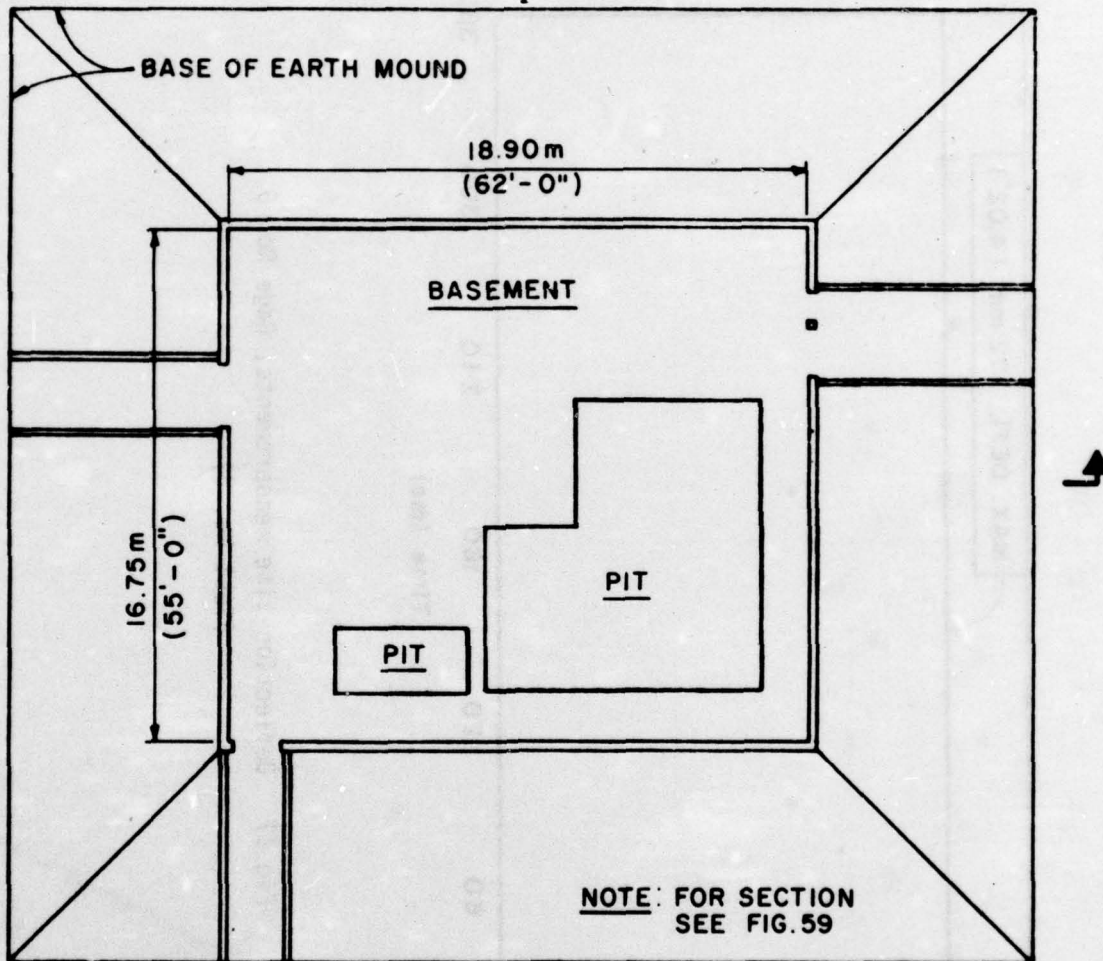


Fig 58 Floor plan - Building 9502, RAAP

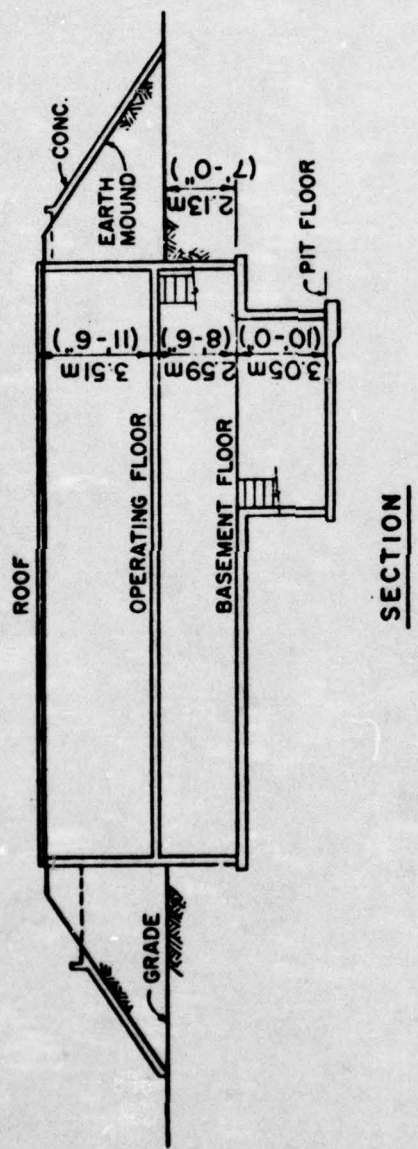


Fig 59 Section - Building 9502, RAAP

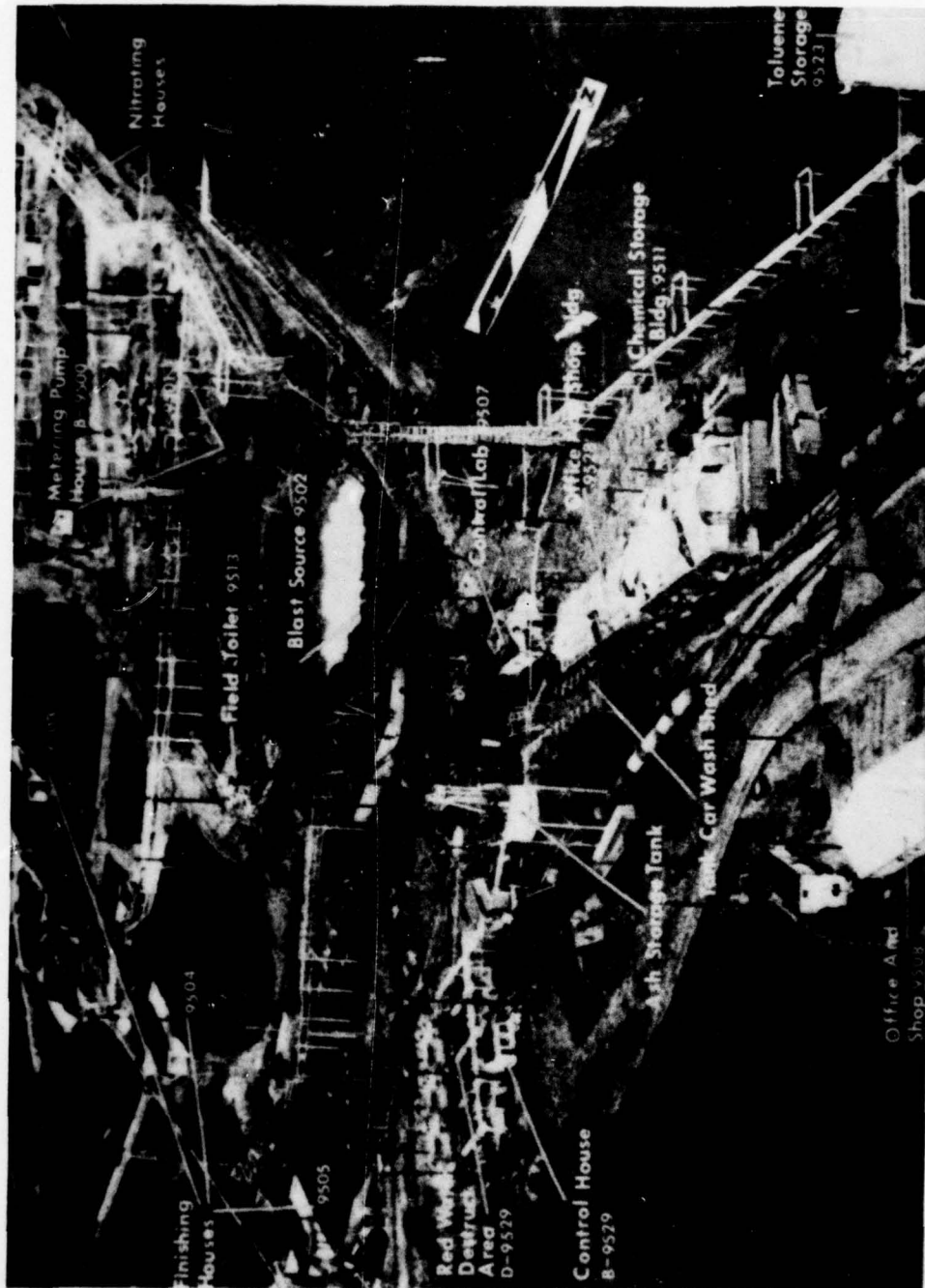


Fig 60 Post-explosion view of Building 9502, RAAP

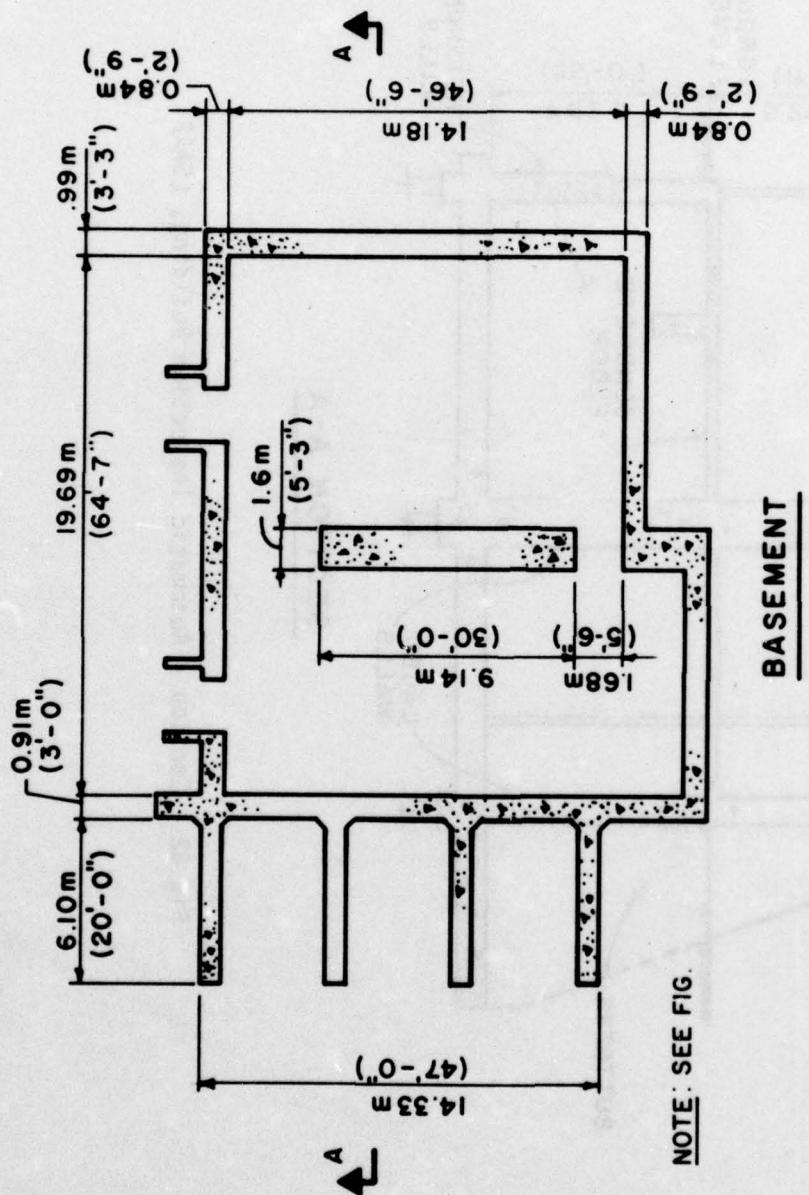


Fig 61 Floor plan - Automatic Inspection Building, LSAAP

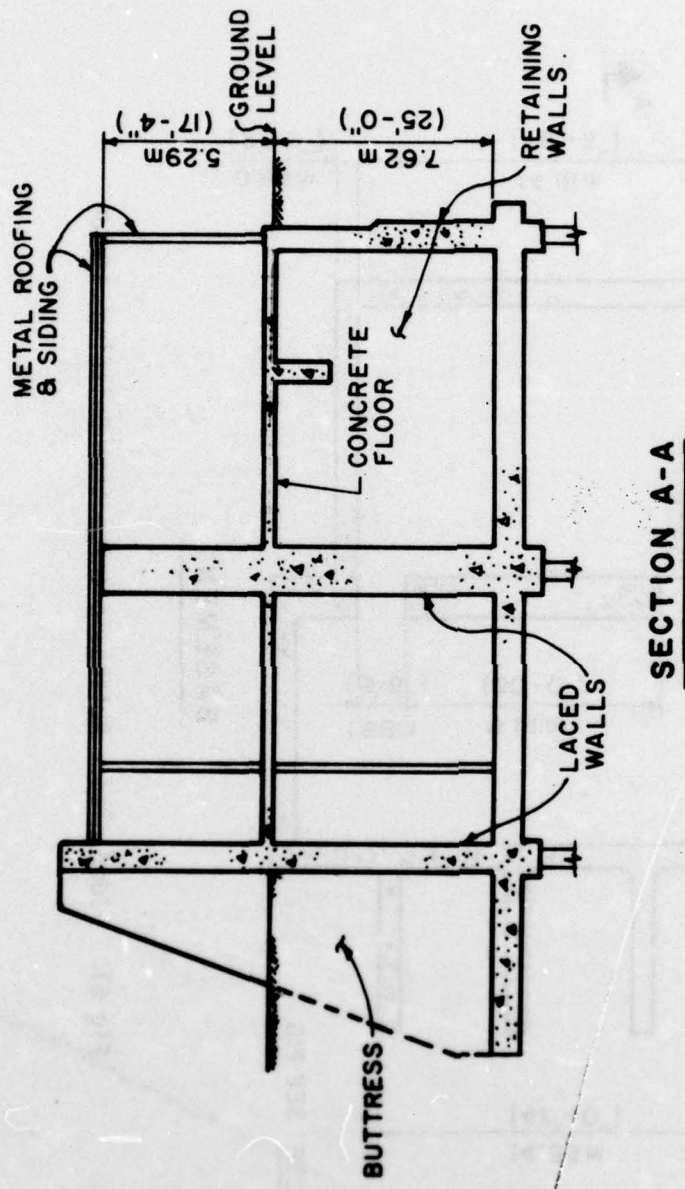


Fig 62 Section - Automatic Inspection Building, LSAAP

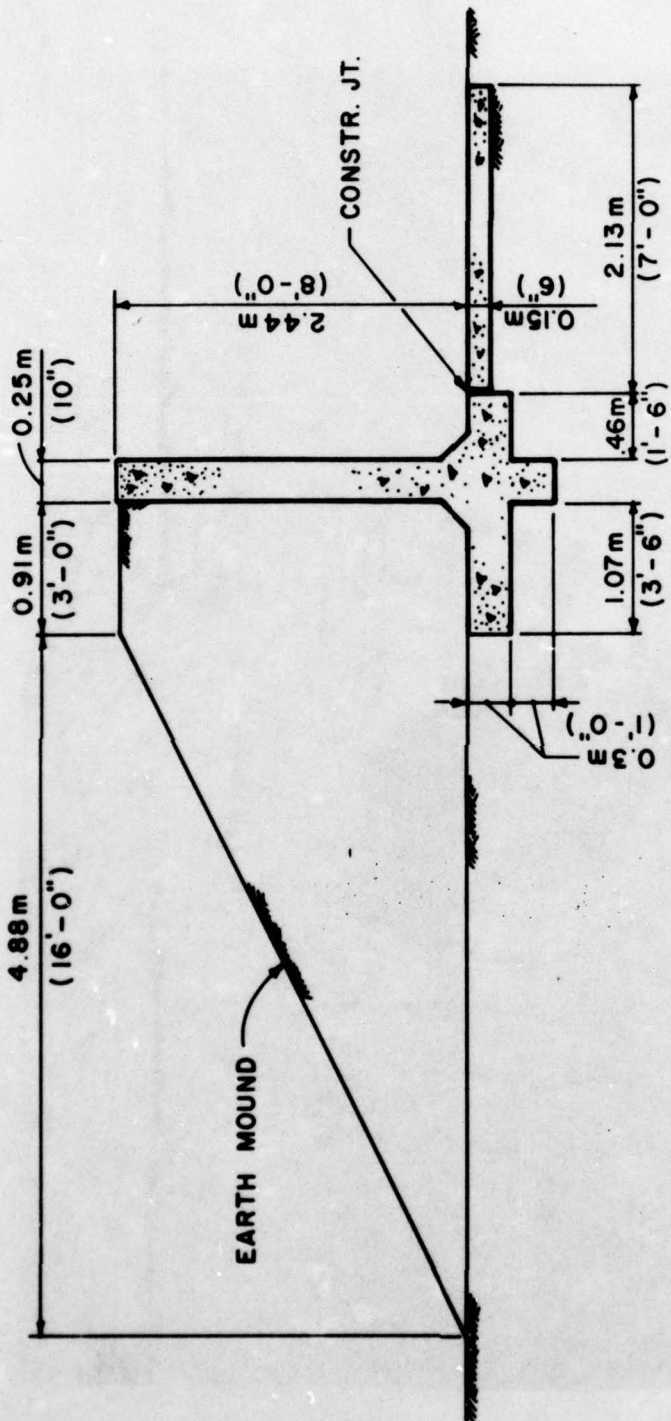


Fig 63 Section - Single Revetted Barricades Test Structure



Fig 64 Post-explosion view of Wall No. 1 - Barricade Tests

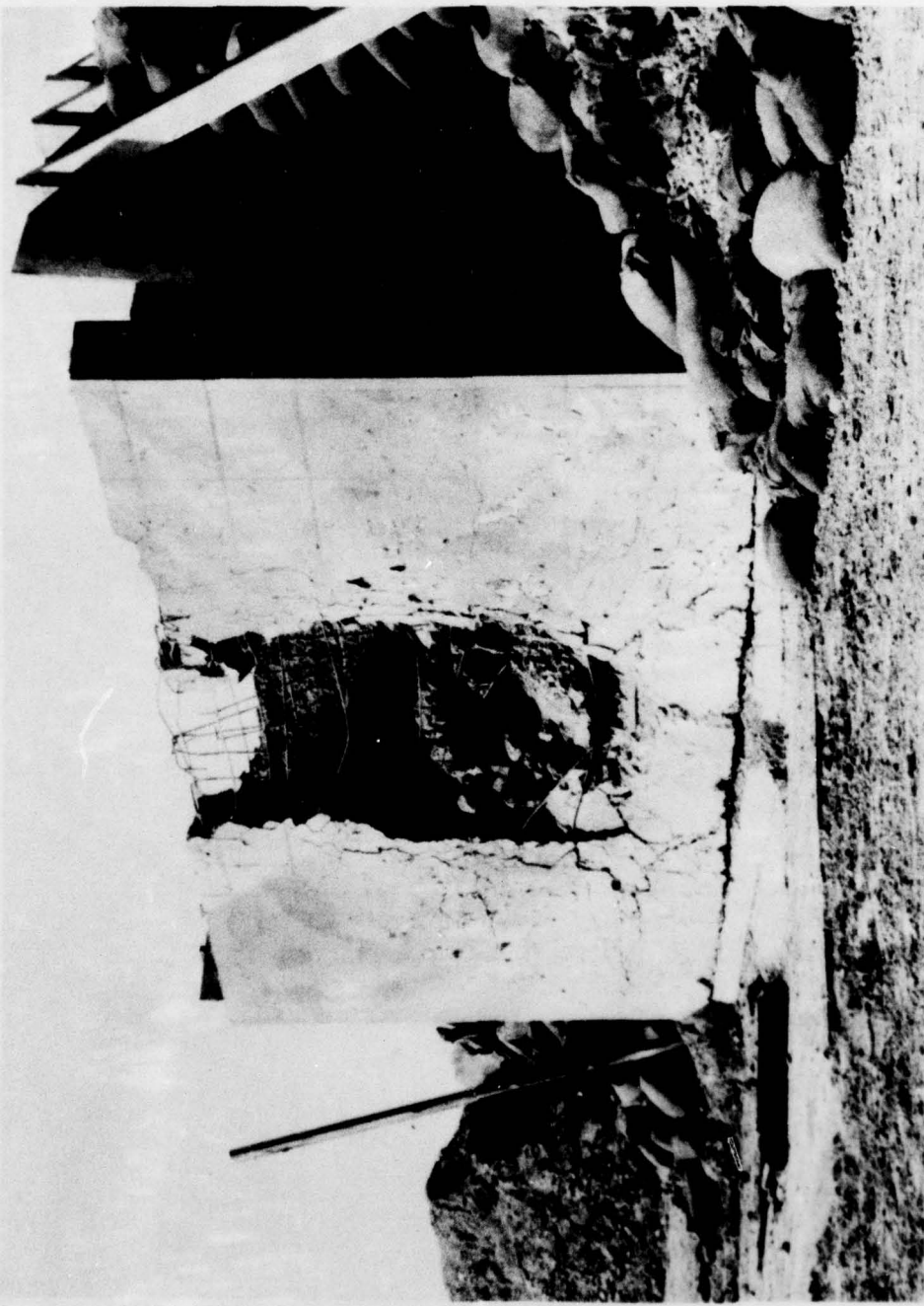


Fig 65 Post-explosion view of Wall No. 2 - Barricade Tests

APPENDIX

INTERNATIONAL SYSTEM OF UNITS

PRECEDING PAGE ~~BLANK NOT FILMED~~

APPENDIX

INTERNATIONAL SYSTEM OF UNITS

General

This appendix deals with the conversion of quantities from the U. S. System of measurement to the International System of Units which is officially abbreviated as SI in all languages. It includes units most frequently used in the various fields of science and industry and conforms to the Metric Practice Guide as presented in the American Society for Testing and Materials Standard E 380.

SI Units and Prefixes

SI consists of seven base units, two supplementary units, a series of derived units consistent with the base and supplementary units, and a series of approved prefixes for the formation of multiples and sub-multiples of various units. A summary of the base units, supplementary units, derived units and prefixes is given below:

Base Units

Quantity	Unit	Symbol
Length	meter	m
Mass	kilogram	kg
Time	second	s
Electric current	ampere	A
Thermodynamic temperature	kelvin	K
Amount of substance	mole	mol
Luminous intensity	candela	cd

Supplementary Units

Quantity	Unit	Symbol
Plane angle	radian	rad
Solid angle	steradian	sr

Derived Units

Quantity	Unit	Symbol or Formula
Acceleration	meter per second squared	m/s^2
Activity (radioactive source)	disintegration per second	(disintegration)/s
Angular acceleration	radian per second squared	rad/s^2
Angular velocity	radian per second	rad/s
Area	square meter	m^2
Density	kilogram per cubic meter	kg/m^3
Electric capacitance	farad	F or A.s/V
Electrical conductance	siemens	S or A/V
Electric field strength	volt per meter	V/m
Electric inductance	henry	H or V.s/A
Electric potential difference	volt	V or W/A
Electric resistance	ohm	Ω or V/A
Electromotive force	volt	V or W/A
Energy	joule	J or N.m
Entropy	joule per kelvin	J/K
Force	newton	N or kg.m/s^2
Frequency	hertz	Hz or (cycle)/s
Illuminance	lux	$1x$ or $1\text{m}/\text{m}^2$
Luminance	candela per square meter	cd/m^2
Luminous flux	lumen	$1m$ or cd.sr
Magnetic field strength	ampere per meter	A/m
Magnetic flux	weber	Wb or V.s
Magnetic flux density	tesla	T or Wb/m^2
Magnetomotive force	ampere	A
Power	watt	W or J/s
Pressure	pascal	Pa or N/m^2
Quantity of electricity	coulomb	C or A.s
Quantity of heat	joule	J or N.m
Radiant intensity	watt per steradian	W/s.r
Specific heat	joule per kilogram-kelvin	J/kg.K
Stress	pascal	Pa or N/m^2
Thermal conductivity	watt per meter-kelvin	$\text{W}/\text{m.K}$
Velocity	meter per second	m/s
Viscosity, dynamic	pascal-second	Pa.s
Viscosity, kinematic	square meter per second	m^2/s
Voltage	volt	V or W/A

Derived Units (continued)

Quantity	Unit	Symbol or Formula
Volume	cubic meter	m^3
Wavenumber	reciprocal meter	(wave)/m
Work	joule	J or N.m

Prefixes

Multiplication		Prefix	Symbol
1,000,000,000,000 = 10^{12}		tera	T
1,000,000,000 = 10^9		giga	G
1,000,000 = 10^6		mega	M
1,000 = 10^3		kilo	k
100 = 10^2		hecto*	h
10 = 10^1		deka*	da
0.1 = 10^{-1}		deci*	d
0.01 = 10^{-2}		centi*	c
0.001 = 10^{-3}		milli	m
0.000,001 = 10^{-6}		micro	u
0.000,000,001 = 10^{-9}		nano	n
0.000,000,000,001 = 10^{-12}		pico	p
0.000,000,000,000,001 = 10^{-15}		femto	f
0.000,000,000,000,000,001 = 10^{-18}		atto	a

*To be avoided where possible

Selection of prefixes representing steps of 1,000 is recommended for most multiple and submultiple prefixes. An exception is made in the case of area and volume used alone. When expressing a quantity by a numerical value and a unit, prefixes should preferably be chosen so that the numerical value lies between 0.1 and 1,000, except where certain multiples or submultiples have been agreed to for particular use. The same unit, multiple or submultiple is used for tabular values even though the series exceeds the preferred range 0.1 to 1,000. Double prefixes should not be used. Prefixes should not be used in the denominator of compound units, except for the kilogram which is a base unit of SI. However, prefixes may be applied to numerator of a combined unit. With SI units of higher order such as m^2 , m^3 , etc., the prefix is also raised to the same order; e.g., mm^3 is $10^{-9}m^3$ and not $10^{-3}m^3$. In such cases, the use of cm^2 , cm^3 , dm^2 , dm^3 and similar nonpreferred prefixes is acceptable.

Mass, Force and Weight

The principal departure of SI from the gravimetric form of metric engineering units is the separate and distinct units for mass and force. The kilogram is restricted to the unit of mass. The newton is the unit of force and should be used in place of kilogram-force. Likewise, the newton instead of kilogram-force should be used in combination units which include force; e.g., pressure or stress ($N/m^2=Pa$), energy ($N.m=J$), and power ($N.m/s=W$).

Considerable confusion exists in the use of the terms mass and weight. Mass is a property of matter to which it owes its inertia. If a body or particle of matter at rest on the earth's surface is released from the forces holding it at rest, it will experience the acceleration of free fall (or acceleration of gravity, g). The force required to restrain it against free fall is commonly called weight. This force is proportional to the mass of the body and is often expressed in mass units (kg), but as it is a force it should be expressed in force units (N). The acceleration of free fall (g) varies in time and space; weight (which is proportional to it) does too, although mass does not. Further confusion arises in the measuring of weight because of the buoyant effect of the medium in which the weighing is performed. In common parlance the term weight is used where the technically correct word is mass and, therefore, the use of the term weight should be avoided in technical practice.

Conversion and Rounding Rules

Conversion of quantities should be handled with careful regard to the implied correspondence between the accuracy of the data and the given number of digits. In all conversions, the number of significant digits retained should be such that accuracy is neither sacrificed nor exaggerated. Proper conversion procedure is to multiply the specific quantity by the conversion factor exactly as given and then round to the appropriate number of significant digits.

The following table contains conversion factors that give exact or seven-figure accuracy where the nature of the dimension makes this degree of accuracy practical:

Selected Conversion Factors

To convert from	to	Multiply by
atmosphere (technical = 1 kfg/cm ²)	pascal (Pa)	9.806 650×10 ⁴
bar	pascal (Pa)	1.000 000×10 ⁵
board foot	meter ³ (m ³)	2.359 737×10 ⁻³
British thermal unit (International Table)	joule (J)	1.055 056×10 ³
Btu (International Table) - in./s·ft ² ·°F (k, thermal conductivity)	watt/meter-kelvin (W/m·K)	5.192 204×10 ²
Btu (International Table) /hour	watt (W)	2.930 711×10 ⁻¹
calorie (International Table)	joule (J)	4.186 800*
centipoise	pascal-second (Pa·s)	1.000 000×10 ⁻³
centistokes	meter ² /second (m ² /s)	1.000 000×10 ⁻⁶
degree (angle)	radian (rad)	1.745 329×10 ⁻²
degree Fahrenheit	degree Celsius	t°C=(t°F-32)/1.8
fluid ounce (U.S.)	meter ³ (m ³)	2.957 353×10 ⁻⁵
foot	meter (m)	3.048 000×10 ⁻¹
foot ²	meter ² (m ²)	9.290 304×10 ⁻²
foot ³ (volume and section modulus)	meter ³ (m ³)	2.831 685×10 ⁻²
foot/second	meter/second (m/s)	3.048 000×10 ⁻¹
foot-pound-force	joule (J)	1.355 818
foot-pound-force/second	watt (W)	1.355 818
foot/second ²	meter/second ² (m/s ²)	3.048 000×10 ⁻¹
gallon (U.S. liquid)	meter ³ (m ³)	3.785 412×10 ⁻³
horsepower (electric)	watt (W)	7.460 000×10 ²
inch	meter (m)	2.540 000×10 ⁻²
inch ²	meter ² (m ²)	6.451 600×10 ⁻⁴
inch ³ (volume and section modulus)	meter ³ (m ³)	1.638 706×10 ⁻⁵
inch of mercury (60°F)	pascal (Pa)	3.376 85×10 ³
inch of water (50°F)	pascal (Pa)	2.488 4 ×10 ²
kilogram-force (kgf)	newton (N)	9.806 650*
kilogram-force/millimeter ²	pascal (Pa)	9.806 650×10 ⁶
kilogram-mass	kilogram (kg)	1.000 000*
kip (1000 lbf)	newton (N)	4.448 222×10 ³
kip/inch ² (ksi)	pascal (Pa)	6.894 757×10 ⁶
lux	lumen/meter ² (lm/m ²)	1.000 000*
minute (angle)	radian (rad)	2.908 882×10 ⁻⁴
ounce-force (avoirdupois)	newton (N)	2.780 139×10 ⁻¹

*Exact

Selected Conversion Factors (Continued)

To convert from	to	Multiply by
ounce-mass (avoirdupois)	kilogram (kg)	2.834 952x10 ⁻²
ounce-mass/yard ²	kilogram/meter ² (kg/m ²)	3.390 575x10 ⁻²
ounce (avoirdupois) (mass)/inch ³	kilogram/meter ³ (kg/m ³)	1.729 994x10 ³
ounce (U.S. fluid)	meter ³ (m ³)	2.957 353x10 ⁻⁵
pint (U.S. liquid)	meter ³ (m ³)	4.731 765x10 ⁻⁴
pound-force (lbf avoirdupois)	newton (N)	4.448 222
pound/force/inch ² (psi)	pascal (Pa)	6.894 757x10 ³
pound-mass (1bm avoirdupois)	kilogram (kg)	4.535 924x10 ⁻¹
pound-mass-inch ² (moment of inertia)	kilogram-meter ² (kg·m ²)	2.926 397x10 ⁻⁴
pound-mass/inch ³	kilogram/meter ³ (kg/m ³)	2.767 990x10 ⁴
quart (U.S. liquid)	meter ³ (m ³)	9.463 529x10 ⁻⁴
second angle	radian (rad)	4.848 137x10 ⁻⁶
ton (short, 2000 1bm)	kilogram (kg)	9.071 847x10 ²
watt-hour	joule (J)	3.600 000*x10 ³
yard	meter (m)	9.144 000*x10 ⁻¹
yard ²	meter ² (m ²)	8.361 274x10 ⁻¹
yard ³	meter ³ (m ³)	7.645 549x10 ⁻¹

*Exact

DISTRIBUTION LIST

Copy No.

Commander	
US Army Armament Research and	
Development Command	
ATTN: DRDAR-CC	1
DRDAR-LCM-E	2
DRDAR-LCM-S	3-26
DRDAR-SF	27
DRDAR-TSS	28-32
Dover, NJ 07801	
Chairman	
Dept of Defense Explosive Safety Board	
Forrestal Bldg, GB-270	33-34
Washington, DC 20314	
Administrator	
Defense Documentation Center	
ATTN: Accessions Division	35-46
Cameron Station	
Alexandria, VA 22314	
Commander	
Department of the Army	
Office, Chief Research, Development & Acquisition	
ATTN: DAMA-CSM-P	47
Washington, DC 20310	
Office, Chief of Engineers	
ATTN: DAEN-MCZ	48
Washington, DC 20314	
Commander	
US Army Materiel Development &	
Readiness Command	
ATTN: DRCSF	49
DRCDE	50
DRCRP	51
DRCIS	52
5001 Eisenhower Avenue	
Alexandria, VA 22333	
Commander	
DARCOM Installations & Services Agency	
ATTN: DRCIS-RI	53
Rock Island, IL 61201	

Director

Industrial Base Engineering Activity

ATTN: DRXIB-MT & EN
Rock Island, IL 61201

54

Commander

**US Army Materiel Development &
Readiness Command**

ATTN: DRCPM-PBM 55
DRCPM-PBM-S 56
DRCPM-PBM-L 57-58
DRCPM-PBM-E 59-60

Dover, NJ 07801

Commander

US Army Armament Materiel Readiness Command

ATTN: DRSAR-SF 61-63
DRSAR-SC 64
DRSAR-EN 65
DRSAR-PPI 66
DRSAR-PPI-C 67
DRSAR-RD 68
DRSAR-IS 69
DRSAR-ASF 70

Rock Island, IL 61201

Commander

Frankford Arsenal

ATTN: SARFA-T 71
Philadelphia, PA 19137

Director

DARCOM Field Safety Activity

ATTN: DRXOS-ES 72-73
Charlestown, IN 47111

Commander

US Army Engineer Division

ATTN: HNDED 74
PO Box 1600, West Station
Huntsville, AL 35809

Commander

Radford Army Ammunition Plant 75
Radford, VA 24141

Commander	
Badger Army Ammunition Plant	76
Baraboo, WI 53913	
Commander	
Indiana Army Ammunition Plant	77
Charlestown, IN 47111	
Commander	
Holston Army Ammunition Plant	78
Kingsport, TN 37660	
Commander	
Lone Star Army Ammunition Plant	79
Texarkana, TX 75501	
Commander	
Milan Army Ammunition Plant	80
Milan, TN 38358	
Commander	
Iowa Army Ammunition Plant	81
Middletown, IA 52638	
Commander	
Joliet Army Ammunition Plant	82
Joliet, IL 60436	
Commander	
Longhorn Army Ammunition Plant	83
Marshall, TX 75670	
Commander	
Louisiana Army Ammunition Plant	84
Shreveport, LA 71130	
Commander	
Cornhusker Army Ammunition Plant	85
Grand Island, NB 68801	
Commander	
Ravenna Army Ammunition Plant	86
Ravenna, OH 44266	
Commander	
Newport Army Ammunition Plant	87
Newport, IN 47966	

Commander	
Volunteer Army Ammunition Plant	88
Chattanooga, TN 37401	
Commander	
Kansas Army Ammunition Plant	89
Parsons, KS 67357	
District Engineer	
US Army Engineering District, Mobile	
Corps of Engineers	90
PO Box 2288	
Mobile, AL 36628	
District Engineer	
US Army Engineering District, Ft. Worth	91
Corps of Engineers	
PO Box 17300	
Ft. Worth, TX 76102	
District Engineer	
US Army Engineering District, Omaha	
Corps of Engineers	92
6014 US PO & Courthouse	
215 N 17th Street	
Omaha, NB 78102	
District Engineer	
US Army Engineering District, Baltimore	
Corps of Engineers	93
PO Box 1715	
Baltimore, MD 21203	
District Engineer	
US Army Engineering District, Norfolk	
Corps of Engineers	94
803 Front Street	
Norfolk, VA 23510	
Division Engineer	
US Army Engr District, Huntsville	
PO Box 1600, West Station	95
Huntsville, AL 35807	
Commander	
Naval Ordnance Station	96
Indianhead, MD 20640	

Commander		
U.S Army Construction Engr Research Laboratory	97	
Champaign, IL 61820		
Commander		
Dugway Proving Ground	98	
Dugway, UT 84022		
Commander		
Savanna Army Depot	99	
Savanna, IL 61704		
Civil Engineering Laboratory		
Naval Construction Battalion Center		
ATTN: L51	100	
Port Hueneme, CA 93043		
Commander		
Naval Facilities Engineering Command		
(Code 04, J. Tyrell)	101	
200 Stovall Street		
Alexandria, VA 22322		
Commander		
Southern Division		
Naval Facilities Engineering Command		
ATTN: J. Watts	102	
PO Box 10068		
Charleston, SC 29411		
Commander		
Western Division		
Naval Facilities Engineering Command		
ATTN: W. Moore	103	
San Bruno, CA 94066		
Officer In Charge		
Trident	104	
Washington, DC 20362		
Officer in Charge of Construction		
Trident	105	
Bangor, WA 98348		
Commander		
Atlantic Division		
Naval Facilities Engineering Command		
Norfolk, VA 23511	106	

Commander
Naval Ammunition Depot
Naval Ammunition Production Engineering Center **107**
Crane, IN 47522